

**EMPIRICAL MODEL FOR ESTIMATING THE AVERAGE
HORIZONTAL VALUES OF PSEUDO-ABSOLUTE SPECTRAL
ACCELERATIONS GENERATED BY CRUSTAL EARTHQUAKES**

**VOLUME 1
Sites with $V_{s30} = 450$ to 900 m/s**

By

I. M. Idriss
Professor Emeritus
University of California, Davis
e-mail: imidriss@aol.com

Interim Report Issued for USGS Review

January 19, 2007

TABLE OF CONTENTS

1.0	INTRODUCTION	1
2.0	DATA SELECTION	1
2.1	General	1
2.2	Incorporation of Average Shear Wave Velocity in the Top 30 m, V_{s30}	2
2.3	Earthquake Mechanism	3
2.4	Other Parameters	3
3.0	EMPIRICAL MODEL FOR ESTIMATING EARTHQUAKE GROUND MOTIONS	3
3.1	General	3
3.2	Data Selection	3
3.3	PAA($T = 0.01\text{sec}$) -- Peak Ground Acceleration (pga)	4
	3.3.1 Treatment of Data in Terms of Magnitude Bins	4
	3.3.2 Selection of "Adopted Form"	5
	3.3.3 Examination of Residuals	5
	3.3.4 Comparison with Other Events	5
3.4	Pseudo Absolute Spectral Acceleration for Other Periods	6
4.0	COMPARISONS WITH OTHER ATTENUATION RELATIONSHIPS	6
4.1	General	6
4.2	Comparisons with pre-NGA Relationships	6
4.3	Comparisons with other NGA Relationships	8
5.0	CONCLUDING REMARKS	9
6.0	REFERENCES	10
7.0	ACKNOWLEDGEMENTS	11

LIST OF FIGURES

- Figure 1 Magnitude-distance distribution of NGA free field records
- Figure 2 Magnitude-distance distribution of records selected for use this study
- Figure 3 Magnitude- v_{s30} distribution of records selected for use this study
- Figure 4 Magnitude-pga distribution of records selected for use this study
- Figure 5 Magnitude-pgv distribution of records selected for use this study
- Figure 6 Magnitude-pgd distribution of records selected for use this study
- Figure 7 Magnitude- distance distribution of records used in deriving earthquake ground motion model for sites having v_{s30} ranging from 450 – 900 m/s
- Figure 8 Magnitude- v_{s30} distribution of records used in deriving earthquake ground motions model for sites having v_{s30} ranging from 450 – 900 m/s
- Figure 9 Magnitude-pga distribution of records used in deriving earthquake ground motions model for sites having v_{s30} ranging from 450 – 900 m/s
- Figure 10 Magnitude-pgv distribution of records used in deriving earthquake ground motions model for sites having v_{s30} ranging from 450 – 900 m/s
- Figure 11 Magnitude-pgd distribution of records used in deriving earthquake ground motions model for sites having v_{s30} ranging from 450 – 900 m/s
- Figure 12 Calculated values of PAA for $T = 0.01$ sec versus pga
- Figure 13 Comparison of recorded pga values at distances ranging from 0.1 to 20 km with those calculated at a distance of 10 km based on using magnitude bins for sites having v_{s30} ranging from 450 – 900 m/s
- Figure 14 Comparison of recorded pga values at distances ranging from 20 to 40 km with those calculated at a distance of 30 km based on using magnitude bins for sites having v_{s30} ranging from 450 – 900 m/s
- Figure 15 Calculated values of pga based on using magnitude bins for sites having v_{s30} ranging from 450 – 900 m/s
- Figure 16 Values of pga versus magnitude at a distance of 30 km based on using a number of approaches
- Figure 17 Adopted form used in deriving attenuation relationship
- Figure 18 Comparison of calculated values of pga using adopted form with those calculated

based on using magnitude bins for sites having v_{s30} ranging from 450 – 900 m/s

- Figure 19 Residuals versus magnitude, closest distance and v_{s30} using the derived equation for estimating peak horizontal acceleration (pga)
- Figure 20 Comparison of peak horizontal accelerations recorded during the 1999 Chi-Chi earthquake with calculated values using the derived equation for $M = 7.62$ & mechanism 3
- Figure 21 Residuals – peak horizontal acceleration recorded during the five Chi-Chi earthquake aftershocks obtained using the derived equation with magnitude and mechanism as shown in the legend
- Figure 22 Comparison of peak horizontal accelerations recorded during the 1999 Hector Mine earthquake with calculated values using the derived equation with $M = 7.1$ & mechanism 0
- Figure 23 Comparison of peak horizontal accelerations recorded during the 1989 Loma Prieta earthquake with calculated values using the derived equation with $M = 6.9$ & mechanism 3
- Figure 24 Comparison of peak horizontal accelerations recorded during the 1994 Northridge and the 1971 San Fernando earthquakes with calculated values using the derived equation with $M = 6.7$ & mechanism 2
- Figure 25 Comparison of median values of pga calculated using the new NGA relationship and the relationship by Idriss (2006)
- Figure 26 Comparison of 84-percentile values of pga calculated using the new NGA relationship and the relationship by Idriss (2006)
- Figure 27 Comparison of median values of spectral acceleration for $T = 1.0$ sec calculated using the new NGA relationship and the relationship by Idriss (2006)
- Figure 28 Comparison of 84-percentile values of spectral acceleration for $T = 1.0$ sec calculated using the new NGA relationship and the relationship by Idriss (2006)
- Figure 29 Comparison of the median values of pga calculated using the NGA relationships – $M = 7.5$ and strike slip mechanism
- Figure 30 Comparison of the median values of spectral acceleration for $T = 1.0$ sec calculated using the NGA relationships – $M = 7.5$ and strike slip mechanism

APPENDICES

- Appendix A FREE-FIELD EARTHQUAKE GROUND MOTIONS OBTAINED FROM NGA FLATFILE AND USED IN THIS STUDY
- Appendix B DERIVED PARAMETERS – SPECTRAL VALUES FOR $\tau = 0.02$, $\tau = 0.03$ AND $\tau = 0.04$ SEC
- Appendix C DERIVED PARAMETERS – SPECTRAL VALUES FOR $\tau = 0.2$ SEC
- Appendix D DERIVED PARAMETERS – SPECTRAL VALUES FOR $\tau = 1$ SEC
- Appendix E DERIVED PARAMETERS – SPECTRAL VALUES FOR $\tau = 3$ SEC
- Appendix F ATTENUATION RELATIONSHIP DERIVED BY I. M. IDRIS IN 2002

EMPIRICAL MODEL FOR ESTIMATING THE AVERAGE HORIZONTAL VALUES OF PSEUDO-ABSOLUTE SPECTRAL ACCELERATIONS GENERATED BY CRUSTAL EARTHQUAKES

by

I. M. Idriss
Professor Emeritus
University of California, Davis
e-mail: imidriss@aol.com

1.0 INTRODUCTION

This Volume presents the results obtained from an empirically-based model constructed for estimating the average peak horizontal acceleration (pga) and the average horizontal values of pseudo-spectral acceleration (PAA) for periods of 0.02, 0.03, 0.04, 0.2, 1 and 3 seconds. The objective of the NGA program is to derive such estimates for periods ranging from 0.01 to 10 seconds. At this time, however, only estimates for pga and for the periods listed above are included in this edition of the Volume.

As described below, the approach taken in this study is the use of "bins" of average shear wave velocity, V_{s30} , and only the parameters for the model pertaining to the range of $V_{s30} = 450$ to 900 m/s are presented in this Volume at this time (January 2007).

2.0 DATA SELECTION

2.1 General

Three thousand five hundred and fifty-one (3,551) strong motion records obtained during 173 earthquakes were included in the PEER NGA Flatfile Version 7.2. Only shallow crustal earthquakes were considered in the NGA project.

Only "free-filed" records were utilized in the study. Accordingly, the following records were excluded from the NGA Flatfile: (i) records in basements of any building; (ii) records at dam crests, toes, or abutments; and (iii) records in the first floor of buildings three stories or higher. Thus, the number of free-field records reduces to 3,319 obtained in 125 shallow crustal earthquakes. The magnitude-distance distribution of these free-field records is shown in Figure 1; note that the closest distance to the source is used in Figure 1 and throughout this study.

The list of the earthquakes considered in deriving the parameters for the empirical model used in this study is provided in Appendix A, and includes only records obtained at distances within 200 km of the source. There are 120 earthquakes listed in Appendix A and the total number of records is 3,253, which can be summarized as follows:

- Seventy-two earthquakes in California – number of records = 1,233
- Six earthquakes in Taiwan – the Chi-Chi main shock (414 records), and five aftershocks (1,383 records)
- Seventy-eight earthquakes in: other parts of the USA (Alaska, Idaho, and Nevada), in Canada, Georgia, Greece, Iran, Italy, Mexico, and Turkey – number of records = 223

The magnitude-distance, magnitude- v_{s30} , magnitude-peak ground acceleration (pga), magnitude-peak ground velocity (pgv), and magnitude- peak ground displacement (pgd) distributions of the records referenced in Appendix A are presented in Figures 2, 3, 4, 5 and 6, respectively.

The information gleaned from these figures may be summarized as follows:

- Figure 2 (magnitude-distance distribution) shows that there only 17 recordings at distances less than or equal to 5 km and 33 at distances less than or equal to 10 km; note that for $M \geq 7$, only 3 recordings were obtained in California. Thus, it is difficult to "mathematically" constrain the values at small distances, particularly for large magnitude earthquakes. Thus, reliance must be placed on some physical attributes and on judgment.
- Figure 3 (magnitude- v_{s30} distribution) shows that only a few recordings (47) were at sites with $v_{s30} \geq 900$ m/s and a similar number (56) of recordings at sites with v_{s30} less than 180 m/s.
- Figures 4, 5 and 6 (magnitude-pga, magnitude-pgv, magnitude-pgd distributions, respectively) show that except for a handful of recordings, the values of pga are less than about 0.8g, the values of pgv are less than about 100 cm/s, and the values of pgd are less than about 70 cm.
- Figures 4, 5 and 6 (magnitude-pga, magnitude-pgv, magnitude-pgd distributions, respectively) show that pga is far less dependent on magnitude than pgv and that pgd is somewhat more dependent on magnitude than pgv.

2.2 Incorporation of Average Shear Wave Velocity in the Top 30 m, V_{s30}

Each strong station has been assigned a value of V_{s30} . Shear wave velocities have been measured at or near the sites of only about 1/3 of these strong motion stations. The values of V_{s30} assigned to the other sites were estimated based a variety of techniques, which are referenced in the Flatfile documentation and are not repeated in this Volume.

Initial analyses indicated that pga and spectral ordinates for periods, τ , less than about 3 sec are not materially dependent on the value of v_{s30} , in the range of about 450 to 900 m/s. Accordingly, the recordings at sites having this range of average shear wave velocities were used to derive relationships in this range independently of v_{s30} .

Because the number of the recordings for $v_{s30} > 900$ m/s is only 47, it is felt that it would be best to develop relationships for such sites using the approach outlined in Appendix – [*Note to the reviewers*: the appendix and the parameters for the model pertaining to $v_{s30} > 900$ m/s will be included in Revision 2 to this Volume].

Revision 3 will cover the parameters for the model(s) pertaining to $v_{s30} = 180$ to 450 m/s and for the model pertaining to $v_{s30} < 180$ m/s.

2.3 Earthquake Mechanism

The mechanism for each earthquake listed in the Flatfile was referenced by either a number from 0 to 4 or by a rake angle. The rake angle, however, was not provided for each earthquake and has not been used in this study as an independent parameter.

Instead, earthquakes assigned a mechanism of 0 (e.g., the Denali earthquake) and earthquakes assigned a mechanism of 1 (e.g., the Irpinia earthquake) were combined as a single group and considered to be representative of "strike slip" events. Note that the sense of movement on the Denali fault is a strike slip (USGS, Fact Sheet 014-03) and that on the Irpinia fault is normal (Pantosti et al, 1993).

Earthquakes assigned a mechanism of 2 (e.g., the Northridge earthquake) and earthquakes assigned a mechanism of 3 (e.g., the Loma Prieta earthquake) were combined as a single group and considered to be representative of "reverse" events. Appendix A includes recordings from only three earthquakes with mechanism 4. The Anza-02, with 72 recordings, is described to have occurred on the San Jacinto fault zone and the earthquake focal mechanism exhibited mixed left-lateral strike-slip and thrust motion on a vertical fault striking N35E (Hauksson et al, 2001). Accordingly, these recordings were combined with those from the "reverse" events.

2.4 Other Parameters

The Flatfile included a number of parameters, such as: depth to the top of rupture; sediment (or basin) depth in terms of depth to shear wave velocities of 1.0, 1.5, and 2.5 km/s ($Z_{1.0}$, $Z_{1.5}$, and $Z_{2.5}$, respectively); and parameters relevant to assessing directivity; and location relative to hanging wall/foot wall, as appropriate. The influence of these parameters will be evaluated at a later date.

3.0 EMPIRICAL MODEL FOR ESTIMATING EARTHQUAKE GROUND MOTIONS

3.1 General

The following form was adopted in this study for estimating the median values of pseudo absolute spectral acceleration, $PAA(\mathcal{T})$:

$$\ln[PAA(\mathcal{T})] = \alpha_1(\mathcal{T}) + \alpha_2(\mathcal{T})M - [\beta_1(\mathcal{T}) + \beta_2(\mathcal{T})M] \ln(R_{rup} + 10) + \gamma(\mathcal{T})R_{rup} + \varphi(\mathcal{T})F \quad [1]$$

The variables included in Equation [1] are defined as follows: $PAA(\mathcal{T})$ in g's is the pseudo-absolute acceleration for period, \mathcal{T} , at a spectral damping ratio of 5%; M is moment magnitude; R_{rup} is closest distance to the rupture surface in km; $\gamma(\mathcal{T})$ is a "distance" adjustment factor (partially accounts for anelastic attenuation); $\varphi(\mathcal{T})$ is the source mechanism (or style of faulting) factor; F refers to source mechanism designator with $F = 0$ for "strike slip" events and $F = 1$ for "reverse" events; and $\alpha_1(\mathcal{T})$, $\alpha_2(\mathcal{T})$, $\beta_1(\mathcal{T})$, and $\beta_2(\mathcal{T})$ are parameters obtained from the regression process.

3.2 Data Selection

After a number of iterations, it was found that the average shear wave velocity in the upper 30 m, v_{s30} , in the range of about 450 to 900 m/s, had very little influence on pga and on spectral

ordinates for periods, τ , less than about 3 sec. Accordingly, the recordings at sites having this range of average shear wave velocities were used to derive only one set of relationships in this range.

Table 1 provides a list of the earthquakes used and the number of sites at which the value of $v_{s,30}$ varies from 450 to 900 m/sec. There are 74 earthquakes listed in Table 1 and the total number of records is 987, which can be summarized as follows:

- Forty-four earthquakes in California – number of records = 201
- Six earthquakes in Taiwan – the Chi-Chi main shock (172 records), and five aftershocks (555 records)
- Other earthquakes in: other parts of the USA (Alaska, Idaho, and Nevada), in Canada, Georgia, Greece, Iran, Italy, Mexico, and Turkey – number of records = 59

The magnitude-distance, magnitude- $v_{s,30}$, magnitude-pga, magnitude-pgv, and magnitude-pgd distributions of the records referenced in Table 1 are presented in Figures 7, 8, 9, 10 and 11, respectively.

The observations offered in Section 2.1 regarding Figures 2 through 6 apply as well to Figures 6 through 11 (i.e., the trends of the subset are essentially the same as those of the entire set).

3.3 $PAA(T = 0.01 \text{ sec})$ -- Peak Ground Acceleration (pga)

The Flatfile includes values of pga (directly obtained from the recorded accelerograms) and of the calculated pseudo-absolute acceleration $PAA(T)$ for $T = 0.01$ sec. The values of $PAA(T)$ for $T = 0.01$ sec are about zero to 2% greater than the values of pga, except for some 24 records from California in which the difference varies from about 3 to 4%. Accordingly, the calculated values listed in the Flatfile for $PAA(T)$ for $T = 0.01$ sec are used in this study to represent pga.

3.3.1 Treatment of Data in Terms of Magnitude Bins: The first step undertaken in this study for developing a relationship to estimate pga was to divide the data into $\frac{1}{2}$ magnitude bins, viz: $M = 7\frac{1}{2}$ to 8; 7 to $7\frac{1}{2}$; $6\frac{1}{2}$ to 7 ; ... etc. The number of data points obtained in each magnitude bin is listed below:

Magnitude Range	Average Magnitude	Number of Data Points
$7\frac{1}{2} \leq M < 8$	7.62	180
$7 \leq M < 7\frac{1}{2}$	7.18	29
$6\frac{1}{2} \leq M < 7$	6.76	92
$6 \leq M < 6\frac{1}{2}$	6.23	452
$5\frac{1}{2} \leq M < 6$	5.89	148
$5 \leq M < 5\frac{1}{2}$	5.24	46
$4\frac{1}{2} \leq M < 5$	4.85	40
Total		987

Equation [1] was used to derive a relationship expressing median pga as a function of distance for each magnitude bin. The values of the coefficients α , β , and γ were obtained using standard least square techniques (e.g., Draper and Smith 1998).

The calculated values of pga at a distance of 10 km are shown in Figure 13 in comparison with the values recorded in the distance range of 0.1 to 10 km and values recorded in the distance range of 10 to 20 km. Similar plots of the calculated values of pga at a distance of 30 km are shown in Figure 14 in comparison with the values recorded in the distance range of 20 to 30 km and values recorded in the distance range of 30 to 40 km. These comparisons indicate that the calculated values based on using magnitude bins provide reasonable representation of the recorded data.

3.3.2 Selection of "Adopted Form": The values of pga calculated based on using magnitude bins are plotted in Figure 15 as a function of magnitude at distances of 3, 10, 30 and 100 km. The trends presented in Figure 15 indicate that the values of pga increase as magnitude increases for $M \leq 6\frac{3}{4}$, but decrease at higher magnitudes. The main reason for the drop-off at about $M = 7.62$ (obtained from the analysis of the $7\frac{1}{2} \leq M < 8$ magnitude bin) is the fact that of the 180 data points in that magnitude bin, 172 were recorded in Taiwan during the Chi-Chi earthquake.

As described in the report by Chiou and Youngs (2006), theoretical considerations indicate that variations of pga with magnitude at a distance of 30 km would follow the trend shown in Figure 16. In addition to the curves based on theoretical considerations, the trend obtained using the relationship by Abrahamson and Silva (1997) and the relationship by Idriss (2002) are also presented in Figure 16. The form and the applicable factors and parameters for the relationship by Idriss (2002) are summarized in Appendix F.

Accordingly, the parameters in Eq. [1] were derived to produce the curve designated in Figure 17 as the "adopted form" by minimizing the residuals and obtaining an average residual equal to essentially zero, excluding the values recorded during the magnitude 7.62 Chi-Chi earthquake. The resulting parameters are listed below and in Table 2:

$\tau = 0.01$ sec (i.e., pga)							
M range	$\alpha_1(\tau)$	$\alpha_2(\tau)$	$\beta_1(\tau)$	$\beta_2(\tau)$	$\gamma(\tau)$	$\phi(\tau)$	SE**
$M \leq 6\frac{3}{4}$	5.6362	-0.4104	2.9832	-0.2339	0.00047	0.12	0.66
$M \geq 6\frac{3}{4}$	3.7113	-0.1252	2.9832	-0.2339	0.00047	0.12	0.66

**SE represents the standard error term

The resulting values of pga are plotted in Figure 18 as a function of magnitude at distances of 3, 10, 30 and 100 km.

3.3.3 Examination of Residuals: The residuals calculated using the parameters listed above are presented in Figure 19 in terms of residuals versus magnitude, residuals versus distance, and residuals versus $v_{s,30}$. The residuals obtained for the Chi-Chi main shock ($M = 7.62$) are shown separately and the trend of the residuals is shown for all events with and without the Chi-Chi main shock. The results in Figure 19 indicate that the fitted parameters provide an excellent representation of the data in the magnitude range of 5.2 to 7.2, for almost the entire distance and $v_{s,30}$ ranges. The data for magnitudes smaller than about 5.2 and larger than 7.2 are rather sparse (except for the Chi-Chi main shock). The trend of the residuals shows practically no bias for all magnitudes larger than 5.2, when the residuals for the Chi-Chi main shock are excluded.

Obviously, the pga values recorded during the Chi-Chi main event are overestimated. The latter observation is more clearly depicted in Figure 20.

The residuals obtained for the five Chi-Chi aftershocks are presented in Figure 21 in terms of residuals versus distance. Note that in the aggregate, the derived relationship for pga provides an excellent representation, for distances greater than about 10 km, of the values recorded during these five aftershocks, but that recordings from an individual aftershock can be either well over- or well under-estimated. Note, however, that the number of data points is quite small at distances less than about 20 km.

3.3.4 Comparisons with Other Events: The values recorded during the Hector Mine earthquake are shown in Figure 22 together with the curve calculated using the derived relationship for pga with $M = 7.1$ and mechanism 0. Similar plots for the values recorded during the Loma Prieta earthquake are shown in Figure 23, and those recorded during the Northridge and the San Fernando earthquakes are presented in Figure 24.

The plots in these figures indicate that the degree of fit varies for each earthquake but that the overall comparisons (as depicted in Figure 19) indicate the reasonableness of the derived relationship.

3.4 Pseudo-Absolute Spectral Acceleration for Other Periods

The parameters for the 34 periods listed in Table 2 will be derived following the approach outlined in Section 3.2. Detailed comparisons of the derived and recorded values for each period will be done and plots comparable to those presented in Figures 19 through 24 will be examined for each period. Revision 1 of this Volume will only include the parameters and the figures for periods, $\tau = 0.02, 0.03, 0.04, 0.2, 1$ and 3 seconds, which are presented in Appendices B, C, D and E. The parameters derived for these periods are listed in Table 2. More details regarding these parameters and the parameters for the other periods listed in Table 2 will be included in Revision 2 of this Volume.

4.0 COMPARISONS WITH OTHER ATTENUATION RELATIONSHIPS

4.1 General

The values of pga and spectral accelerations for periods of 0.2 and 1.0 sec using Equation [1] and the parameters and factors listed in Table 2 are compared to corresponding values obtained using pre-NGA relationships and to other NGA relationships. For ease of reference, the new relationship will be designated IMI07.

4.2 Comparison with pre-NGA Relationships

The median values of pga, calculated using IMI07, at distances of 1, 10, 30 and 100 km are plotted versus magnitude in Figure 25 together with the corresponding values calculated using the relationship derived by the author in 2002 (see Appendix F). The values shown in the upper part of Figure 25 are for a strike slip mechanism and in the lower part of the figure are for a reverse mechanism. Corresponding comparisons are presented in Figure 26 for the 84-percentile values of pga.

The information presented in Figures 25 and 26 indicates the following:

- The median values (Figure 25) calculated using the new NGA relationship (IMI07) are smaller than those calculated using the pre-NGA relationship for strike slip as well as for reverse mechanisms.

- The decrease in the median values for strike slip mechanism (upper part of Figure 25) varies from less than 1% for $M = 4\frac{1}{2}$ at a distance of 1 km to about 17% for $M = 8\frac{1}{2}$ at the same distance. At a distance of 100 km, the decrease is less than 1% for $M = 4\frac{1}{2}$ and about 25% for $M = 8\frac{1}{2}$.
- The decrease in median values for reverse mechanism (lower part of Figure 25) is greater, varying from about 41% to 45% for all magnitudes and distances.
- The 84-percentile values for strike slip mechanism (upper part of Figure 26) calculated using the new NGA relationship (IMI07) are about 5 to 15% less than those calculated using the pre-NGA relationship for all distances and $M < 6.75$. For $M > 6.75$, the 84-percentile values for strike slip mechanism calculated using the new NGA relationship (IMI07) vary from about 5% smaller to about 2% larger than those calculated using the pre-NGA relationship for all distances.
- The 84-percentile values calculated using the new NGA relationship (IMI07) are smaller than those calculated using the pre-NGA relationship for reverse mechanism (lower part of Figure 26). The decrease varies from about 22% for $M = 4\frac{1}{2}$ at a distance of 1 km to about 16% for $M = 8$ at the same distance. At a distance of 100 km, the decrease varies from about 17% to 24% for $M = 4\frac{1}{2}$ to 8. These trends are different from those obtained for the strike slip mechanism upper part of Figure 26) because of the significant decrease in the mechanism factor (ϕ).

Corresponding comparisons are presented in Figures 27 and 28 for spectral ordinates at a period of 1.0 sec. The information presented in Figures 27 and 28 indicates the following:

- The median values calculated using the new NGA relationship (IMI07) are generally comparable to those calculated using the pre-NGA relationship for strike slip mechanism (upper part of Figure 27), but are somewhat smaller at all distances and $M > 7$. At a distance of 1 km, the median values calculated using IMI07 are about 8% larger for $M = 4\frac{1}{2}$, about 23% smaller for $M = 6\frac{1}{2}$, and about 15% for $M = 8\frac{1}{2}$. At a distance of 100 km, the decrease is less than 1% for $M = 4\frac{1}{2}$ and about 25% for $M = 8\frac{1}{2}$.
- The median values calculated using the new NGA relationship (IMI07) are smaller than those calculated using the pre-NGA relationship for reverse mechanism (lower part of Figure 27), except at a distance of 100 km for $M < 5$. At a distance of 1 km, the median values calculated using IMI07 are about 9% smaller for $M = 4\frac{1}{2}$ and about 26% smaller for $M = 8\frac{1}{2}$. At a distance of 100 km, the median values calculated using IMI07 are about 7% larger for $M = 4\frac{1}{2}$, about 19% smaller for $M = 6\frac{1}{2}$, and about 23% for $M = 8\frac{1}{2}$.
- The 84-percentile values for strike slip mechanism (upper part of Figure 28) calculated using the new NGA relationship (IMI07) are about 10 to 23% less than those calculated using the pre-NGA relationship at distances of 1, 10 and 30 km and for $5 < M < 6\frac{1}{2}$. For $M > 6.75$, the 84-percentile values for strike slip mechanism calculated using the new NGA relationship (IMI07) vary from about 11% smaller to about 8% larger than those calculated using the pre-NGA relationship at distances of 1, 10 and 30 km. At a distance of 100 km, the 84-percentile values calculated using IMI07 are about 10% larger for $M =$

$4\frac{1}{2}$, becoming essentially equal for $5 < M < 6\frac{1}{2}$, and varying from about 22% larger for $M = 6.75$ to about 13% smaller for $M = 8\frac{1}{2}$.

- The 84-percentile values calculated using the new NGA relationship (IMI07) are smaller than those calculated using the pre-NGA relationship for reverse mechanism (lower part of Figure 28) at essentially all distances and for all magnitudes. The decrease varies from about 20% to 31% at a distance of 1 km in the magnitude range of $4\frac{1}{2}$ to $6\frac{1}{2}$, and from about 15% to 17% for $M > 6.75$ at the same distance. At a distance of 100 km, the 84-percentile values calculated using IMI07 are about 6% smaller for $M = 4\frac{1}{2}$, about 14% smaller for $M = 6\frac{1}{2}$, and varying from about 4% larger for $M = 6.75$ to about 25% smaller for $M = 8$.

4.3 Comparison with other NGA Relationships

The median values of pga calculated using the NGA attenuation relationships derived by Abrahamson and Silva (2006), Boore and Atkinson (2006), Campbell and Bozorgnia (2006), Chiou and Youngs (2006), and Idriss (2007) are shown in Figure 29. The median values of spectral acceleration at a period of 1.0 sec, also calculated the same five relationships, are presented in Figure 30.

At a distance of 0.1 km, the median values of pga range from about 0.42 to 0.75g with an average value of about 0.55g. The range of the median values of pga at a distance of 1 km are about 0.42 to 0.68g, with an average value of about 0.52g. The corresponding values at distances of 10 km, 30 km and 100 km are: 0.26 to 0.33g with an average of 0.29g; 0.11 to 0.16g with an average of 0.13g; and 0.034 to 0.046g with an average of 0.041, respectively. Thus, the ratio of the maximum to the minimum value of calculated median pga at these distances ranges from about 1.3 to 1.8.

At a distance of 0.1 km, the median values of spectral acceleration at a period of 1.0 sec range from about 0.35 to 0.63g with an average value of about 0.49g. The range of the median values of spectral acceleration at a period of 1.0 sec, at a distance of 1 km, are about 0.35 to 0.58g, with an average value of about 0.46g. The corresponding values at distances of 10 km, 30 km and 100 km are: 0.21 to 0.33g with an average of 0.25g; 0.096 to 0.17g with an average of 0.12g; and 0.039 to 0.069g with an average of 0.048, respectively. Thus, the ratio of the maximum to the minimum value of calculated median spectral acceleration at a period of 1.0 sec at these distances ranges from about 1.6 to 1.8.

The relationship derived herein (i.e., IMI07) results in the largest values of pga at distances less than 30 km. The largest values of the median values of spectral acceleration at a period of 1.0 sec are obtained using IMI07 at all distances

Note that the values calculated using the relationships by the other NGA developers represented a site having an average shear wave velocity, v_{s30} , equal to 760 m/s, while the relationship derived herein is representative of sites having values ranging from 450 to 900 m/s, with the average being about 550 m/s. Use of 550 m/s in lieu of 760 m/s would have reduced the median values calculated using the other NGA relationships by about 5 to 15%. That approach is not recommended because the values calculated using IMI07 are essentially independent of v_{s30} in this range.

5.0 CONCLUDING REMARKS

The NGA research effort has added considerably to the quantity and quality of the data available for use in deriving empirically based models for estimating earthquake ground motions generated at various site conditions during crustal earthquakes.

This Volume presents a very simple model for estimating spectral ordinates for a number of period and for a relatively narrow range of average shear wave velocities, v_{s30} . The spectral values appear to be little affected by v_{s30} in this range and the model included in this Volume can be considered to be applicable for the full range (i.e., $v_{s30} = 450$ to 900 m/s).

The efforts completed to date for site with values of v_{s30} less than 450 m/sec are affected by and a different model is being developed to accommodate these effects. The results will be included in Volume 2.

6.0 REFERENCES

1. Abrahamson, N. A. and Silva, W. J. (1997) "Empirical response spectral attenuation relations for shallow crustal earthquakes", *Seismological Research Letters*, vol 68, No. 1, pp 94-109.
2. Boore, D. M, and Atkinson, G. M. (2006) "Boore-Atkinson NGA empirical ground motion model for the average horizontal component of PGA, PGV, and SA at spectral periods of 0.1, 0.2, 1, 2, and 3 seconds", Interim Report for USGS Review, October.
3. Campbell, K. W. and Bozorgnia, Y. (2006) "Campbell-Bozorgnia NGA empirical ground motion model for the average horizontal components of PGA, PGV, and SA at selected spectral periods ranging from 0.01 - 10.0 seconds", Interim Report for USGS Review, October, 2006.
4. Chiou, B. S-J., and Youngs, R. R. (2006) "Chiou and Youngs PEER-NGA empirical ground motion model for the average horizontal component of peak acceleration and pseudo spectral acceleration for spectral periods of 0.01 to 10 seconds", Interim Report for USGS Review, July, 2006.
5. Draper, N. R. and Smith, H. (1998) *Applied Regression Analysis*, Third Edition, John Wiley & Sons, Inc., New York.
6. Hauksson, Egill, Kate Hutton, Lucy Jones and Doug Given (2001) "M5.1 Anza Earthquake of October 30, 2001", Preliminary Report from: Southern California Seismic Network/TriNet, Posted on October 31, 2001 at 15:27:16.
7. URL: <http://pasadena.wr.usgs.gov/eqinthenews/ci9718013/reports/2.html>
8. Pantosti, D., Schwartz, D. P. and Valensise, G. (1993) "Paleo-seismology along the 1980 surface rupture of the Irpinia fault: Implications for earthquake recurrence in the southern Apennines, Italy", *Journal of Geophysical Research*, Vol. 98, No. B4, pp 6561–6578.
9. U.S. Geological Survey Fact Sheet 014-03 "Rupture in South-Central Alaska—The Denali Fault Earthquake of 2002; accessed at <http://pubs.usgs.gov/fs/2003/fs014-03/>

7.0 ACKNOWLEDGEMENTS

This project was sponsored by the Pacific Earthquake Engineering Research Center's Program of Applied Earthquake Engineering Research of Lifeline Systems supported by the California Energy Commission, California Department of Transportation, and the Pacific Gas & Electric Company. The author is grateful for the support provided by this program. His interactions with the other developers, Drs. N. Abrahamson, G. Atkinson, D. Boore, Y. Bozorgnia, K. Campbell, B. Chiou, W. Silva and R. Youngs, have been most invigorating and intellectually satisfying. Mr. Maurice Power of Geomatrix, the Project Manager, deserves a great deal of our thanks for all his efforts in keeping the project on tract. The input of and the discussions with Dr. P. Spudich and ...(names to be added later) are also gratefully acknowledged.

TABLE 1
FREE-FIELD NGA FLATFILE EARTHQUAKE GROUND MOTIONS AT SITES HAVING AVERAGE SHEAR
WAVE VELOCITIES RANGING FROM 450 TO 900 M/S

Earthquake ID	Earthquake Name	Year	Moment Magnitude	Mechanism	Number of Stations	Shear Wave Velocity, V_{s30} (m/s)		Closest Distance (km)	
						Minimum	Maximum	Minimum	Maximum
0170	Big Bear City	2003	4.9	0	6	453	685	32.5	118.6
0166	Gilroy	2002	4.9	0	10	478	730	8.6	130.1
0168	Nenana Mountain, Alaska	2002	6.7	0	1	660	660	199.3	199.3
0161	Big Bear-02	2001	4.5	0	4	488	685	24.8	40.6
0160	Yountville	2000	5.0	0	3	642	713	46.9	62.9
0173	Chi-Chi, Taiwan-04	1999	6.2	0	90	455	845	6.2	172.8
0138	Duzce, Turkey	1999	7.1	0	7	471	782	8.0	131.5
0158	Hector Mine	1999	7.1	0	12	453	725	11.7	196.8
0136	Kocaeli, Turkey	1999	7.5	0	6	523	811	7.2	165.0
0129	Kobe, Japan	1995	6.9	0	5	609	609	7.1	119.6
0147	Northridge-02	1994	6.1	0	4	450	602	8.8	42.1
0148	Northridge-03	1994	5.2	0	3	450	822	21.1	44.5
0126	Big Bear-01	1992	6.5	0	5	623	822	35.2	95.6
0125	Landers	1992	7.3	0	3	685	685	2.2	50.9
0145	Sierra Madre	1991	5.6	0	1	822	822	10.4	10.4
0144	Manjil, Iran	1990	7.4	0	1	724	724	12.6	12.6
0143	Upland	1990	5.6	0	1	660	660	71.8	71.8
0110	Baja California	1987	5.5	0	1	660	660	4.5	4.5
0098	Hollister-04	1986	5.5	0	1	685	685	12.2	12.2
0108	San Salvador	1986	5.8	0	1	545	545	6.3	6.3
0090	Morgan Hill	1984	6.2	0	5	462	730	3.3	45.5
0085	Coalinga-08	1983	5.2	0	1	617	617	18.3	18.3
0070	Irpinia, Italy-03	1981	4.7	0	1	660	660	13.7	13.7
0055	Anza (Horse Canyon)-01	1980	5.2	0	2	685	725	12.7	17.4
0053	Livermore-01	1980	5.8	0	1	517	517	30.5	30.5

TABLE 1 (Cont'd)

Earthquake ID	Earthquake Name	Year	Moment Magnitude	Mechanism	Number of Stations	Shear Wave Velocity, V_{s30} (m/s)		Closest Distance (km)	
						Minimum	Maximum	Minimum	Maximum
0054	Livermore-02	1980	5.4	0	2	517	713	14.1	30.0
0065	Mammoth Lakes-09	1980	4.9	0	1	685	685	9.2	9.2
0064	Victoria, Mexico	1980	6.3	0	1	660	660	14.4	14.4
0048	Coyote Lake	1979	5.7	0	1	663	663	3.1	10.7
0050	Imperial Valley-06	1979	6.5	0	1	660	660	15.2	15.2
0049	Norcia, Italy	1979	5.9	0	1	660	660	4.6	4.6
0044	Izmir, Turkey	1977	5.3	0	1	660	660	3.2	3.2
0041	Gazli, USSR	1976	6.8	0	1	660	660	5.5	5.5
0140	Sitka, Alaska	1972	7.7	0	2	660	660	34.6	106.7
0025	Parkfield	1966	6.2	0	1	528	528	16.0	16.0
0130	Kozani, Greece-01	1995	6.4	1	2	660	660	19.5	74.1
0152	Little Skull Mtn, NV	1992	5.65	1	3	660	660	24.7	100.2
0122	Roermond, Netherlands	1992	5.3	1	3	660	660	57.1	101.3
0091	Lazio-Abruzzo, Italy	1984	5.8	1	1	660	660	18.9	18.9
0088	Borah Peak, ID-02	1983	5.1	1	2	660	660	22.3	49.0
0068	Irpinia, Italy-01	1980	6.9	1	9	460	660	8.8	64.4
0047	Dursunbey, Turkey	1979	5.34	1	1	660	660	9.2	9.2
0036	Oroville-01	1975	5.89	1	1	623	623	8.0	8.0
0039	Oroville-03	1975	4.7	1	2	478	623	6.1	7.6
0171	Chi-Chi, Taiwan-02	1999	5.9	2	123	455	845	7.7	147.1
0172	Chi-Chi, Taiwan-03	1999	6.2	2	102	455	845	9.3	139.1
0174	Chi-Chi, Taiwan-05	1999	6.2	2	127	455	845	32.3	186.2
0175	Chi-Chi, Taiwan-06	1999	6.3	2	113	455	845	13.0	139.8
0127	Northridge-01	1994	6.7	2	28	450	822	5.4	80.0
0151	Northridge-06	1994	5.3	2	12	450	822	14.7	82.6
0123	Cape Mendocino	1992	7.01	2	4	457	713	7.0	28.8

TABLE 1 (Cont'd)

Earthquake ID	Earthquake Name	Year	Moment Magnitude	Mechanism	Number of Stations	Shear Wave Velocity, V_{s30} (m/s)		Closest Distance (km)	
						Minimum	Maximum	Minimum	Maximum
0097	Nahanni, Canada	1985	6.76	2	3	660	660	4.9	9.6
0076	Coalinga-01	1983	6.36	2	1	685	685	27.5	27.5
0077	Coalinga-02	1983	5.09	2	1	617	617	19.9	19.9
0078	Coalinga-03	1983	5.38	2	1	617	617	13.3	13.3
0079	Coalinga-04	1983	5.18	2	1	617	617	15.4	15.4
0080	Coalinga-05	1983	5.77	2	1	617	617	11.4	11.4
0081	Coalinga-06	1983	4.89	2	1	617	617	11.8	11.8
0082	Coalinga-07	1983	5.21	2	1	617	617	12.1	12.1
0046	Tabas, Iran	1978	7.35	2	2	660	767	2.1	13.9
0040	Friuli, Italy-01	1976	6.5	2	3	660	660	14.5	102.2
0030	San Fernando	1971	6.61	2	11	450	874	11.0	92.6
0020	San Francisco	1957	5.28	2	1	874	874	11.0	11.0
0137	Chi-Chi, Taiwan	1999	7.6	3	172	455	845	0.3	172.2
0149	Northridge-04	1994	5.93	3	1	450	450	24.8	24.8
0150	Northridge-05	1994	5.13	3	3	450	526	20.5	31.1
0118	Loma Prieta	1989	6.9	3	25	450	895	3.9	79.8
0113	Whittier Narrows-01	1987	6.0	3	10	450	822	14.7	72.2
0114	Whittier Narrows-02	1987	5.27	3	2	550	822	11.8	19.9
0101	N. Palm Springs	1986	6.06	3	6	685	685	17.0	54.8
0029	Lytle Creek	1970	5.33	3	5	450	813	12.4	103.6
0163	Anza-02	2001	4.92	4	14	488	845	16.9	101.1
0096	Drama, Greece	1985	5.2	4	1	660	660	43.4	43.4
0139	Stone Canyon	1972	4.81	4	1	478	478	12.0	12.0

TABLE 2
DERIVED PARAMETERS FOR EMPIRICAL MODEL USING EQUATION [1]

Period, T	Parameters for $M \leq 6^{3/4}$				Parameters for $M \geq 6^{3/4}$				$\gamma(T)$	$\varphi(T)$	SE Term
	$\alpha_1(T)$	$\alpha_2(T)$	$\beta_1(T)$	$\beta_2(T)$	$\alpha_1(T)$	$\alpha_2(T)$	$\beta_1(T)$	$\beta_2(T)$			
0.01	3.7113	-0.1252	2.9832	-0.2339	5.6362	-0.4104	2.9832	-0.2339	0.00047	0.12	0.66
0.02	3.7113	-0.1252	2.9832	-0.2339	5.6362	-0.4104	2.9832	-0.2339	0.00047	0.12	0.66
0.03	3.7613	-0.1252	2.9832	-0.2339	5.6862	-0.4104	2.9832	-0.2339	0.00047	0.12	0.66
0.04	3.8113	-0.1252	2.9832	-0.2339	5.7362	-0.4104	2.9832	-0.2339	0.00047	0.12	0.66
0.05											
0.06											
0.07											
0.075											
0.08											
0.09											
0.1											
0.12											
0.15											
0.17											
0.2	3.5006	-0.0319	2.8554	-0.2305	3.3005	-0.0023	2.4154	-0.1653	0.00006	0.12	0.72
0.25											
0.3											
0.35											
0.4											
0.45											
0.5											
0.6											
0.7											

TABLE 2 (Cont'd)

Period, T	Parameters for $M \leq 6^{3/4}$				Parameters for $M \geq 6^{3/4}$				$\gamma(T)$	$\phi(T)$	SE Term
	$\alpha_1(T)$	$\alpha_2(T)$	$\beta_1(T)$	$\beta_2(T)$	$\alpha_1(T)$	$\alpha_2(T)$	$\beta_1(T)$	$\beta_2(T)$			
0.75											
0.8											
0.9											
1	-2.1147	0.5707	2.6904	-0.2371	1.2135	0.0777	2.0933	-0.1487	0.00132	0.12	0.77
1.5											
2											
3	-6.2226	0.8805	2.6442	-0.2497	-2.2929	0.2992	1.8270	-0.1286	0.00023	0.08	0.83
4											
5											
6											
7											
8											
9											
10											

$$\ln[PAA(T)] = \alpha_1(T) + \alpha_2(T)M - [\beta_1(T) + \beta_2(T)M] \ln(R_{rup} + 10) + \gamma(T)R_{rup} + \phi(T)F \quad [1]$$

- PAA(T)** Pseudo absolute spectral acceleration for a single degree of freedom structure having a period T in seconds and a damping ratio of 5% – note that $PAA(T = 0.01) = pga$;
- M** Moment magnitude;
- R_{rup}** Closest distance to the rupture surface in km;
- $\gamma(T)$** "Distance" adjustment factor (partially accounts for anelastic attenuation);
- $\phi(T)$** Source mechanism (or style of faulting) factor;
- F** Refers to source mechanism designator with $F = 0$ for "strike slip/normal" events and $F = 1$ for "reverse" events; and

$\alpha_1(T)$, $\alpha_2(T)$, $\beta_1(T)$, and $\beta_2(T)$ are parameters obtained from the regression process

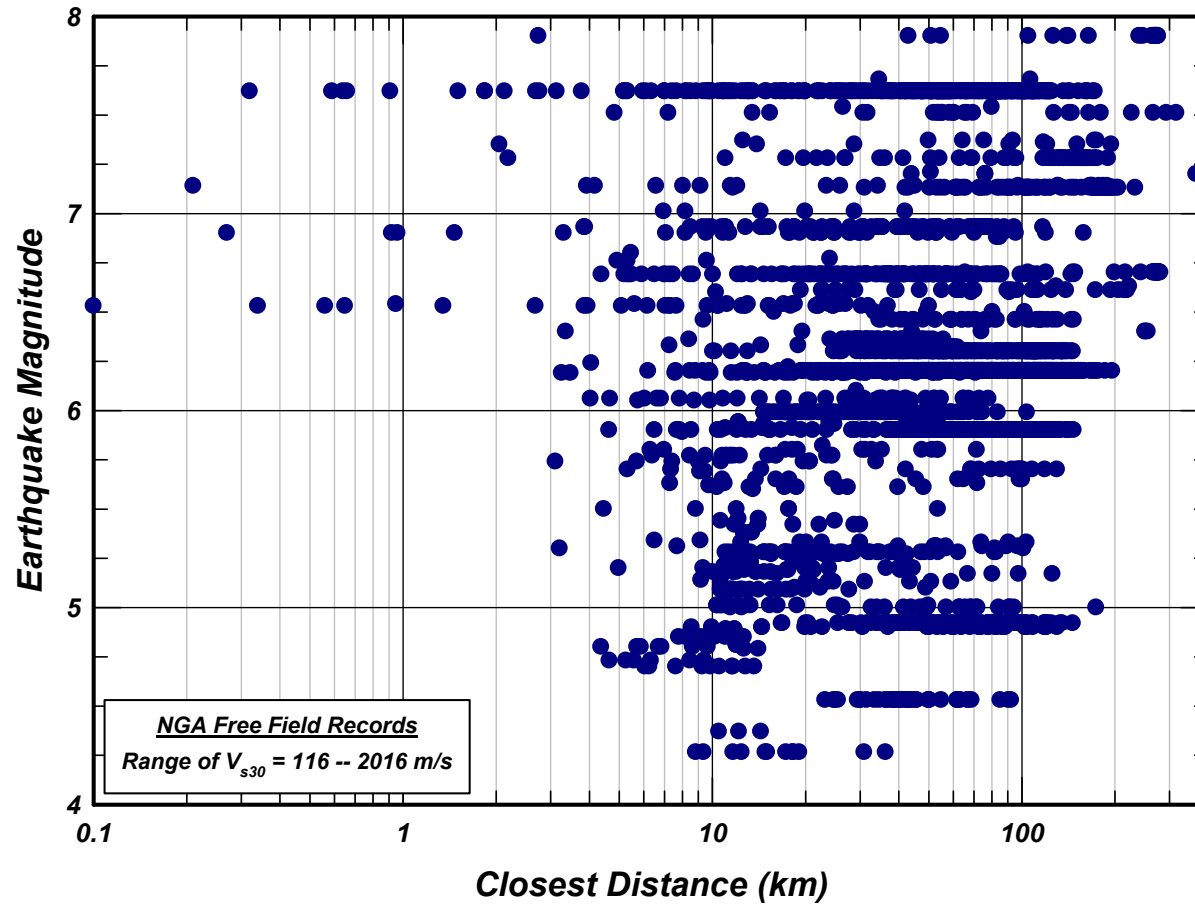


Figure 1 Magnitude-distance distribution of NGA free field records

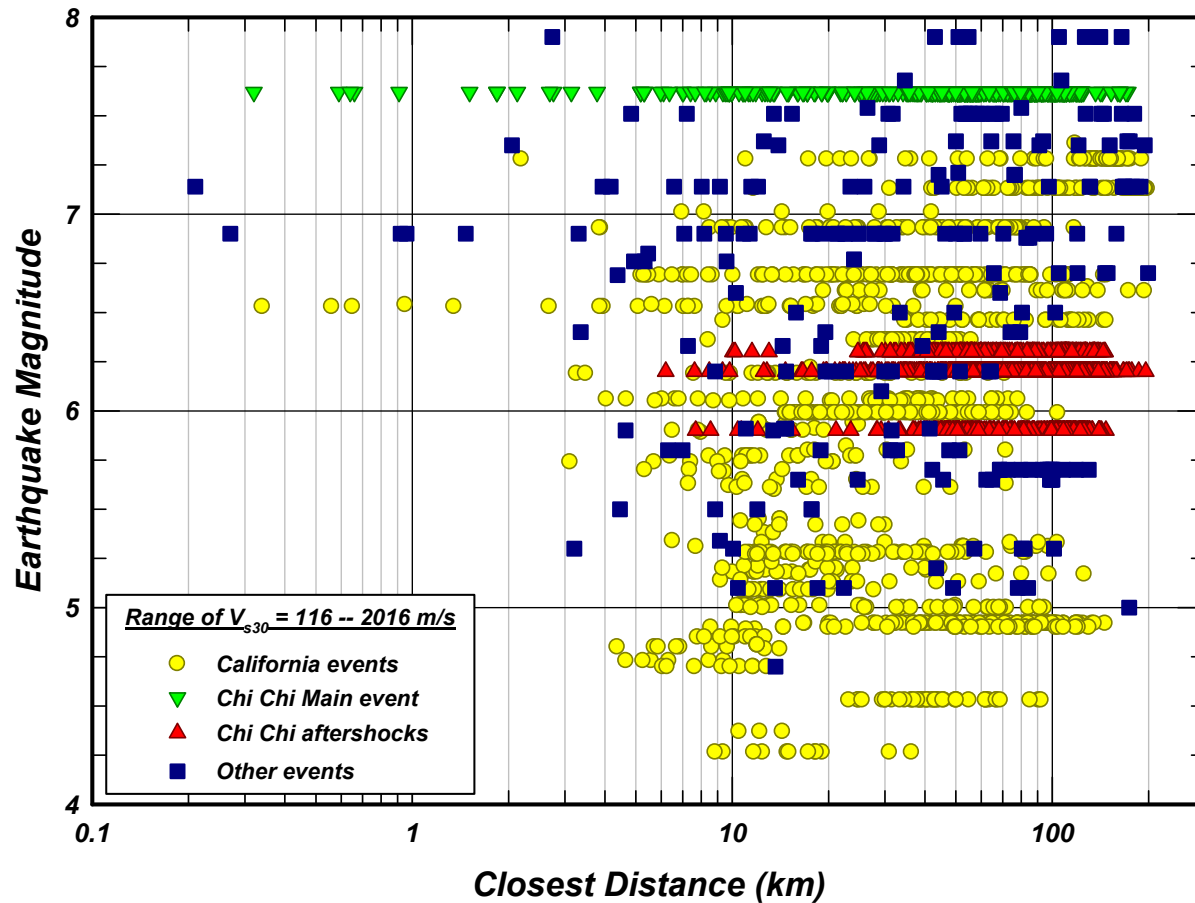


Figure 2 Magnitude-distance distribution of records selected for use this study

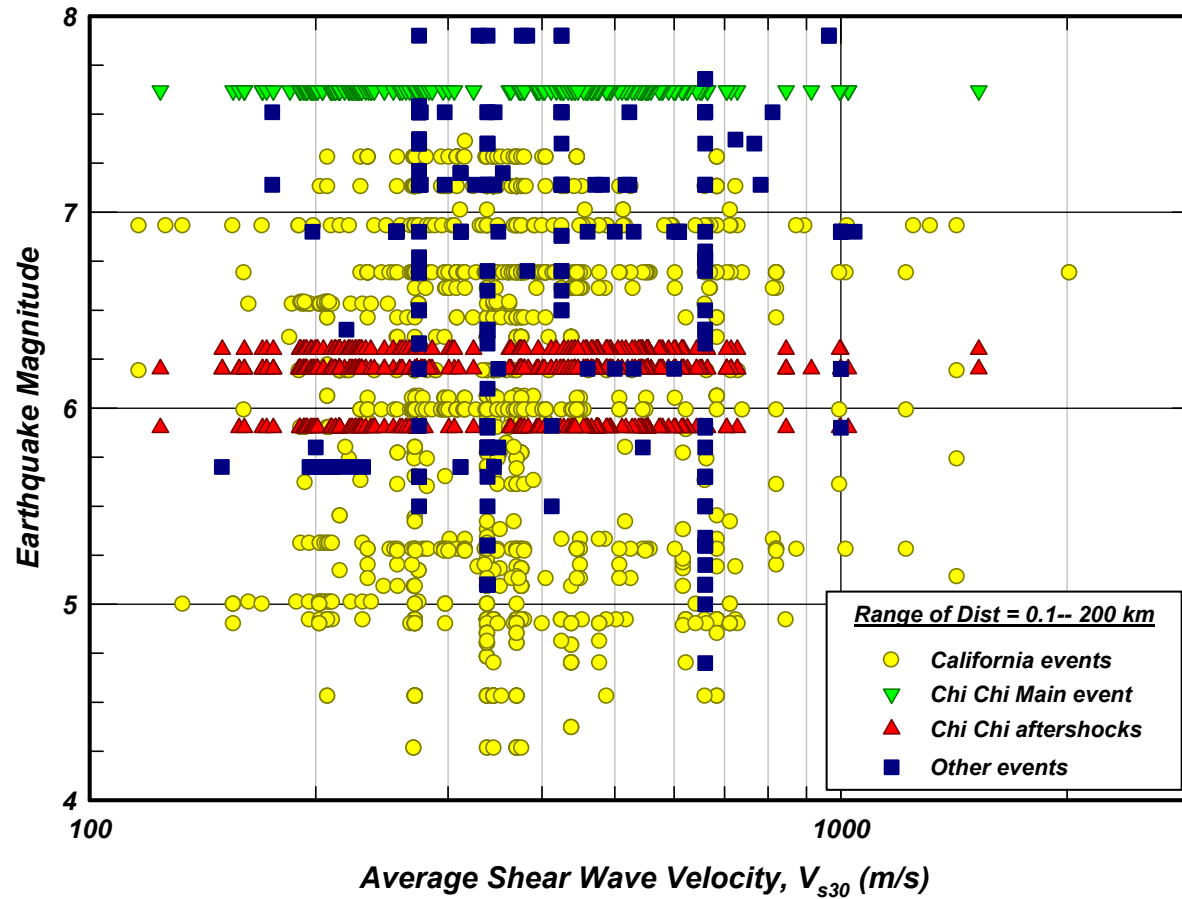


Figure 3 Magnitude- V_{s30} distribution of records selected for use this study

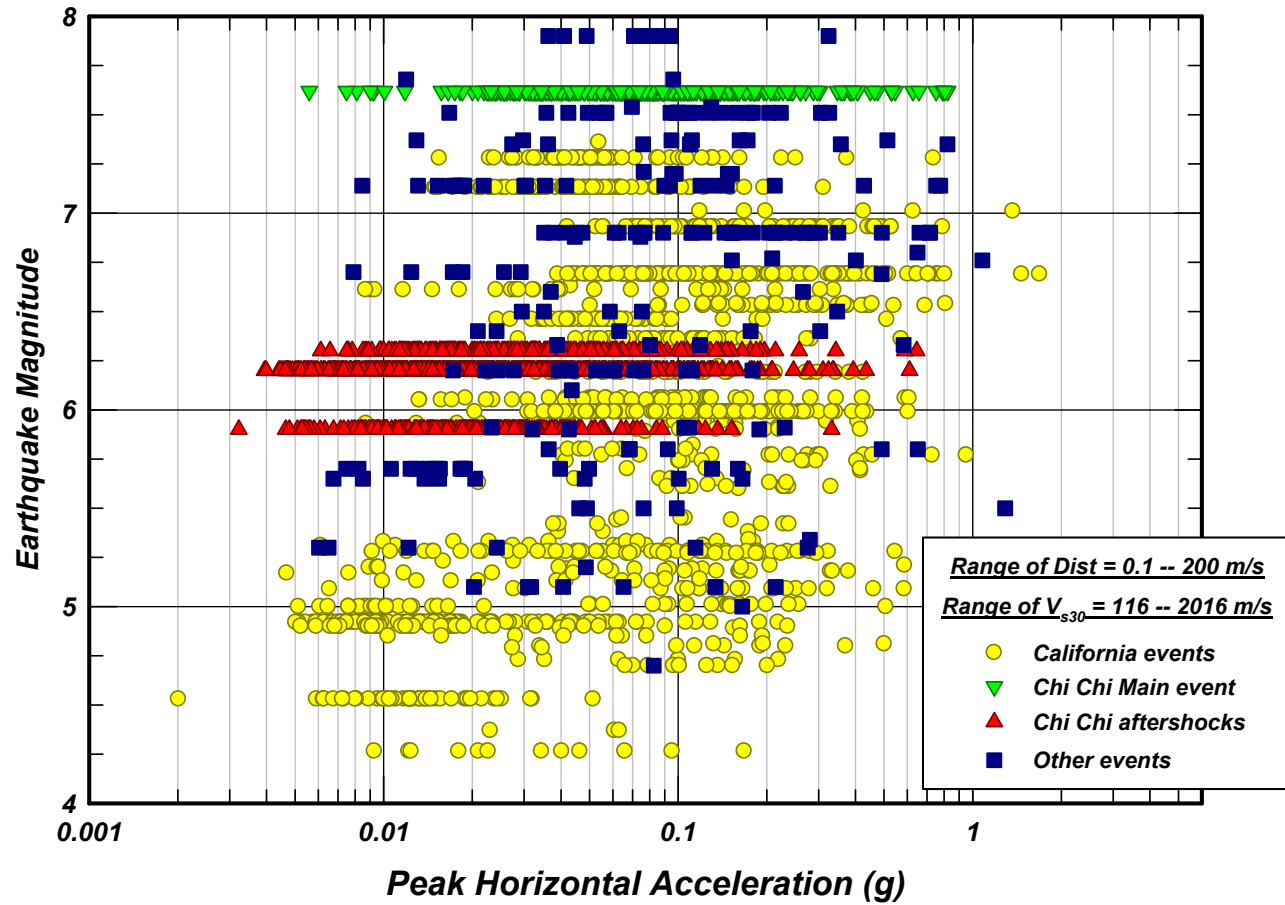


Figure 4 Magnitude-pga distribution of records selected for use this study

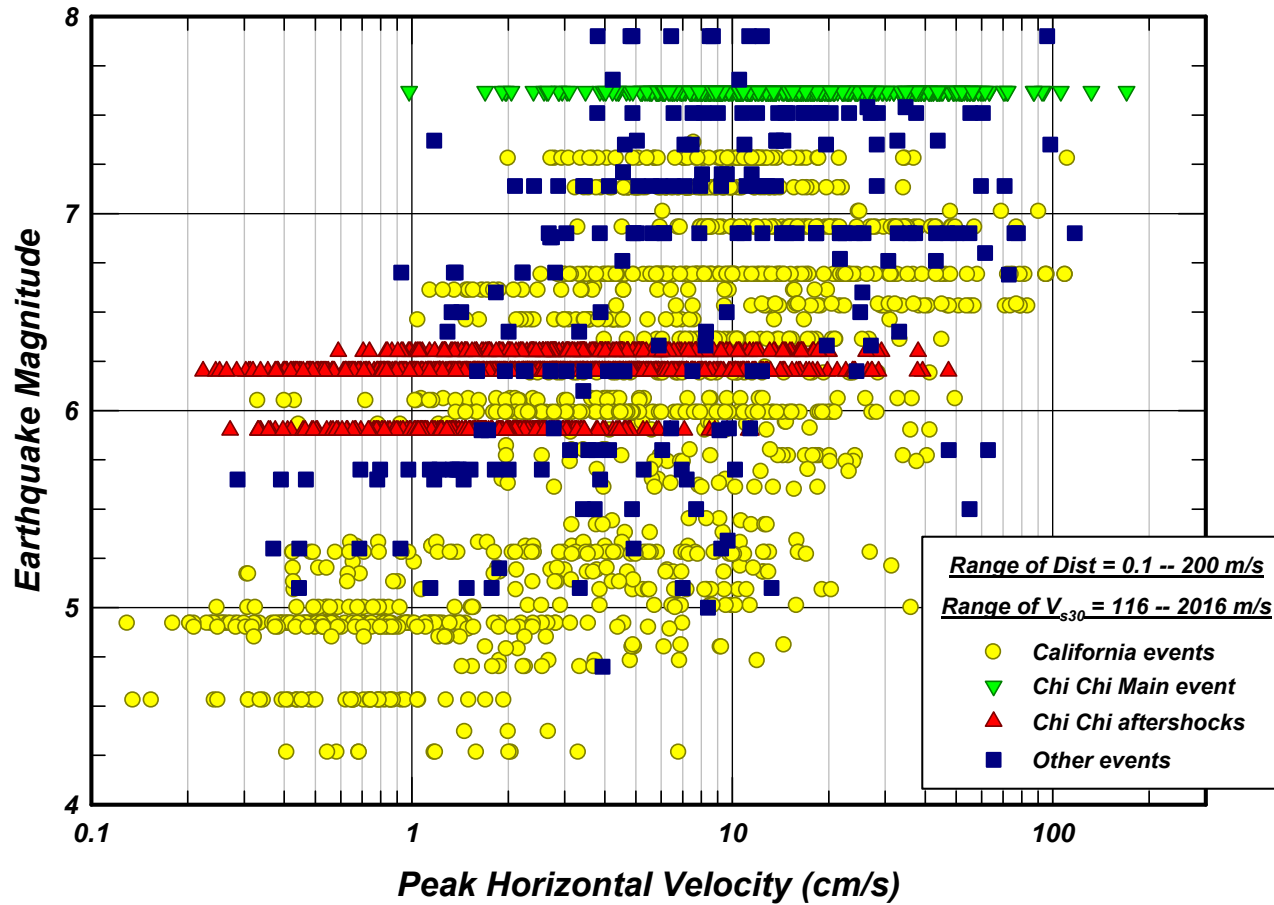


Figure 5 Magnitude-pgv distribution of records selected for use this study

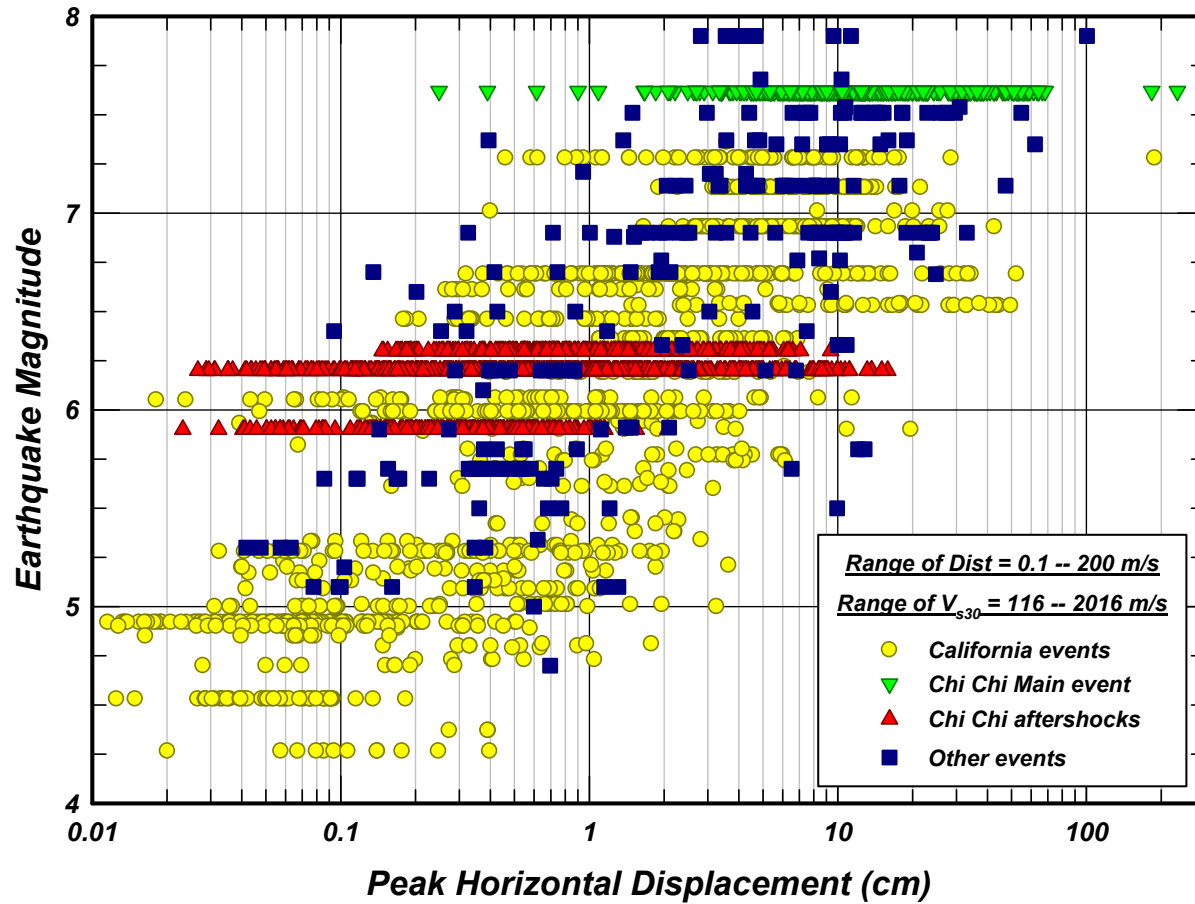


Figure 6 Magnitude-pgd distribution of records selected for use this study

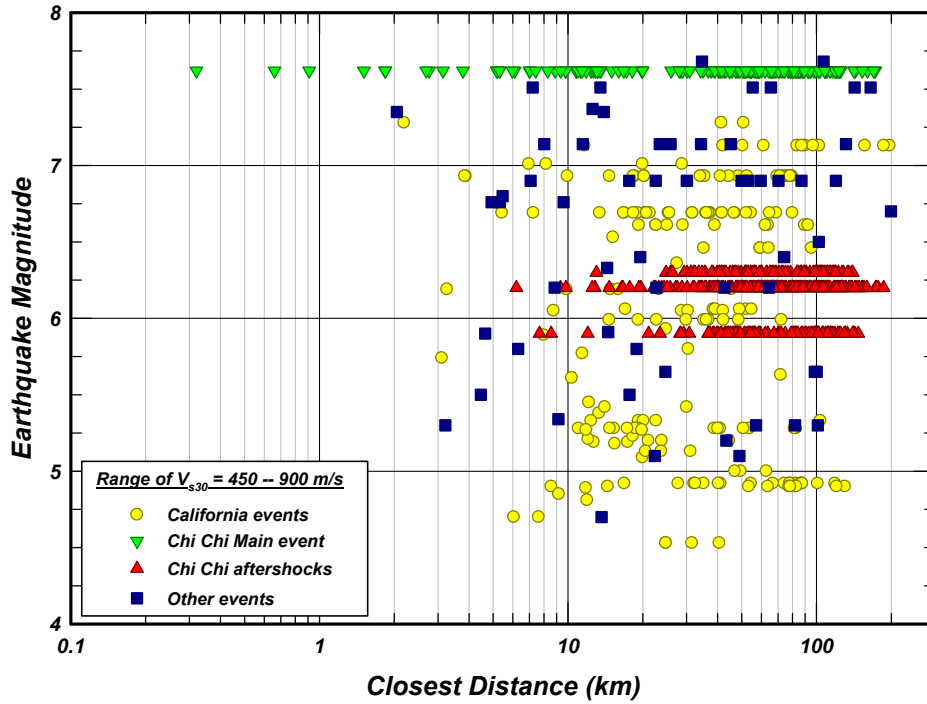


Figure 7 Magnitude- distance distribution of records used in deriving earthquake ground motion model for sites having V_{s30} ranging from 450 – 900 m/s

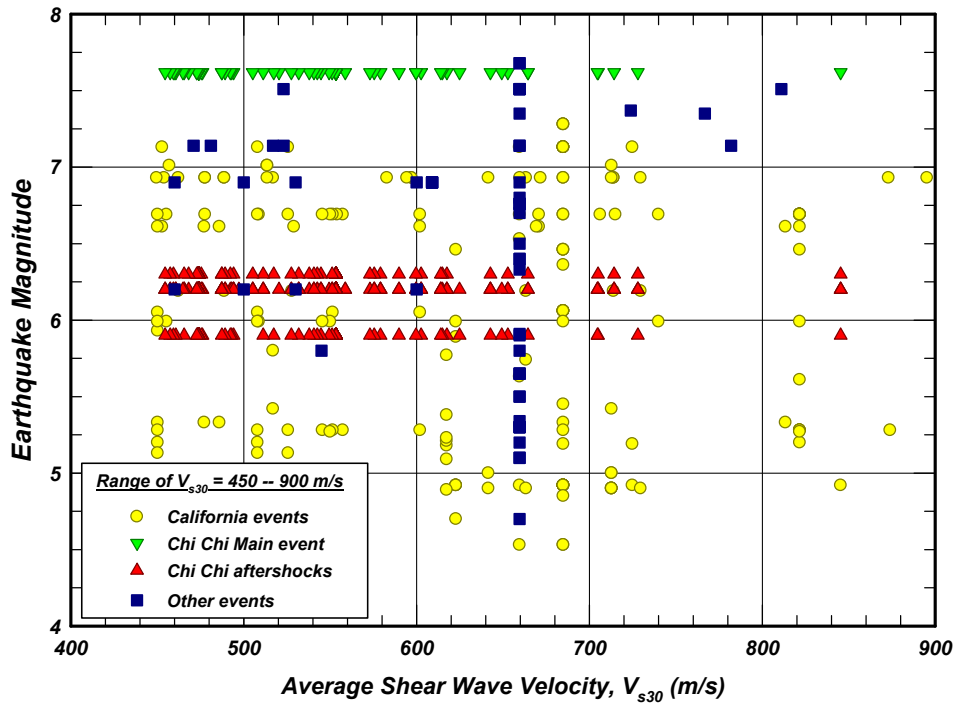


Figure 8 Magnitude- V_{s30} distribution of records used in deriving earthquake ground motions model for sites having V_{s30} ranging from 450 – 900 m/s

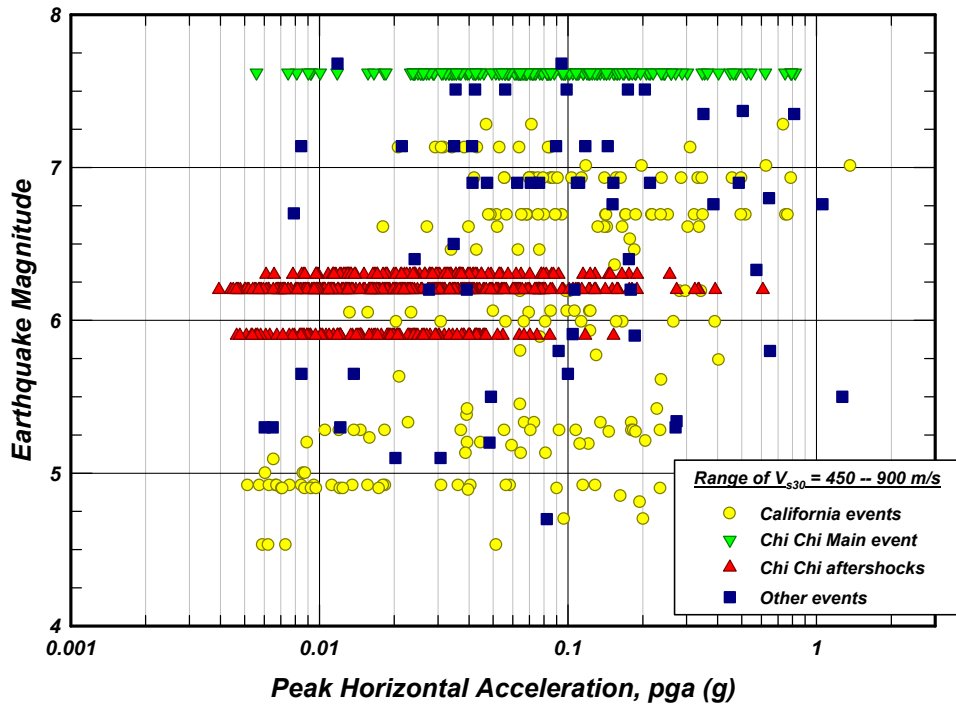


Figure 9 Magnitude-pga distribution of records used in deriving earthquake ground motions model for sites having V_{s30} ranging from 450 – 900 m/s

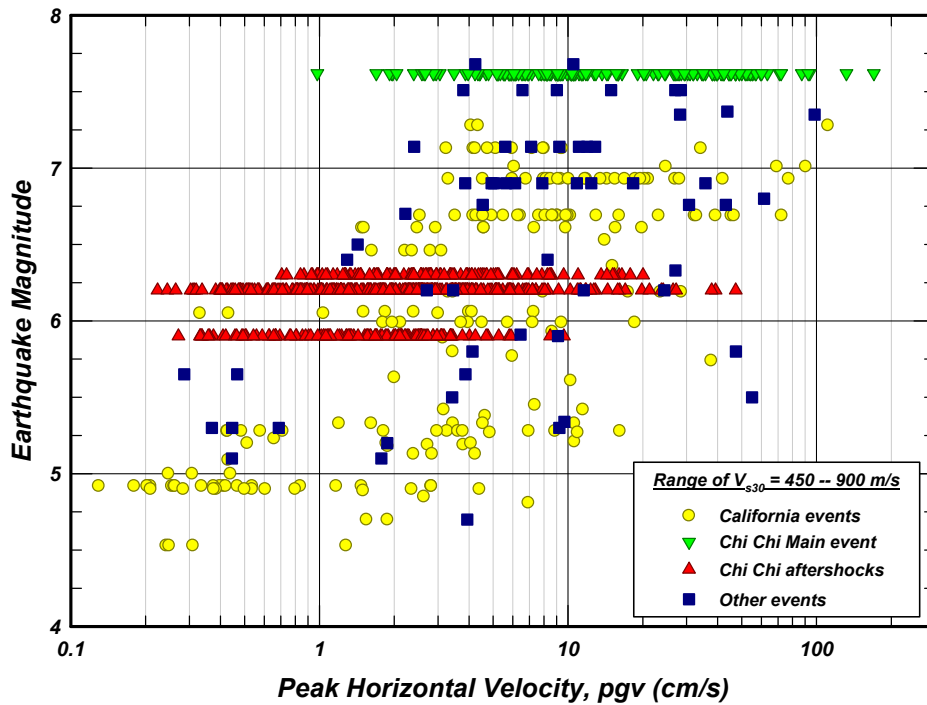


Figure 10 Magnitude-pgv distribution of records used in deriving earthquake ground motions model for sites having V_{s30} ranging from 450 – 900 m/s

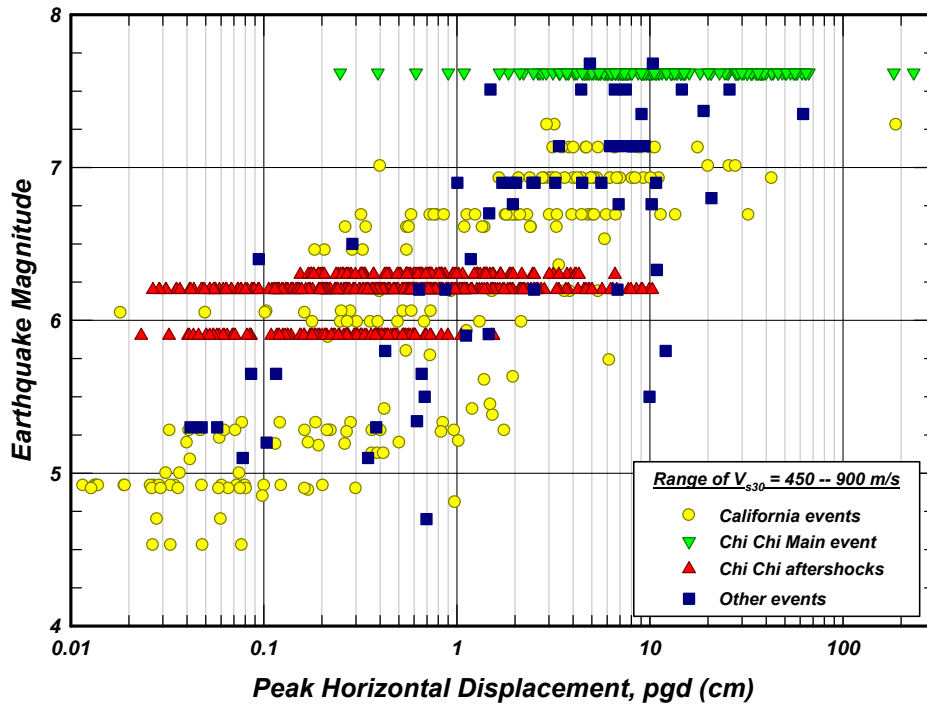


Figure 11 Magnitude-pgd distribution of records used in deriving earthquake ground motions model for sites having V_{s30} ranging from 450 – 900 m/s

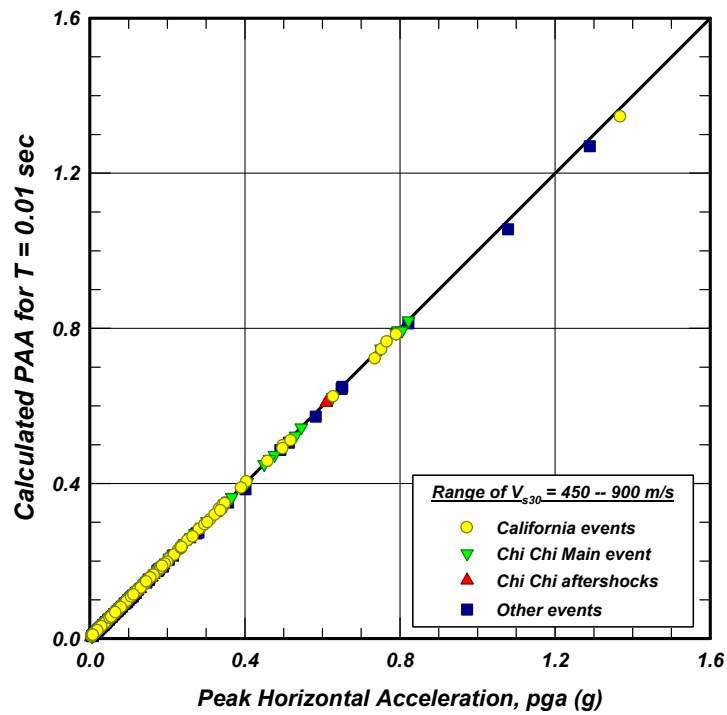


Figure 12 Calculated values of PAA for $T = 0.01 \text{ sec}$ versus pga

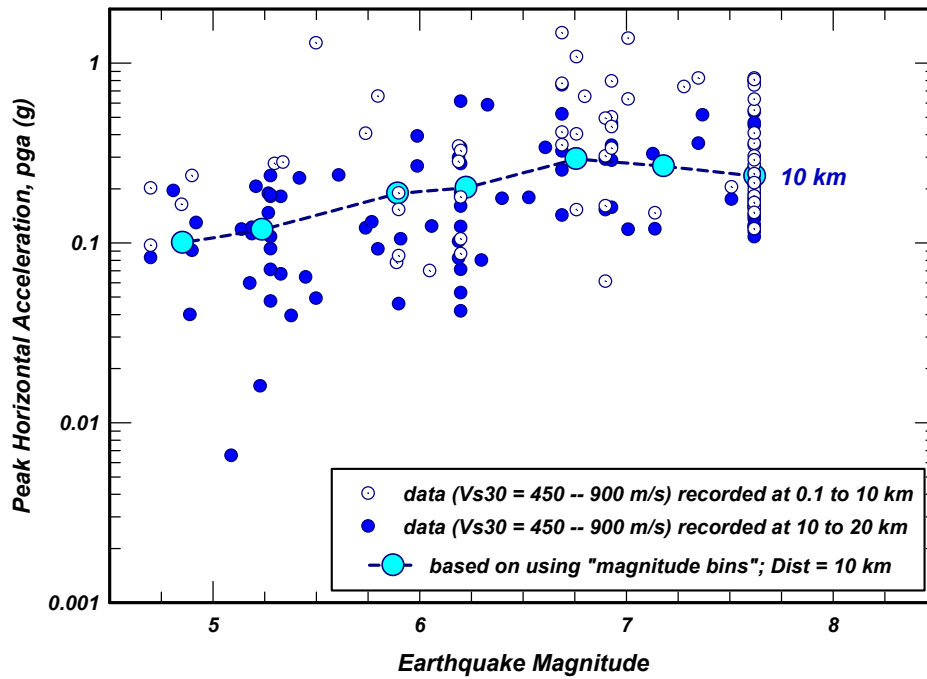


Figure 13 Comparison of recorded pga values at distances ranging from 0.1 to 20 km with those calculated at a distance of 10 km based on using magnitude bins for sites having V_{s30} ranging from 450 – 900 m/s

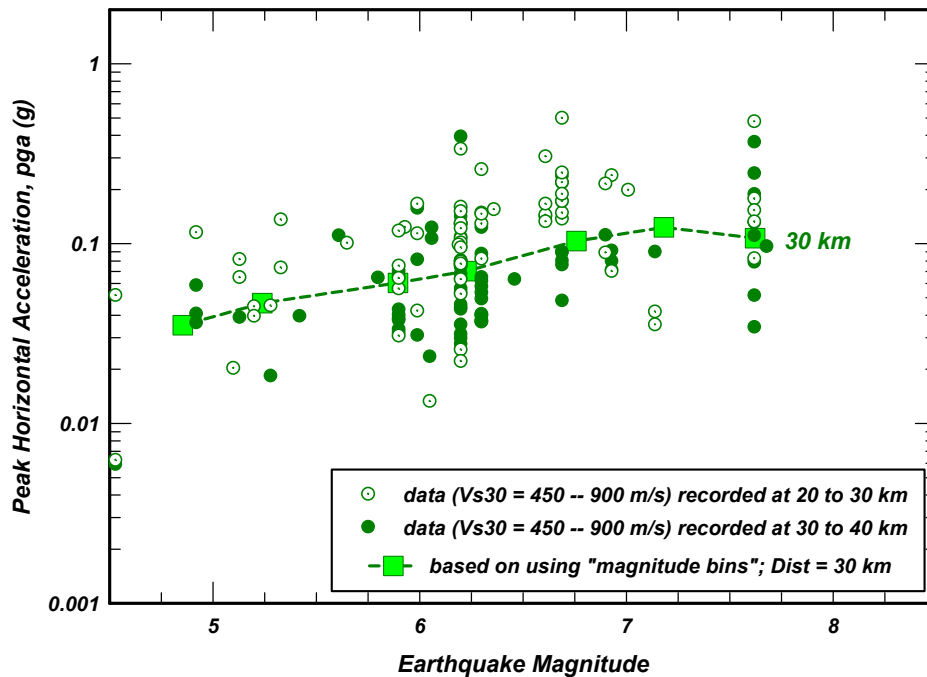


Figure 14 Comparison of recorded pga values at distances ranging from 20 to 40 km with those calculated at a distance of 30 km based on using magnitude bins for sites having V_{s30} ranging from 450 – 900 m/s

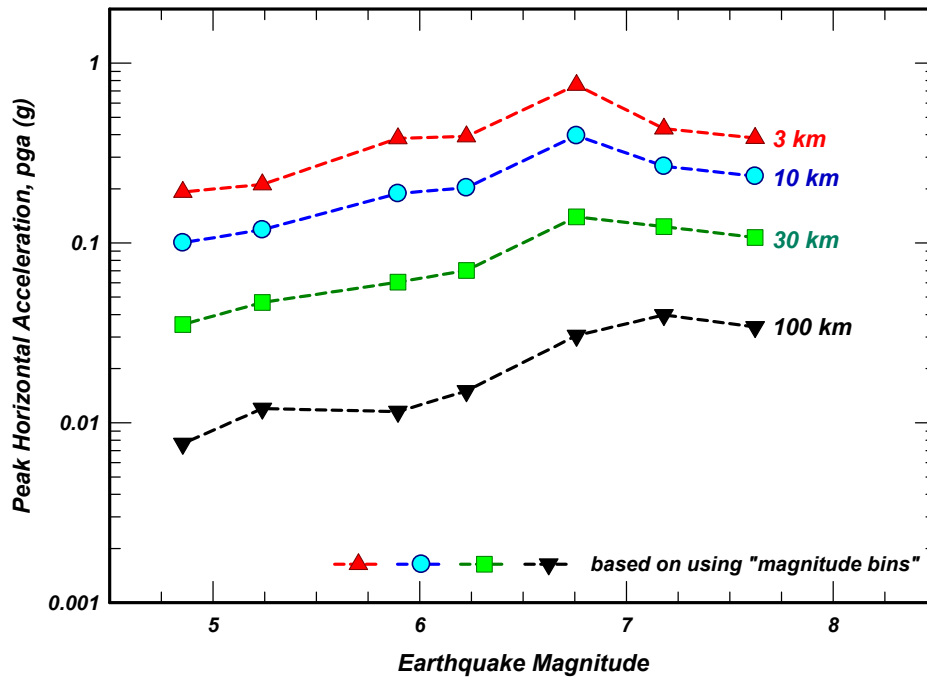


Figure 15 Calculated values of pga based on using magnitude bins for sites having V_{s30} ranging from 450 – 900 m/s

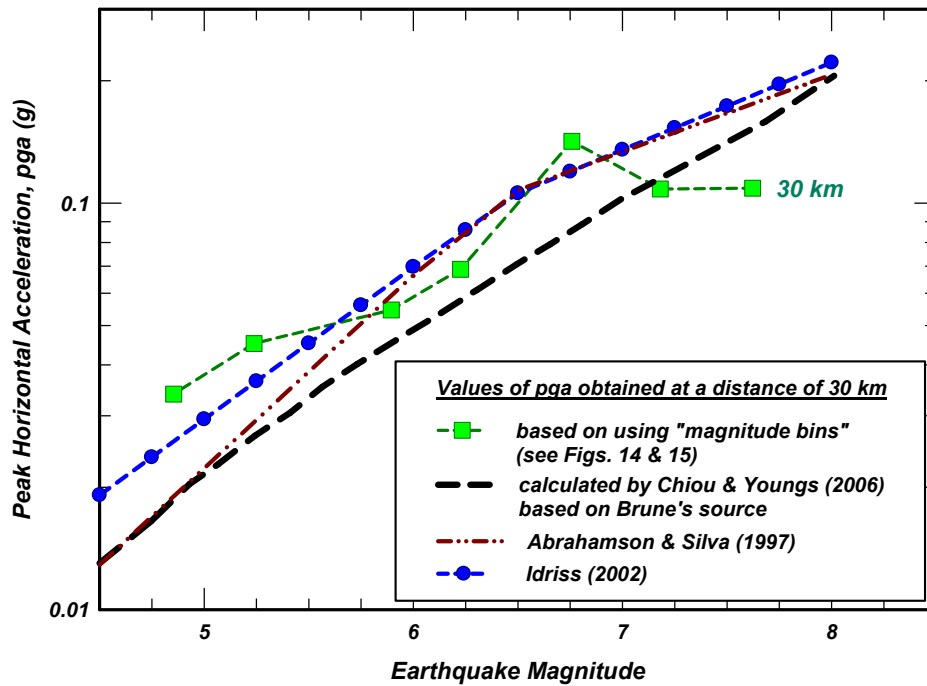


Figure 16 Values of pga versus magnitude at a distance of 30 km based on using a number of approaches

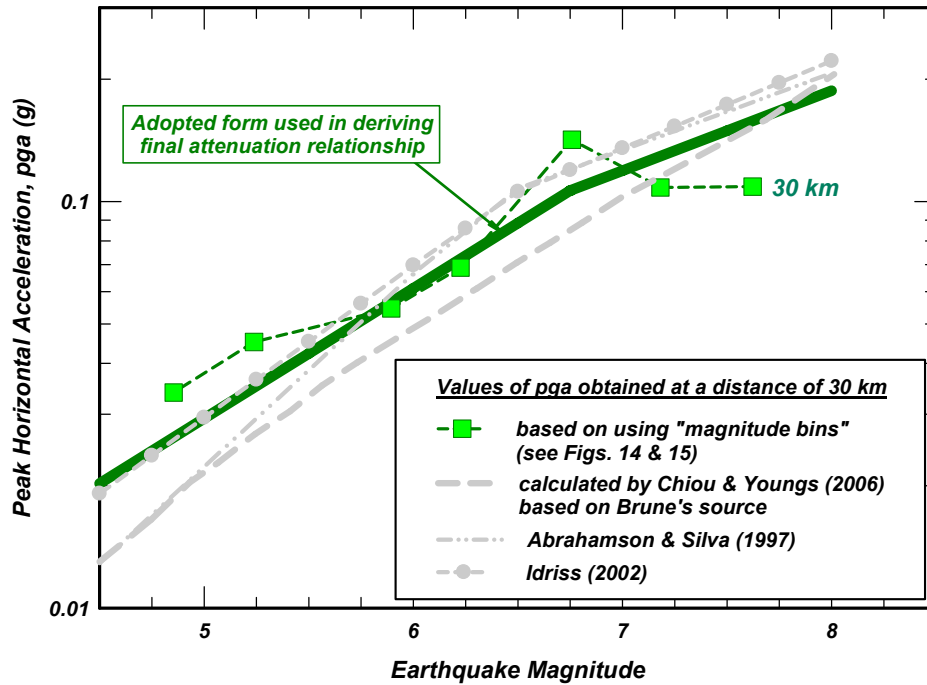


Figure 17 Adopted form used in deriving attenuation relationship

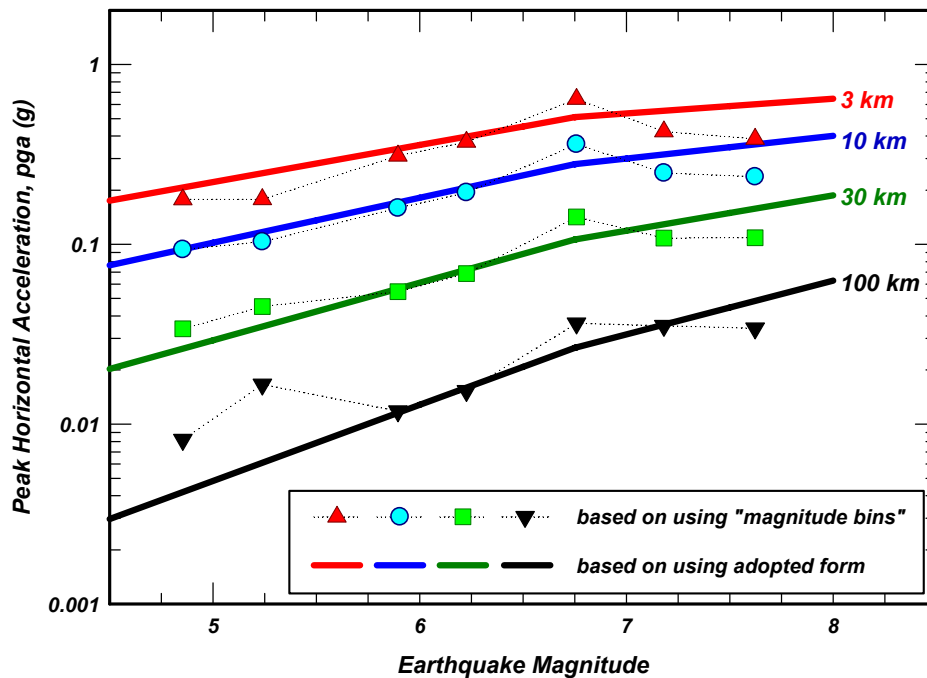


Figure 18 Comparison of calculated values of pga using adopted form with those calculated based on using magnitude bins for sites having V_{s30} ranging from 450 – 900 m/s

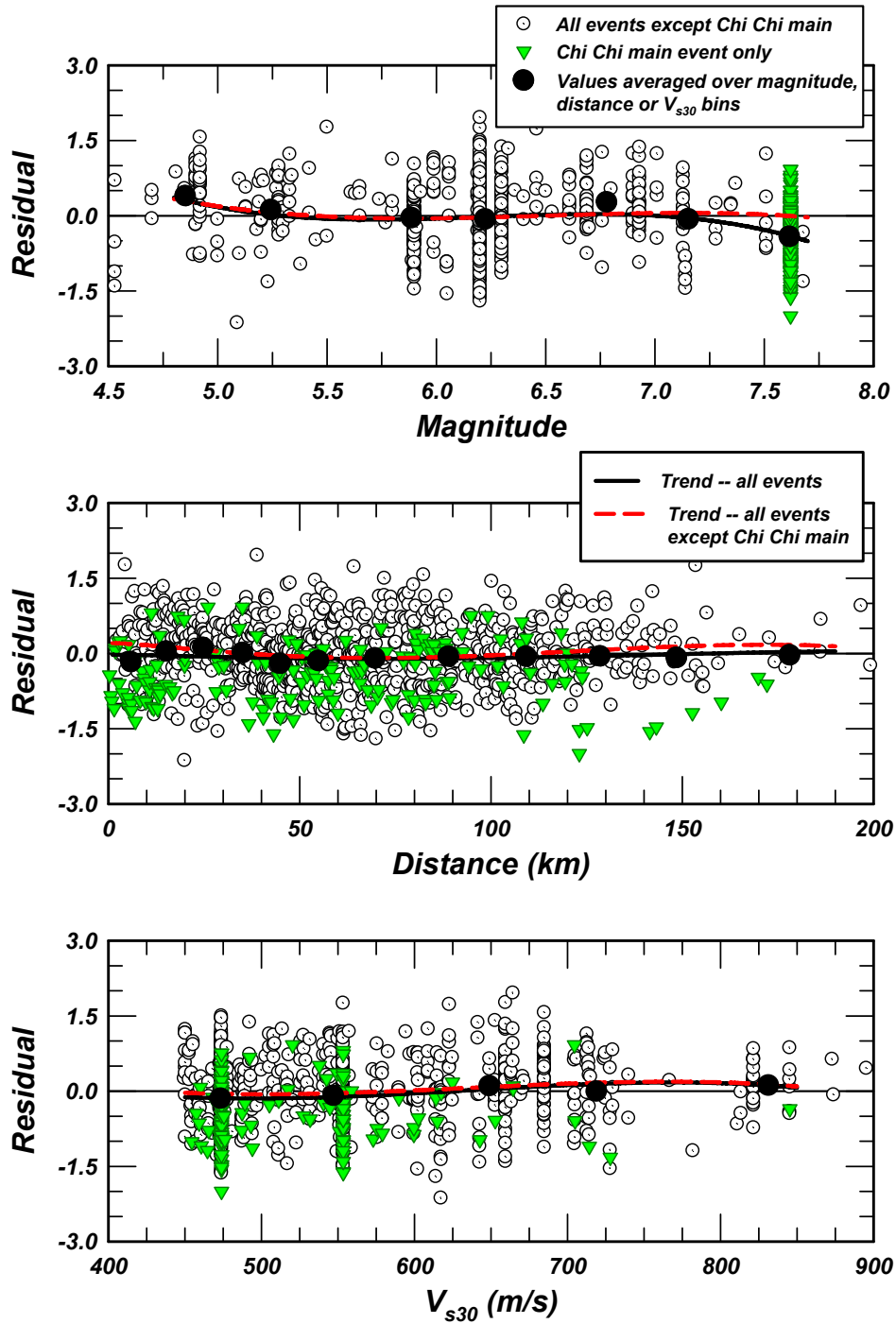


Figure 19 Residuals versus magnitude, closest distance and V_{s30} using the derived equation for estimating peak horizontal acceleration (pga)

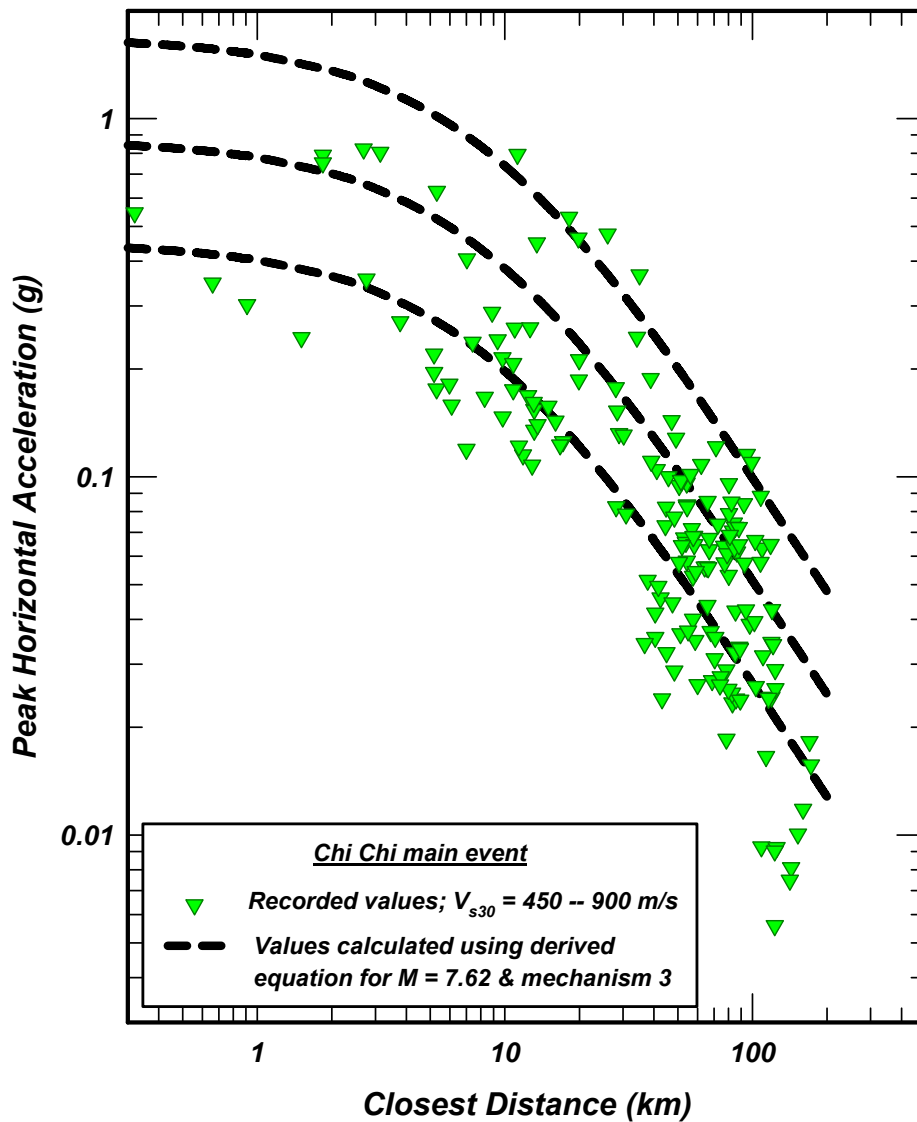


Figure 20 Comparison of peak horizontal accelerations recorded during the 1999 Chi-Chi earthquake with median, 16-percentile and 84-percentile values calculated using the derived equation for $M = 7.62$ & mechanism 3

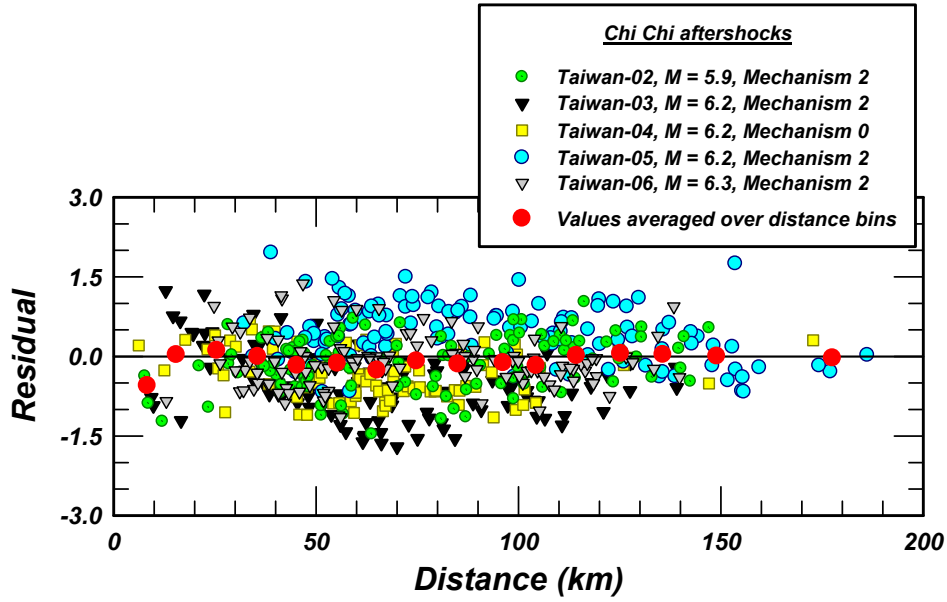


Figure 21 Residuals – peak horizontal acceleration recorded during the five Chi-Chi earthquake aftershocks obtained using the derived equation with magnitude and mechanism as shown in the legend

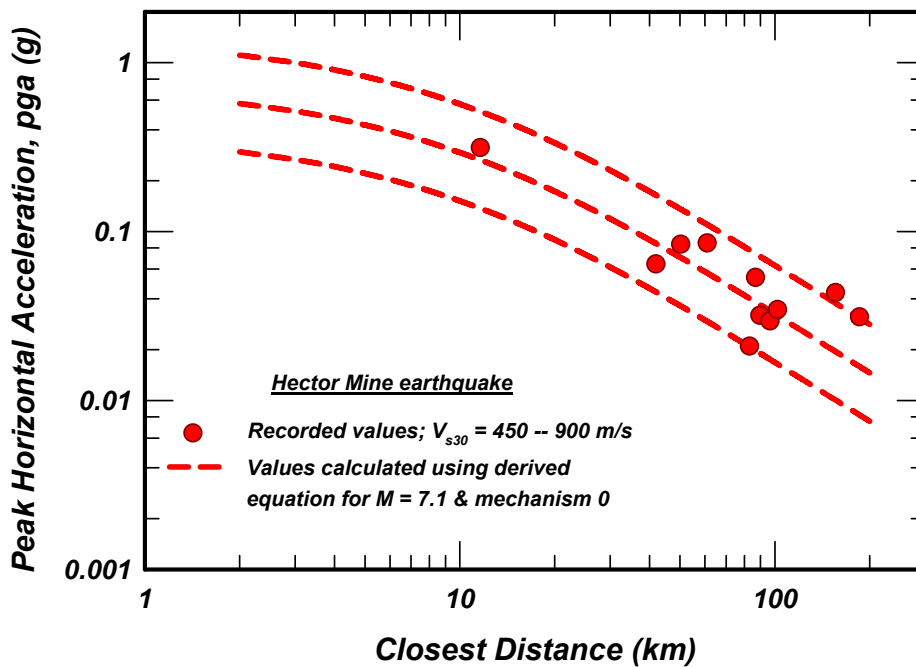


Figure 22 Comparison of peak horizontal accelerations recorded during the 1999 Hector Mine earthquake with median, 16-percentile and 84-percentile values calculated using the derived equation with $M = 7.1$ & mechanism 0

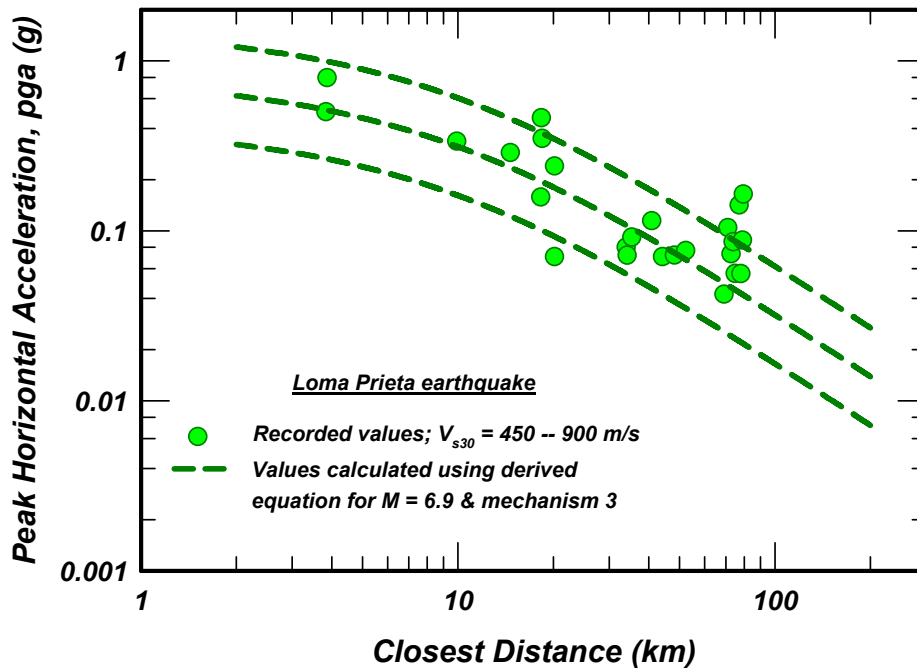


Figure 23 Comparison of peak horizontal accelerations recorded during the 1989 Loma Prieta earthquake with median, 16-percentile and 84-percentile values calculated using the derived equation with $M = 6.9$ & mechanism 3

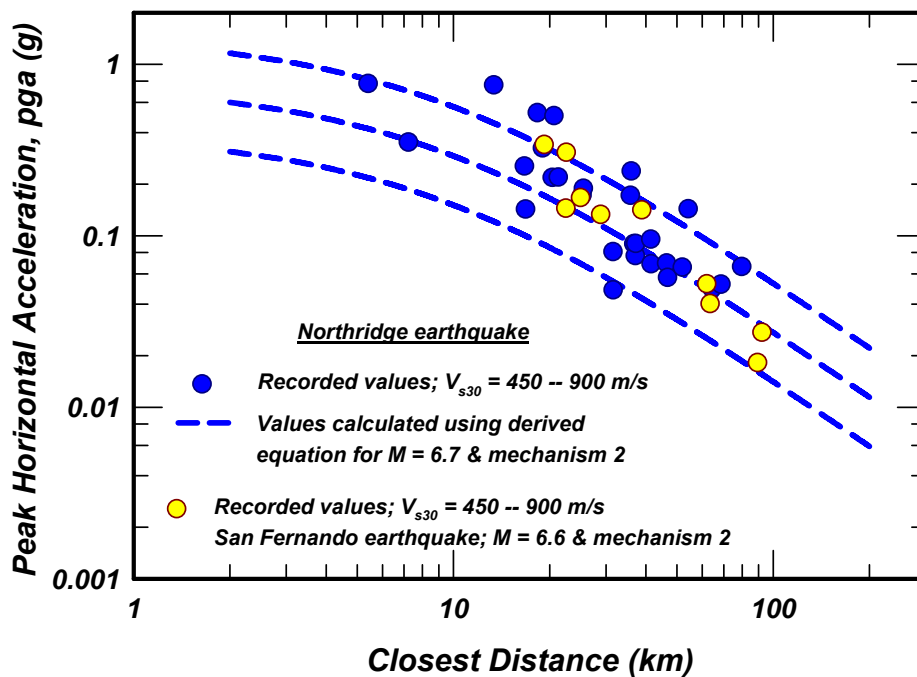


Figure 24 Comparison of peak horizontal accelerations recorded during the 1994 Northridge and the 1971 San Fernando earthquakes with median, 16-percentile and 84-percentile values calculated using the derived equation with $M = 6.7$ & mechanism 2

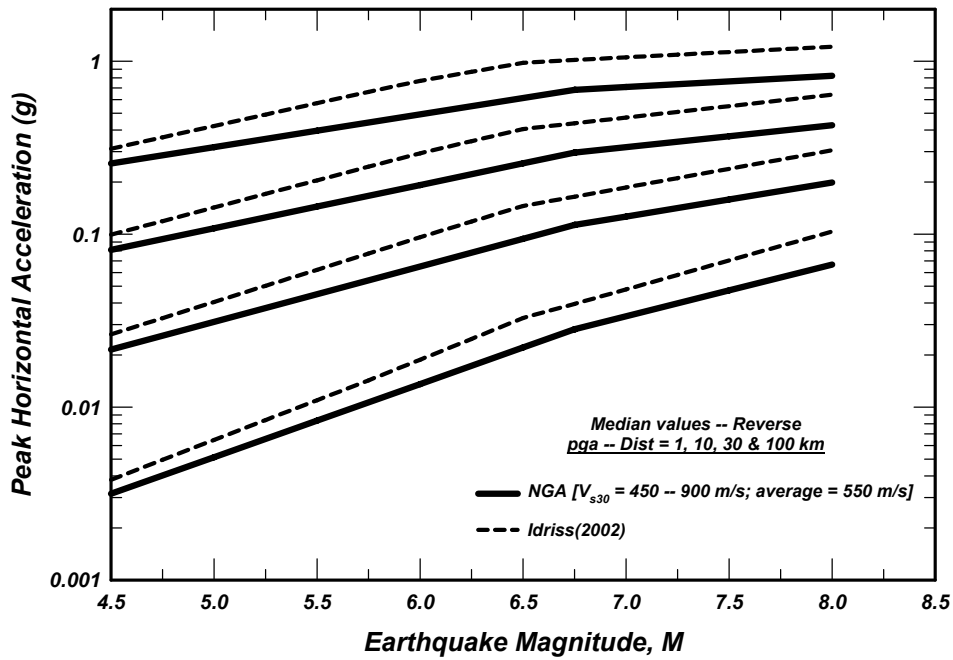
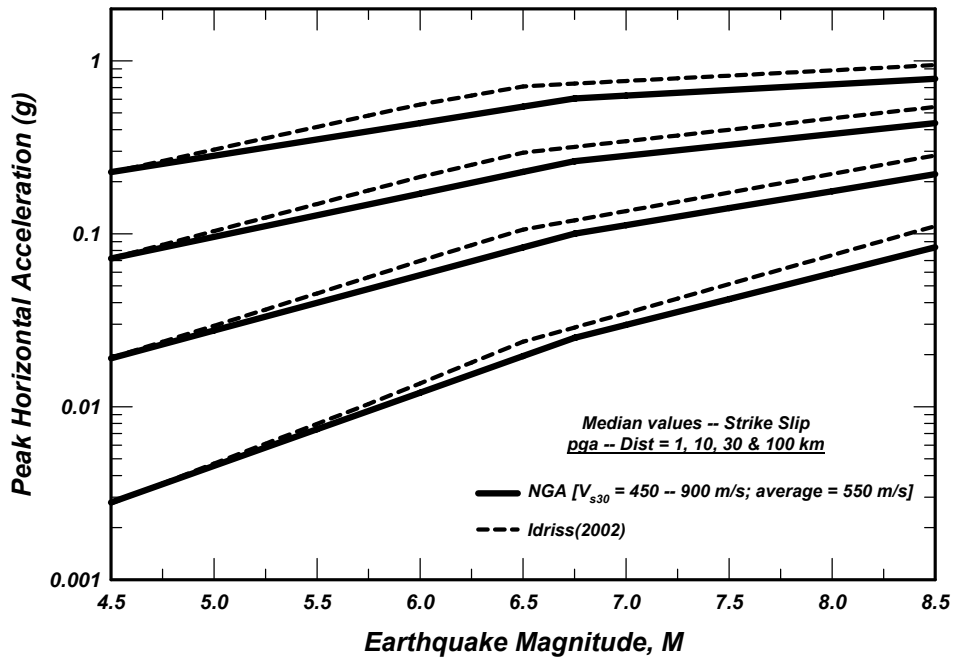


Figure 25 Comparison of median values of pga calculated using the new NGA relationship and the relationship by Idriss (2006)

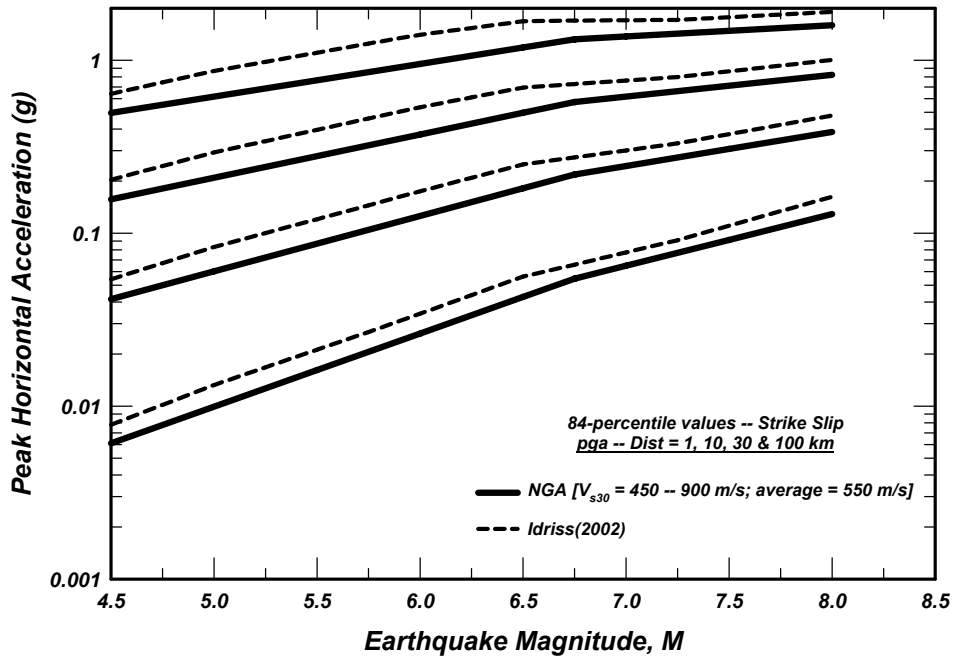
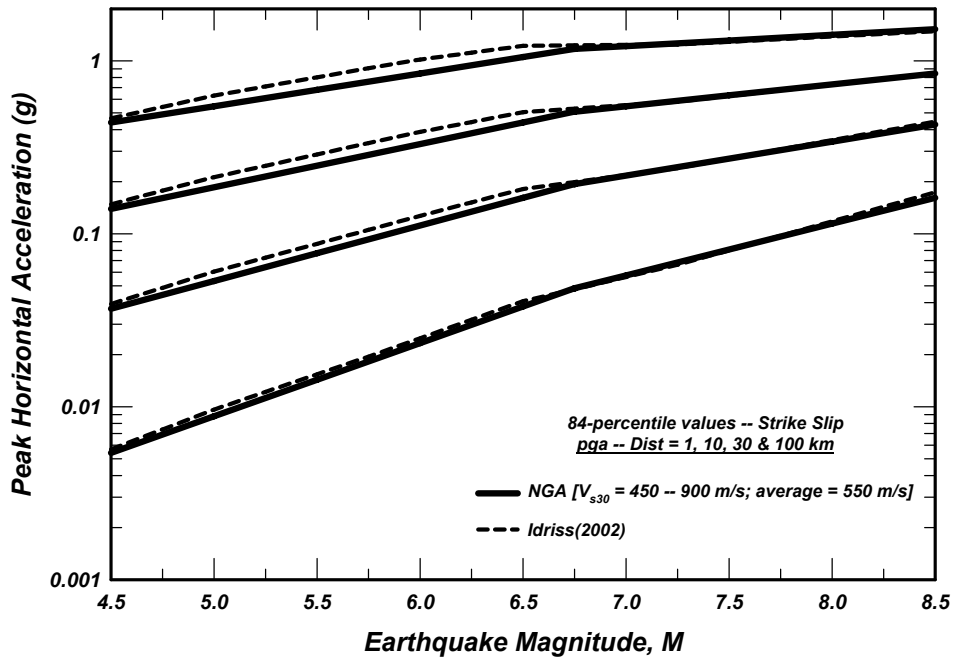


Figure 26 Comparison of 84-percentile values of pga calculated using the new NGA relationship and the relationship by Idriss (2006)

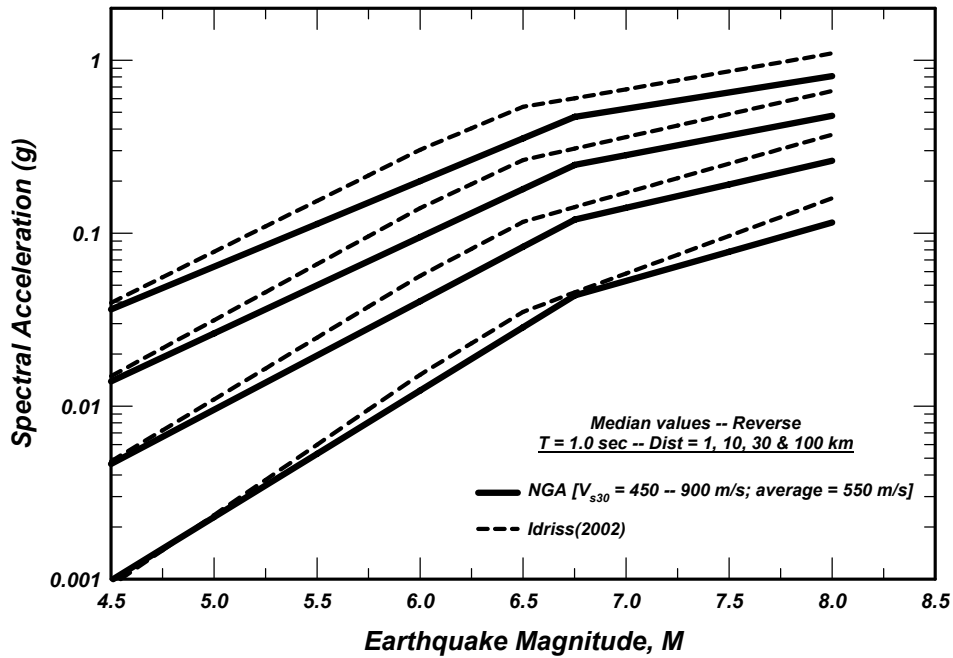
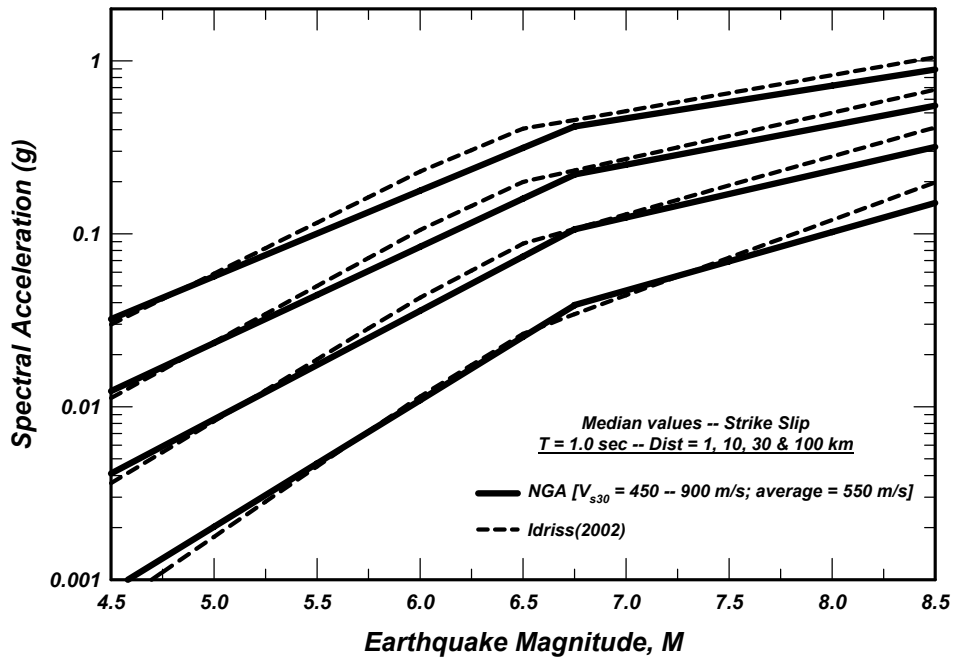


Figure 27 Comparison of median values of spectral acceleration for $T = 1.0$ sec calculated using the new NGA relationship and the relationship by Idriss (2006)

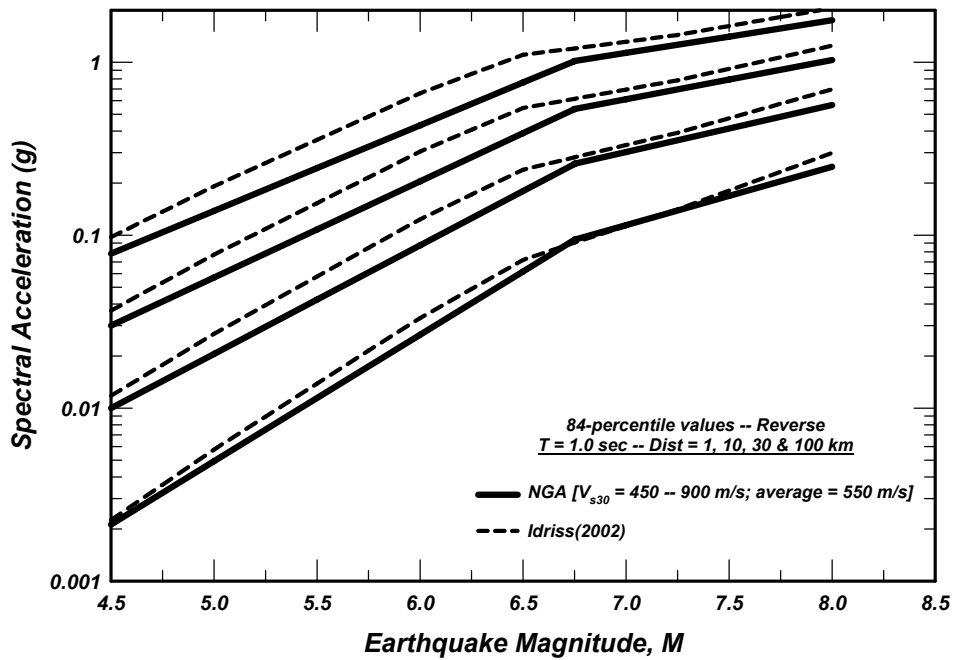
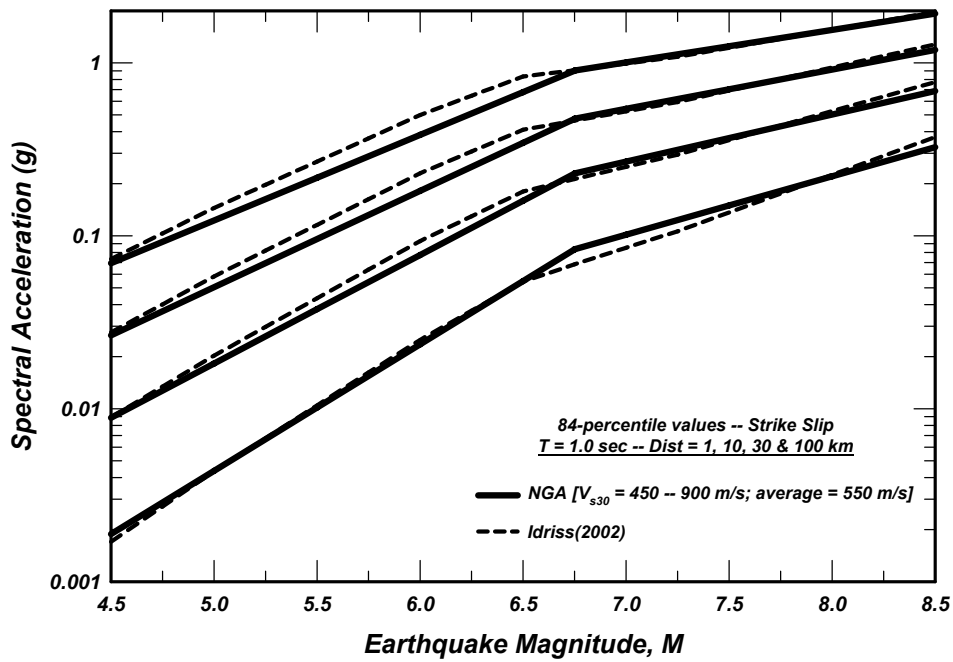


Figure 28 Comparison of 84-percentile values of spectral acceleration for $T = 1.0$ sec calculated using the new NGA relationship and the relationship by Idriss (2006)

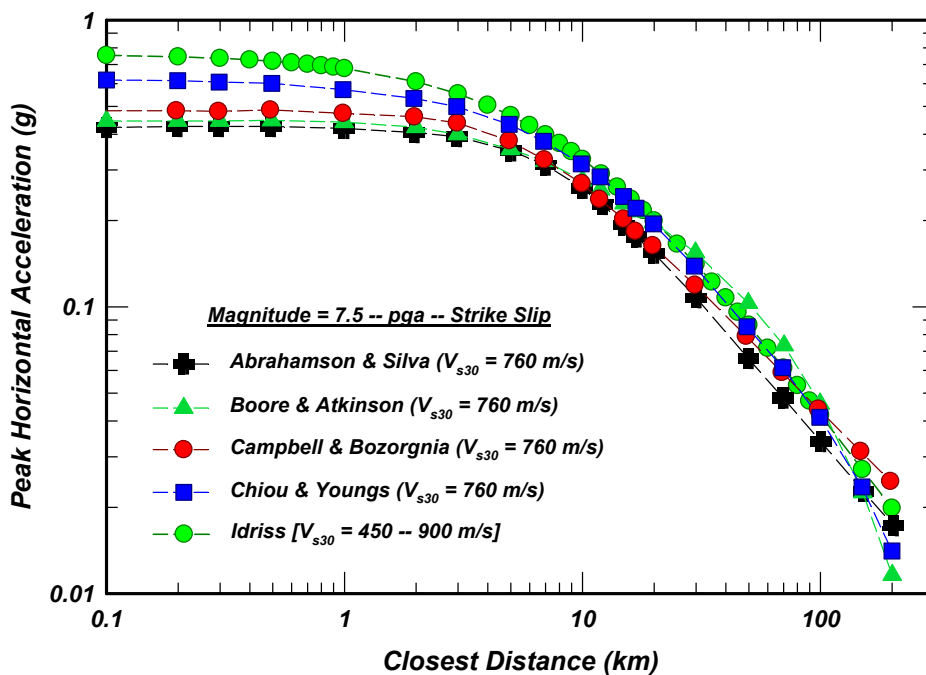


Figure 29 Comparison of the median values of pga calculated using the NGA relationships – M = 7.5 and strike slip mechanism

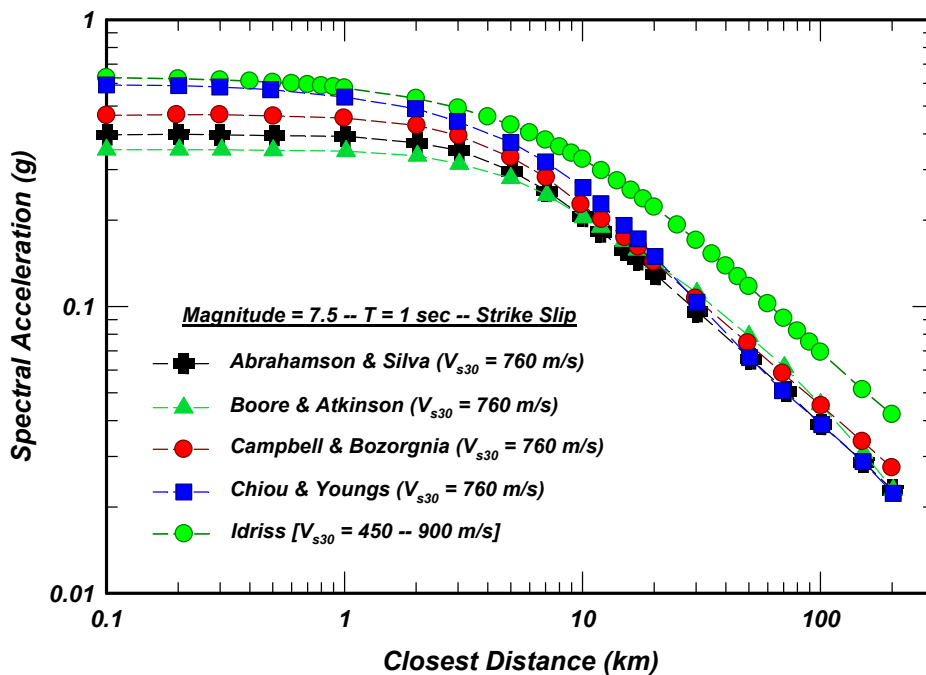


Figure 30 Comparison of the median values of spectral acceleration for T = 1.0 sec calculated using the NGA relationships – M = 7.5 and strike slip mechanism

APPENDIX A

FREE-FIELD EARTHQUAKE GROUND MOTIONS OBTAINED FROM NGA FLATFILE

Earthquake ID	Earthquake Name	Year	Moment Magnitude	Mechanism	Number of Stations	Shear Wave Velocity, V_{s30} (m/s)		Closest Distance (km)	
						Minimum	Maximum	Minimum	Maximum
0170	Big Bear City	2003	4.9	0	35	207	685	25.5	146.2
0165	CA/Baja Border Area	2002	5.3	0	9	191	231	39.9	97.0
0169	Denali, Alaska	2002	7.9	0	9	275	964	2.7	164.7
0166	Gilroy	2002	4.9	0	35	155	730	8.6	130.1
0168	Nenana Mountain, Alaska	2002	6.7	0	5	275	660	104.7	199.3
0167	Yorba Linda	2002	4.3	0	12	270	376	8.8	36.3
0161	Big Bear-02	2001	4.5	0	43	207	685	23.1	92.3
0164	Gulf of California	2001	5.7	0	12	196	345	72.8	130.0
0162	Mohawk Val, Portola	2001	5.2	0	4	275	345	66.9	125.8
0160	Yountville	2000	5.0	0	25	133	713	11.5	94.4
0173	Chi-Chi, Taiwan-04	1999	6.2	0	242	150	914	6.2	172.8
0138	Duzce, Turkey	1999	7.1	0	22	175	782	0.2	188.7
0158	Hector Mine	1999	7.1	0	79	203	725	11.7	198.1
0136	Kocaeli, Turkey	1999	7.5	0	22	175	811	4.8	180.2
0157	San Juan Bautista	1998	5.2	0	1	216	216	16.2	16.2
0129	Kobe, Japan	1995	6.9	0	22	198	1,043	0.3	158.6
0147	Northridge-02	1994	6.1	0	18	235	602	5.8	44.0
0148	Northridge-03	1994	5.2	0	7	235	822	9.3	44.5
0128	Double Springs	1994	5.9	0	1	345	345	12.8	12.8
0126	Big Bear-01	1992	6.5	0	39	207	822	9.4	147.2
0125	Landers	1992	7.3	0	68	207	685	2.2	190.1
0121	Erzican, Turkey	1992	6.7	0	1	275	275	4.4	4.4
0124	New Zealand-04	1992	5.7	0	1	150	150	42.2	42.2
0144	Manjil, Iran	1990	7.4	0	7	275	724	12.6	174.6
0143	Upland	1990	5.6	0	3	230	660	7.3	71.8
0116	Superstition Hills-02	1987	6.5	0	11	191	362	1.0	27.0

Earthquake ID	Earthquake Name	Year	Moment Magnitude	Mechanism	Number of Stations	Shear Wave Velocity, V_{s30} (m/s)		Closest Distance (km)	
						Minimum	Maximum	Minimum	Maximum
0115	Superstition Hills-01	1987	6.2	0	1	207	207	17.6	17.6
0102	Chalfant Valley-01	1986	5.8	0	5	271	345	6.4	24.5
0103	Chalfant Valley-02	1986	6.2	0	10	271	359	7.6	52.0
0104	Chalfant Valley-03	1986	5.7	0	3	271	345	10.8	24.5
0098	Hollister-04	1986	5.5	0	3	216	685	12.2	14.1
0105	Chalfant Valley-04	1986	5.4	0	2	271	271	10.6	24.9
0099	Mt. Lewis	1986	5.6	0	1	282	282	13.5	13.5
0108	San Salvador	1986	5.8	0	2	350	545	6.3	7.0
0090	Morgan Hill	1984	6.2	0	24	116	1,428	3.3	70.9
0094	Bishop (Rnd Val)	1984	5.8	0	1	359	359	22.8	22.8
0089	New Zealand-01	1984	5.5	0	1	275	275	8.8	8.8
0074	Mammoth Lakes-10	1983	5.3	0	1	339	339	6.5	6.5
0075	Mammoth Lakes-11	1983	5.3	0	1	339	339	7.7	7.7
0084	Trinidad offshore	1983	5.7	0	2	312	312	68.6	68.6
0085	Coalinga-08	1983	5.2	0	2	339	617	13.3	18.3
0073	Westmorland	1981	5.9	0	6	191	362	6.5	19.4
0070	Irpinia, Italy-03	1981	4.7	0	1	660	660	13.7	13.7
0055	Anza (Horse Canyon)-01	1980	5.2	0	5	329	725	12.7	40.6
0053	Livermore-01	1980	5.8	0	5	271	517	17.2	53.4
0054	Livermore-02	1980	5.4	0	6	271	713	11.8	30.0
0061	Mammoth Lakes-06	1980	5.9	0	4	271	345	12.2	44.5
0062	Mammoth Lakes-07	1980	4.7	0	6	339	339	4.7	9.4
0063	Mammoth Lakes-08	1980	4.8	0	7	339	371	4.4	9.7
0065	Mammoth Lakes-09	1980	4.9	0	9	339	685	7.8	12.6
0067	Trinidad	1980	7.2	0	3	312	312	76.3	76.3
0064	Victoria, Mexico	1980	6.3	0	4	275	660	7.3	39.3
0057	Mammoth Lakes-02	1980	5.7	0	2	339	371	9.1	9.5
0058	Mammoth Lakes-03	1980	5.9	0	2	339	345	12.5	18.1

Earthquake ID	Earthquake Name	Year	Moment Magnitude	Mechanism	Number of Stations	Shear Wave Velocity, V_{s30} (m/s)		Closest Distance (km)	
						Minimum	Maximum	Minimum	Maximum
0059	Mammoth Lakes-04	1980	5.7	0	2	339	345	5.3	14.4
0060	Mammoth Lakes-05	1980	5.7	0	1	339	339	7.4	7.4
0048	Coyote Lake	1979	5.7	0	9	222	1,428	3.1	33.8
0050	Imperial Valley-06	1979	6.5	0	33	163	660	0.1	50.1
0051	Imperial Valley-07	1979	5.0	0	16	163	275	10.3	49.9
0052	Imperial Valley-08	1979	5.6	0	1	194	194	9.8	9.8
0044	Izmir, Turkey	1977	5.3	0	1	660	660	3.2	3.2
0141	Caldiran, Turkey	1976	7.2	0	1	275	275	50.8	50.8
0041	Gazli, USSR	1976	6.8	0	1	660	660	5.5	5.5
0034	Hollister-03	1974	5.1	0	2	371	1,428	9.2	10.6
0140	Sitka, Alaska	1972	7.7	0	2	660	660	34.6	106.7
0028	Borrego Mtn	1968	6.6	0	0	443	443	129.1	129.1
0025	Parkfield	1966	6.2	0	4	257	528	9.6	17.6
0130	Kozani, Greece-01	1995	6.4	1	9	339	660	10.1	84.0
0134	Dinar, Turkey	1995	6.4	1	2	220	339	3.4	44.2
0152	Little Skull Mtn,NV	1992	5.7	1	8	275	660	16.1	100.2
0122	Roermond, Netherlands	1992	5.3	1	3	660	660	57.1	101.3
0119	Griva, Greece	1990	6.1	1	1	339	339	29.2	29.2
0111	New Zealand-02	1987	6.6	1	1	425	425	68.7	68.7
0091	Lazio-Abruzzo, Italy	1984	5.8	1	5	200	660	18.9	51.3
0088	Borah Peak, ID-02	1983	5.1	1	3	339	660	18.5	49.0
0087	Borah Peak, ID-01	1983	6.9	1	2	425	425	83.0	84.8
0072	Corinth, Greece	1981	6.6	1	1	339	339	10.3	10.3
0068	Irpinia, Italy-01	1980	6.9	1	22	275	1,000	8.2	64.4
0049	Norcia, Italy	1979	5.9	1	3	339	1,000	4.6	31.5
0047	Dursunbey, Turkey	1979	5.3	1	1	660	660	9.2	9.2
0039	Oroville-03	1975	4.7	1	9	345	623	6.1	12.8

Earthquake ID	Earthquake Name	Year	Moment Magnitude	Mechanism	Number of Stations	Shear Wave Velocity, V_{s30} (m/s)		Closest Distance (km)	
						Minimum	Maximum	Minimum	Maximum
0036	Oroville-01	1975	5.9	1	1	623	623	8.0	8.0
0037	Oroville-02	1975	4.8	1	2	438	438	12.7	14.1
0171	Chi-Chi, Taiwan-02	1999	5.9	2	293	124	1,023	7.7	147.1
0172	Chi-Chi, Taiwan-03	1999	6.2	2	241	158	1,000	7.6	139.1
0174	Chi-Chi, Taiwan-05	1999	6.2	2	319	124	1,526	32.3	195.9
0175	Chi-Chi, Taiwan-06	1999	6.3	2	288	150	1,526	10.1	146.3
0127	Northridge-01	1994	6.7	2	155	161	2,016	5.2	147.6
0151	Northridge-06	1994	5.3	2	48	235	1,223	11.3	82.6
0123	Cape Mendocino	1992	7.0	2	6	312	713	7.0	42.0
0120	Georgia, USSR	1991	6.2	2	5	275	275	31.6	63.6
0145	Sierra Madre	1991	5.6	2	8	257	996	10.4	48.2
0097	Nahanni, Canada	1985	6.8	2	3	660	660	4.9	9.6
0076	Coalinga-01	1983	6.4	2	45	185	685	8.4	55.8
0077	Coalinga-02	1983	5.1	2	20	247	617	10.6	27.7
0078	Coalinga-03	1983	5.4	2	3	339	617	12.6	13.5
0079	Coalinga-04	1983	5.2	2	11	339	617	9.5	15.4
0080	Coalinga-05	1983	5.8	2	11	257	617	8.5	16.1
0081	Coalinga-06	1983	4.9	2	2	339	617	11.1	11.8
0082	Coalinga-07	1983	5.2	2	2	339	617	10.9	12.1
0142	St Elias, Alaska	1979	7.5	2	2	275	275	26.5	80.0
0046	Tabas, Iran	1978	7.4	2	7	275	767	2.1	194.6
0040	Friuli, Italy-01	1976	6.5	2	12	275	660	11.0	102.2
0033	Point Mugu	1973	5.7	2	1	298	298	17.7	17.7
0030	San Fernando	1971	6.6	2	29	271	874	11.0	193.9
0012	Kern County	1952	7.4	2	1	316	316	117.8	117.8

Earthquake ID	Earthquake Name	Year	Moment Magnitude	Mechanism	Number of Stations	Shear Wave Velocity, V_{s30} (m/s)		Closest Distance (km)	
						Minimum	Maximum	Minimum	Maximum
0137	Chi-Chi, Taiwan	1999	7.6	3	414	124	1,526	0.3	172.2
0149	Northridge-04	1994	5.9	3	7	235	450	14.7	53.8
0150	Northridge-05	1994	5.1	3	9	235	526	20.1	59.2
0118	Loma Prieta	1989	6.9	3	75	116	1,428	3.9	117.1
0117	Spitak, Armenia	1988	6.8	3	1	275	275	24.0	24.0
0113	Whittier Narrows-01	1987	6.0	3	106	161	1,223	14.7	103.9
0114	Whittier Narrows-02	1987	5.3	3	11	257	822	11.8	42.5
0101	N. Palm Springs	1986	6.1	3	31	207	685	4.0	78.1
0029	Lytle Creek	1970	5.3	3	8	302	813	12.4	103.6
0163	Anza-02	2001	4.9	4	72	196	845	16.8	133.3
0096	Drama, Greece	1985	5.2	4	1	660	660	43.4	43.4
0056	Mammoth Lakes-01	1980	6.1	4	2	339	371	4.7	6.6
0038	Oroville-04	1975	4.4	4	3	438	438	10.5	14.4
0139	Stone Canyon	1972	4.8	4	3	339	478	12.0	12.0

APPENDIX B
DERIVED PARAMETERS – SPECTRAL VALUES
FOR $\tau = 0.02$, $\tau = 0.03$ AND $\tau = 0.04$ SEC

B.1 INTRODUCTION

After careful examination of the recorded values for these periods, it was felt that it would be appropriate to use the expression derived for pga adjusted for the spectral ratio, $PAA(\tau)/pga$, for each period. This approach allows using the same parameters and factors derived for pga , except for the parameter α_1 , which would then be adjusted by adding the value of the spectral ratio selected for that period. The values of the spectral ratio selected for $\tau = 0.02$, 0.03 and 0.04 sec are presented in the following section of this Appendix.

B.2 SPECTRAL RATIOS FOR $\tau = 0.02$, 0.03 AND 0.04 SEC

The cumulative distributions of the spectral ratio for these periods are shown in Figure B-1 and the 50-percentile and 84-percentile values for each are presented in Figure B-2. The 50-percentile, average and 84-percentile values for each period are listed below:

Period, τ (sec)	Spectral Ratio, $PAA(\tau)/pga$		
	50-percentile	Average	84-percentile
0.02	1.005	1.013	1.016
0.03	1.017	1.048	1.064
0.04	1.035	1.095	1.144

The variations of the spectral ratio, $PAA(\tau)/pga$, with magnitude and distance for $\tau = 0.02$ sec are shown in Figure B-3 and the variations of this ratio for this period with V_{s30} and pga are shown in Figure B-4. These variations for $\tau = 0.03$ sec are presented in Figures B-5 and B-6 and variations for $\tau = 0.04$ sec are presented in Figures B-7 and B-8. Also shown in each figure is the average value for each spectral ratio. The average values of this ratio for $\tau = 0.02$, 0.03 and 0.04 sec are equal to about 1.01, 1.05 and 1.10, respectively. However, for $\tau = 0.02$ sec, it was felt reasonable to consider that the spectral ordinates would be essentially equal for those for $\tau = 0.01$ sec (i.e., equal to pga). Accordingly, the parameter α_1 for $\tau = 0.02$, 0.03 and 0.04 sec was increased an amount equal to $\Delta\alpha_1$, approximately equal to the natural logarithm of the average spectral ratio for the corresponding period. The resulting values for the parameter α_1 are listed below:

Period, τ (sec)	$M \leq 6^{3/4}$		$M \geq 6^{3/4}$	
	$\Delta\alpha_1$	α_1	$\Delta\alpha_1$	α_1
0.02	0	3.7113	0	5.6462
0.03	0.05	3.7613	0.05	5.6862
0.04	0.10	3.8113	0.10	5.7362

These values of the parameter α_1 are listed in Table 2.

B.3 EXAMINATION OF RESIDUALS -- $T = 0.04$ SEC

The residuals calculated using the parameters listed above for $T = 0.04$ sec are presented in Figure B-9 in terms of residuals versus magnitude, residuals versus distance, and residuals versus v_{s30} . The results in Figure B-9 indicate that the fitted parameters provide a reasonably accurate representation of the data and that the approach using the spectral ratio and the fitted parameters for *pga* is adequate for estimating the values of $PAA(T)$ for $T = 0.04$ sec.

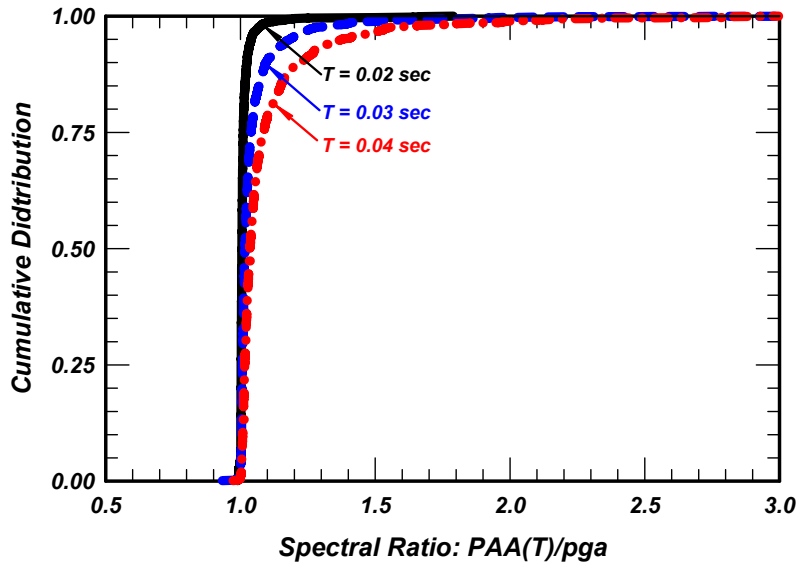


Figure B-1 Cumulative distribution of the spectral ratio $PAA(T)/pga$ for $T = 0.02, 0.03$ and 0.04 sec

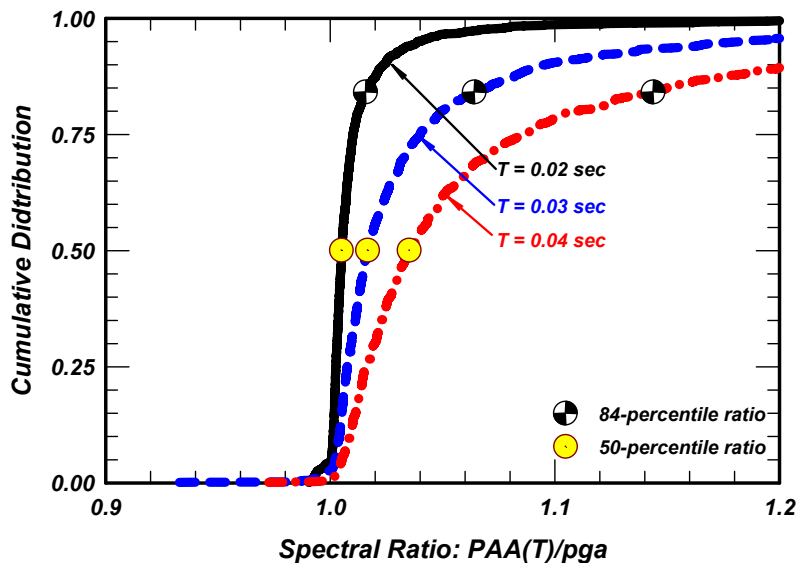


Figure B-2 Median and 84-percentile values of the spectral ratio $PAA(T)/pga$ for $T = 0.02, 0.03$ and 0.04 sec

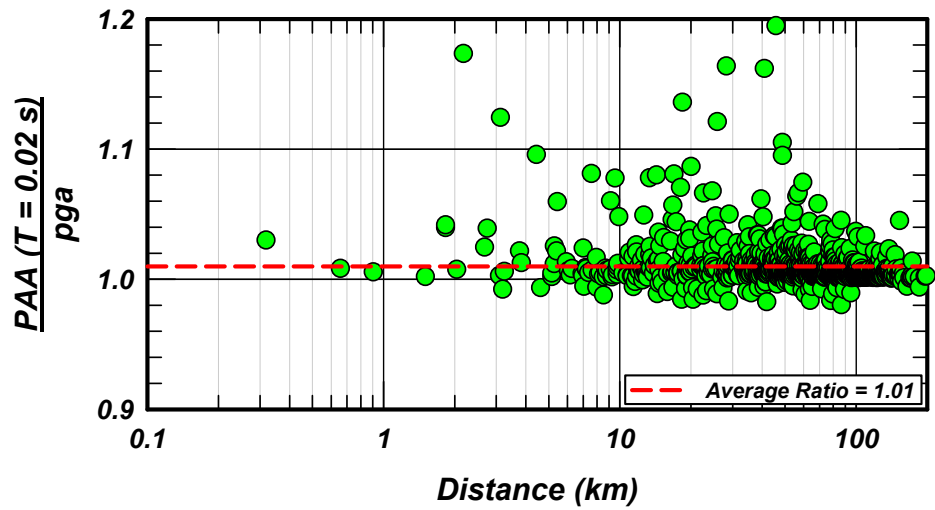
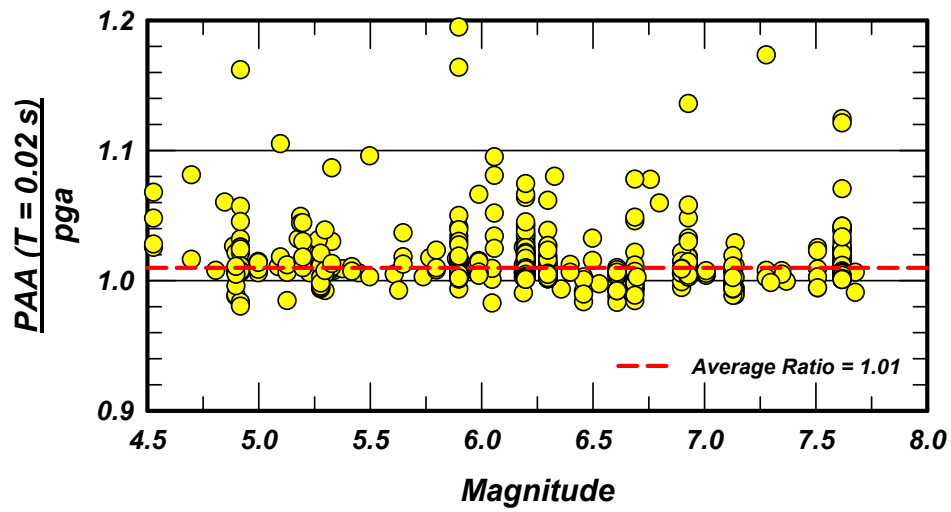


Figure B-3 Variations of the spectral ratio $PAA(T)/pga$ with magnitude and distance for $T = 0.02$ sec

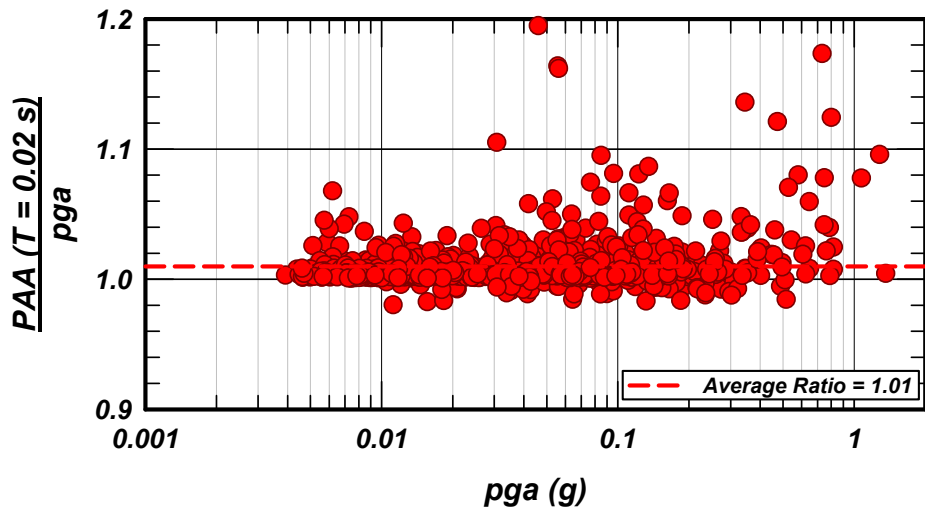
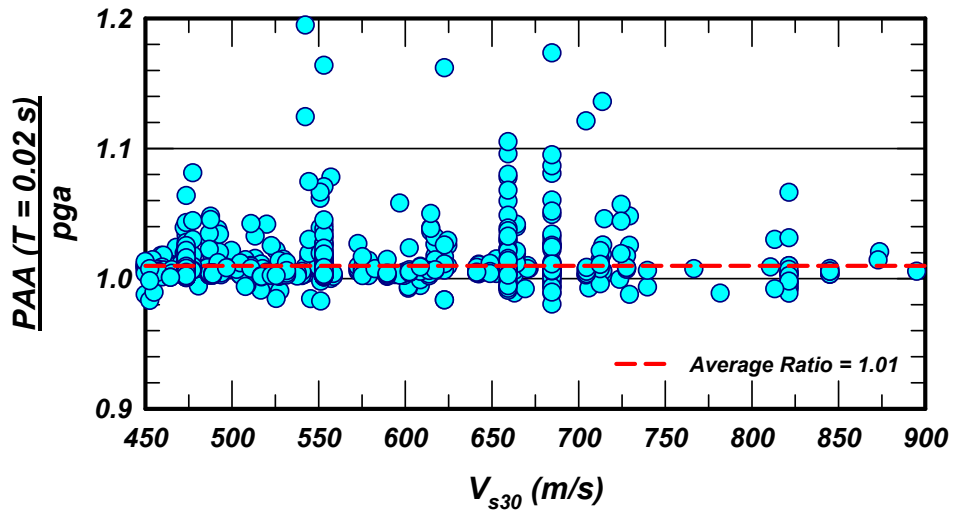


Figure B-4 Variations of the spectral ratio $PAA(T)/pga$ with V_{s30} and pga for $T = 0.02$ sec

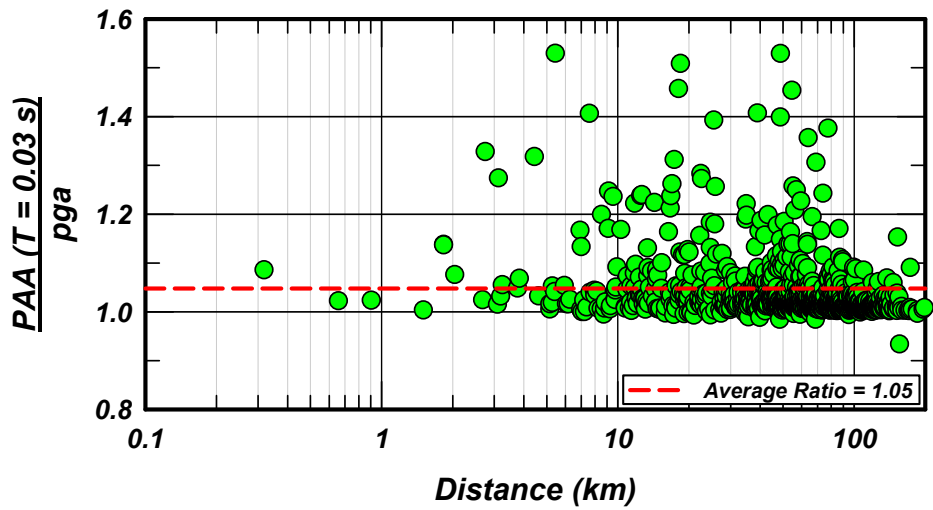
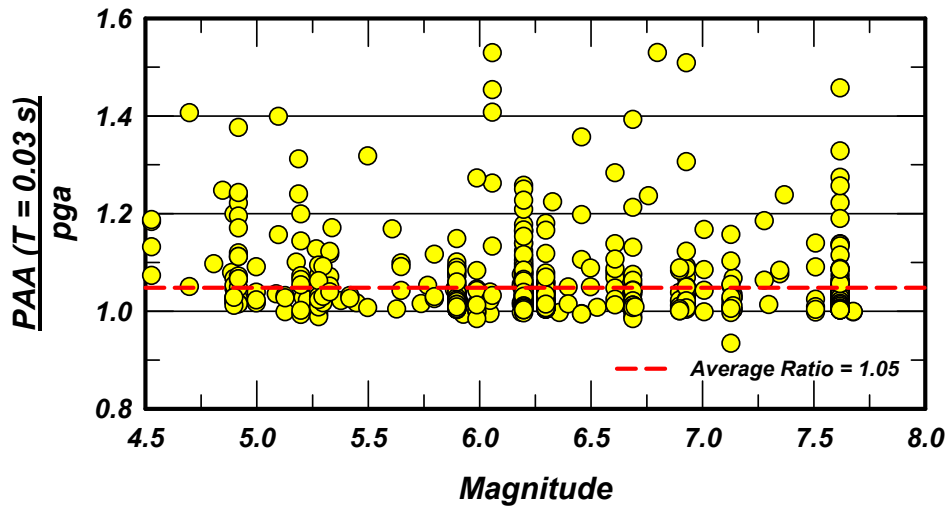


Figure B-5 Variations of the spectral ratio $PAA(T)/pga$ with magnitude and distance for $T = 0.03$ sec

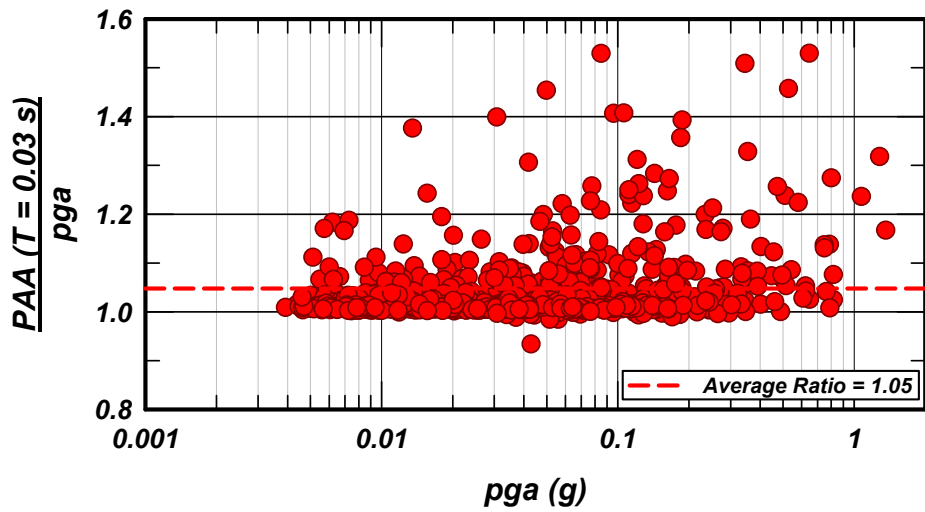
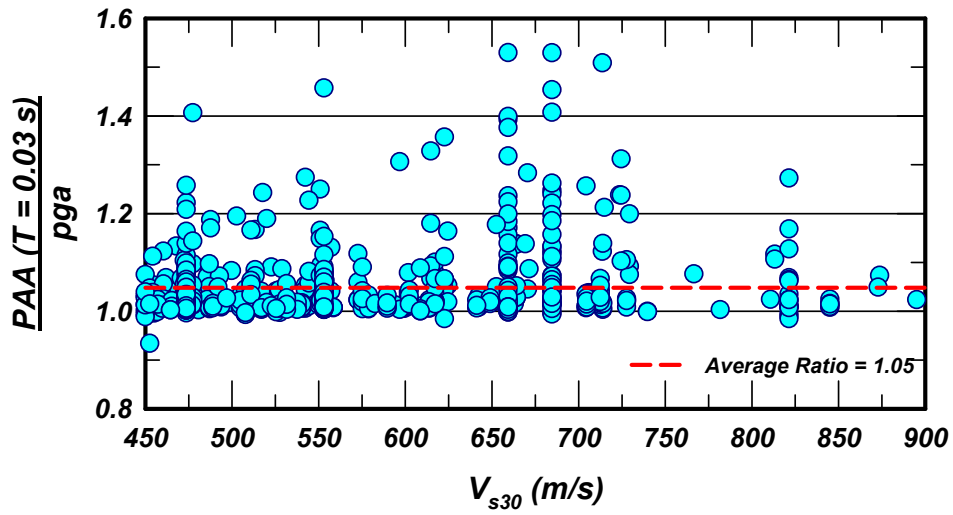


Figure B-6 Variations of the spectral ratio $PAA(T)/pga$ with V_{s30} and pga for $T = 0.03$ sec

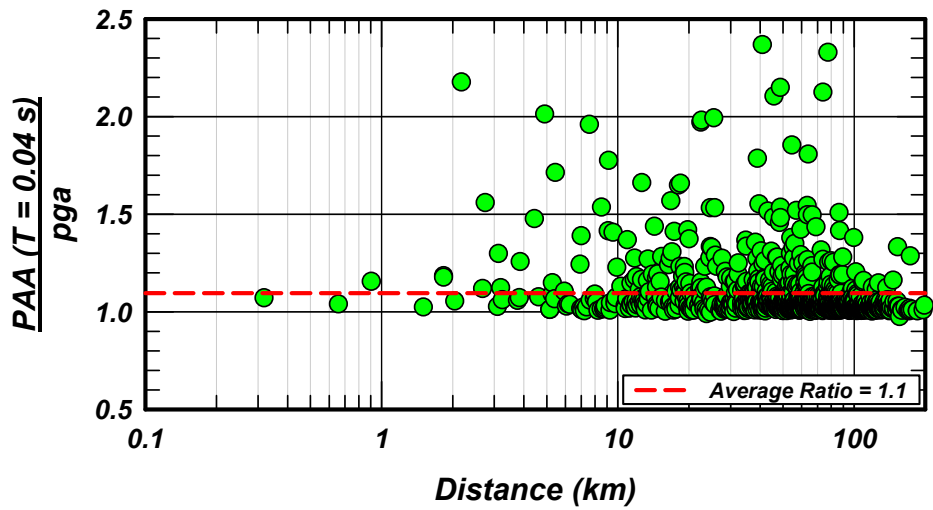
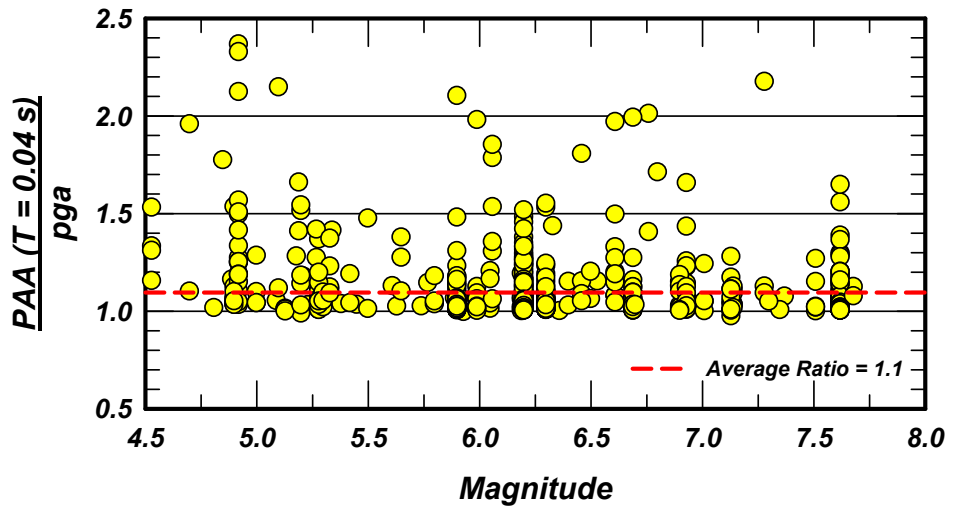


Figure B-7 Variations of the spectral ratio $PAA(T)/pga$ with magnitude and distance for $T = 0.04$ sec

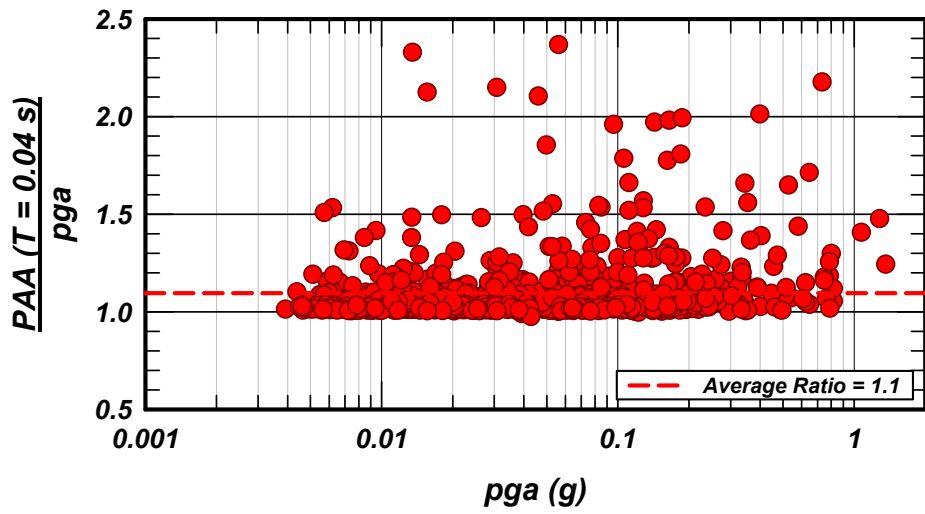
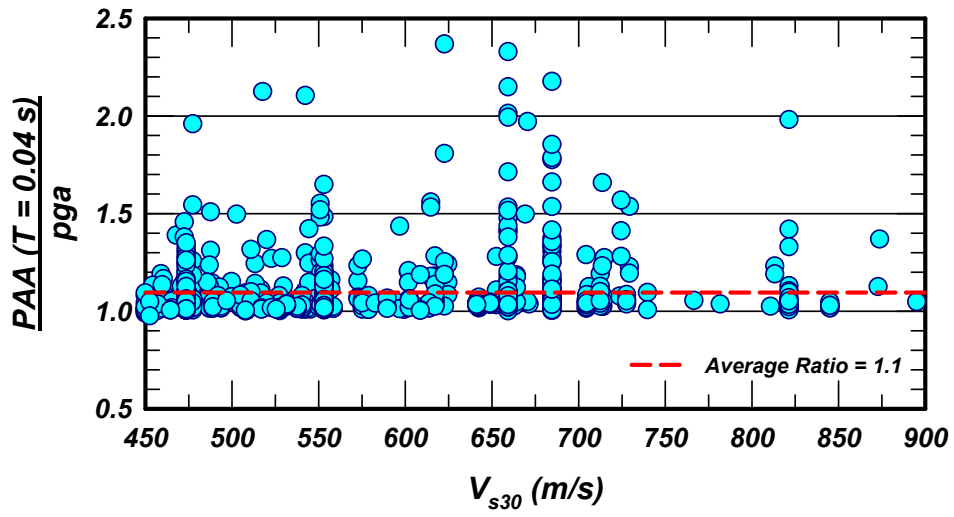


Figure B-8 Variations of the spectral ratio $PAA(T)/pga$ with V_{s30} and pga for $T = 0.04$ sec

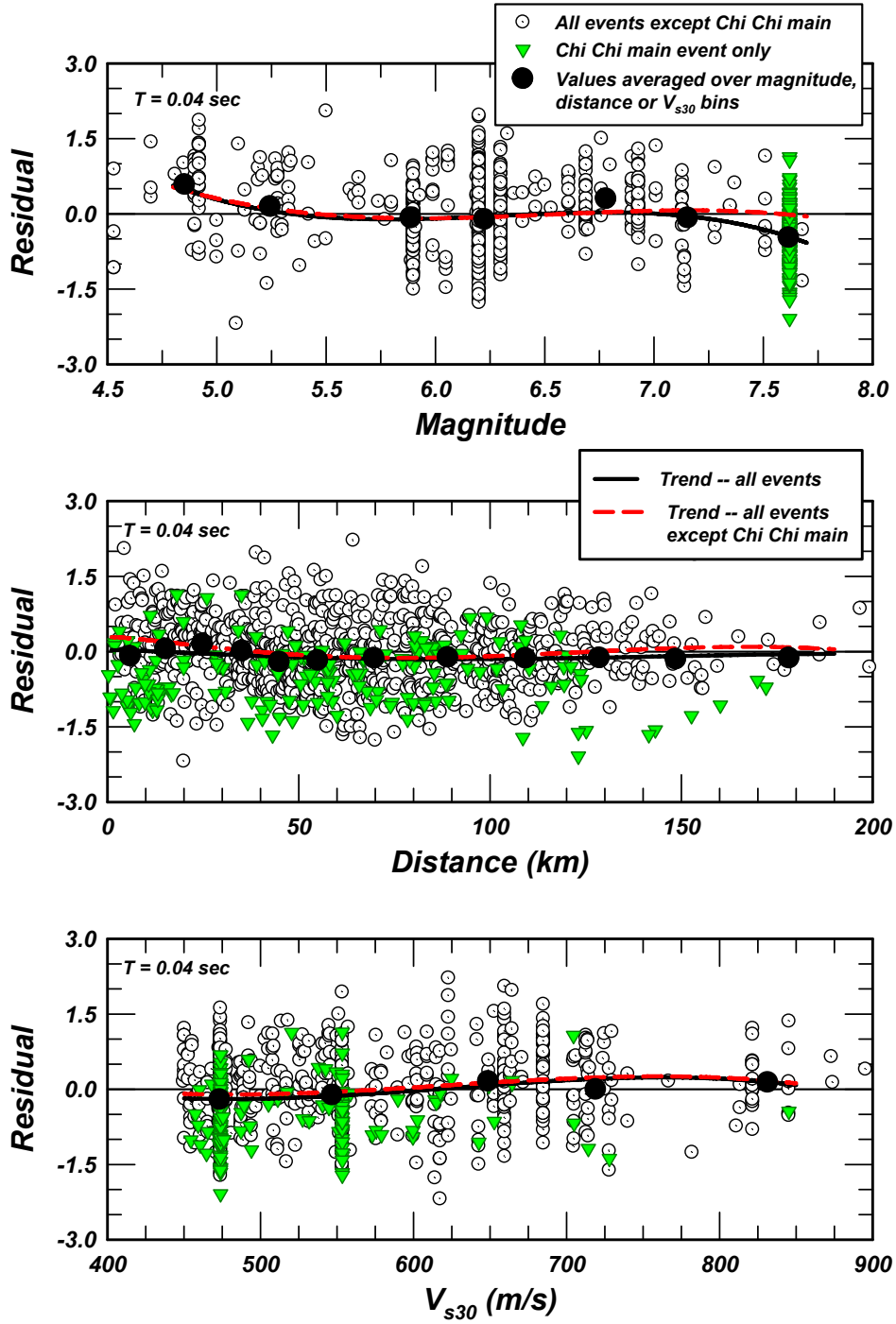


Figure B-9 Residuals versus magnitude, closest distance and V_{s30} using the derived equation for estimating PAA(T) for $T = 0.04 \text{ sec}$

APPENDIX C
DERIVED PARAMETERS – SPECTRAL VALUES FOR $\tau = 0.2$ SEC

C.1 PARAMETERS FOR $\tau = 0.2$ SEC

The parameters, $\alpha_1(\tau)$, $\alpha_2(\tau)$, $\beta_1(\tau)$, and $\beta_2(\tau)$, factors $\gamma(\tau)$ and $\varphi(\tau)$, and standard error term for $\tau = 0.2$ sec derived using Eq. [1], are listed below:

Parameter / Factor for $\tau = 0.2$ sec	Magnitude Range	
	$M \leq 6\frac{3}{4}$	$M > 6\frac{3}{4}$
$\alpha_1(\tau)$	3.5006	3.3005
$\alpha_2(\tau)$	-0.0319	-0.0023
$\beta_1(\tau)$	2.8554	2.4154
$\beta_2(\tau)$	-0.2305	-0.1653
$\gamma(\tau)$	0.00006	
$\varphi(\tau)$	0.12	
SE Term	0.72	

These values are listed and defined in Table 2.

C.2 EXAMINATION OF RESIDUALS -- $\tau = 0.2$ SEC

The residuals calculated using the parameters listed above are presented in Figure C-1 in terms of residuals versus magnitude, residuals versus distance, and residuals versus v_{s30} . The residuals obtained for the Chi-Chi main shock ($M = 7.62$) are shown separately and the trend of the residuals is shown for all events with and without the Chi-Chi main shock. The results shown in Figure C-1 indicate that the fitted parameters provide an excellent representation of the data in the magnitude range of 5.2 to 7.2, for the distance range of about 5 to 150 km, and for v_{s30} values less than about 750 m/s. The trend of the residuals shows practically no bias for all magnitudes larger than 5.2, when the residuals for the Chi-Chi main shock are excluded.

The data for magnitudes smaller than about 5.2 and larger than 7.2 are rather sparse (except for the Chi-Chi main shock); the data for distances beyond 150 km and for v_{s30} greater than 725 m/s are also sparse.

The spectral values (at $\tau = 0.2$ sec) for the motions recorded during the Chi-Chi main event are overestimated. The latter observation is more clearly depicted in Figure C-2.

The residuals obtained for the five Chi-Chi aftershocks are presented in Figure C-3 in terms of residuals versus distance. Note that in the aggregate, the derived relationship for the spectral values at $\tau = 0.2$ sec provides an excellent representation of the values recorded during these five aftershocks in distance range of 15 to about 150 km. Note, however, that the number of data points is quite small at distances less than about 20 km or at distances greater than 150 km.

It is also worth noting that recordings from an individual aftershock can be either well over- or well under-estimated.

The values recorded during the Hector Mine earthquake are shown in Figure C-4 together with the curve calculated using the derived relationship for spectral values at $\tau = 0.2$ sec with $M = 7.1$

and mechanism 0. Similar plots for the values recorded during the Loma Prieta earthquake are shown in Figure C-5, and those recorded during the Northridge and the San Fernando earthquakes are presented in Figure C-6.

The plots in these figures indicate that the degree of fit varies for each earthquake but that the overall comparisons (as depicted in Figure C-1) indicate the reasonableness of the derived relationship.

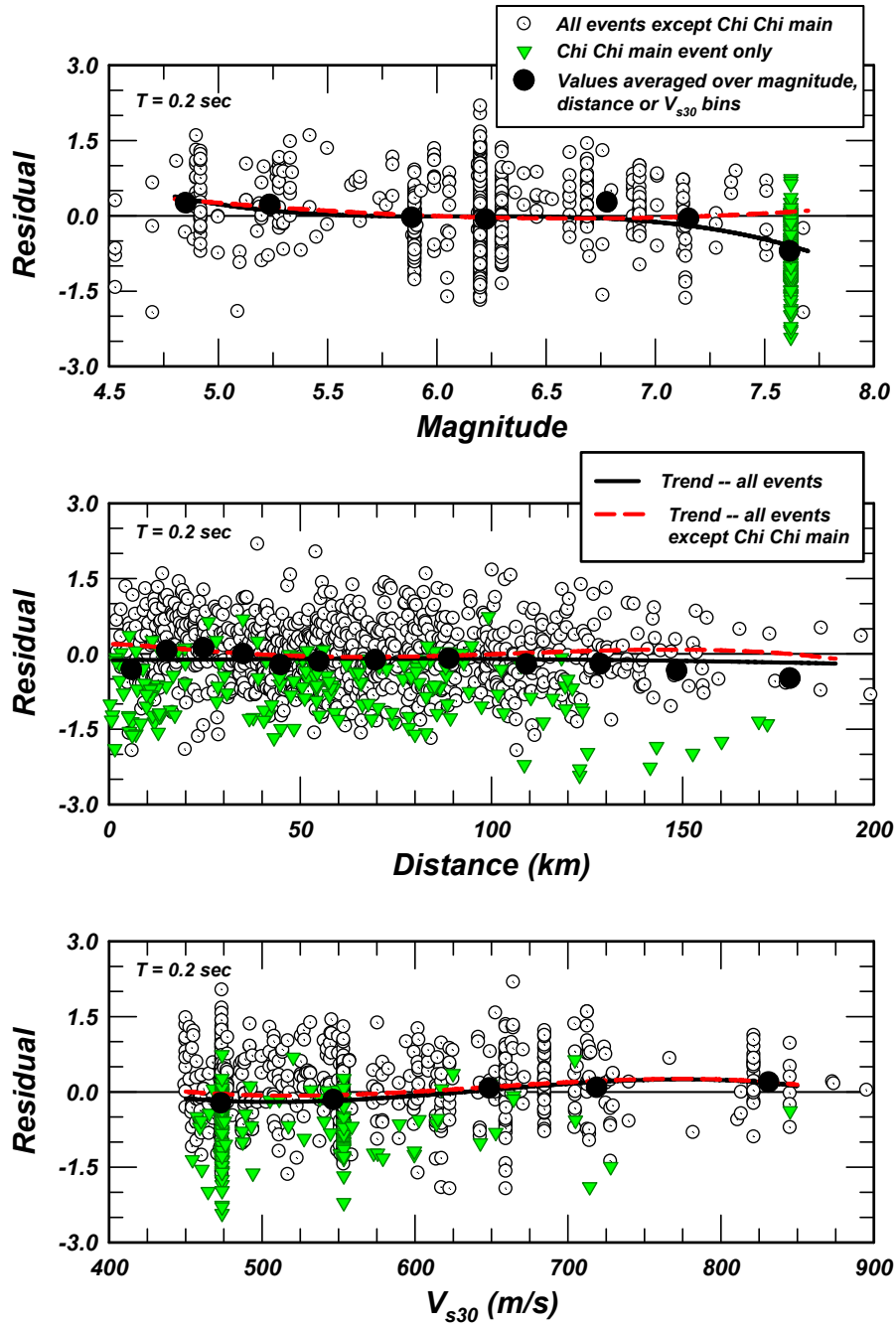


Figure C-1 Residuals versus magnitude, closest distance and V_{s30} using the derived equation for estimating $PAA(T)$ for $T = 0.2$ sec

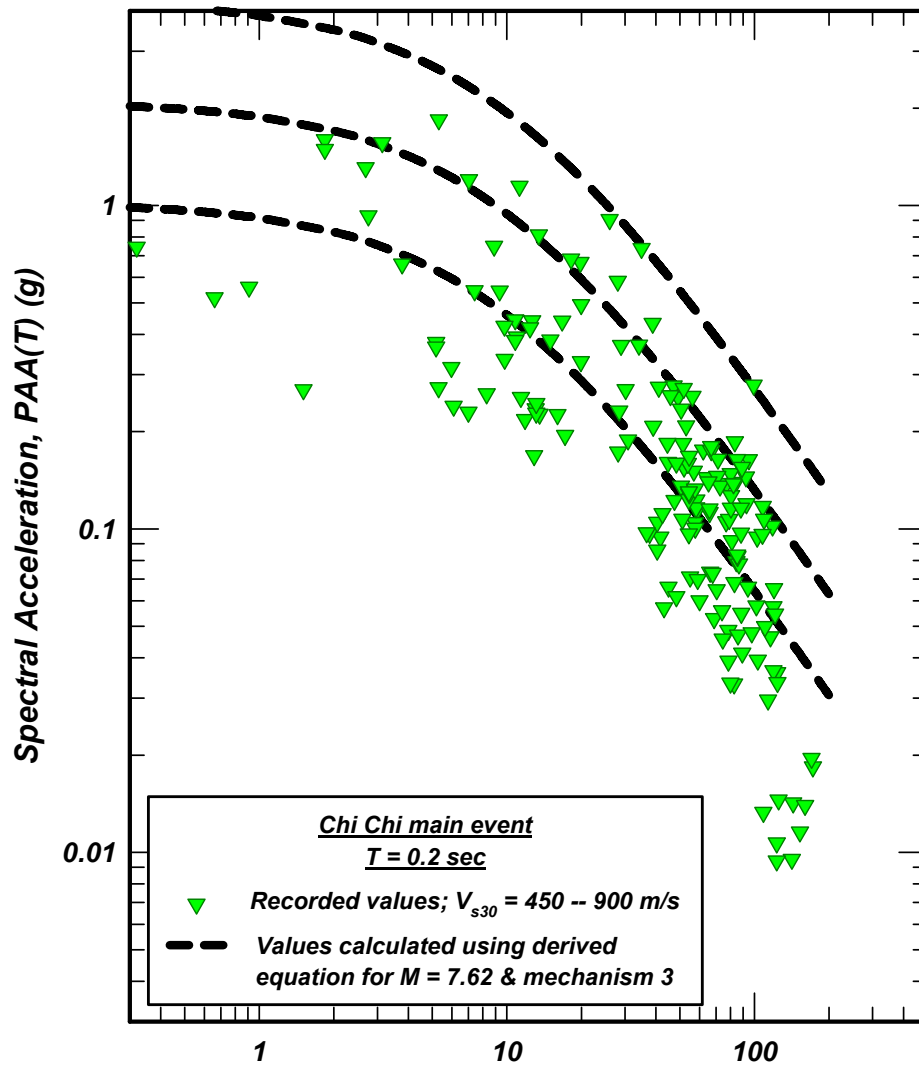


Figure C-2 Comparison of spectral accelerations ($T = 0.2$ sec) recorded during the 1999 Chi-Chi earthquake with median, 16-percentile and 84-percentile values calculated using the derived equation for $M = 7.62$ & mechanism 3

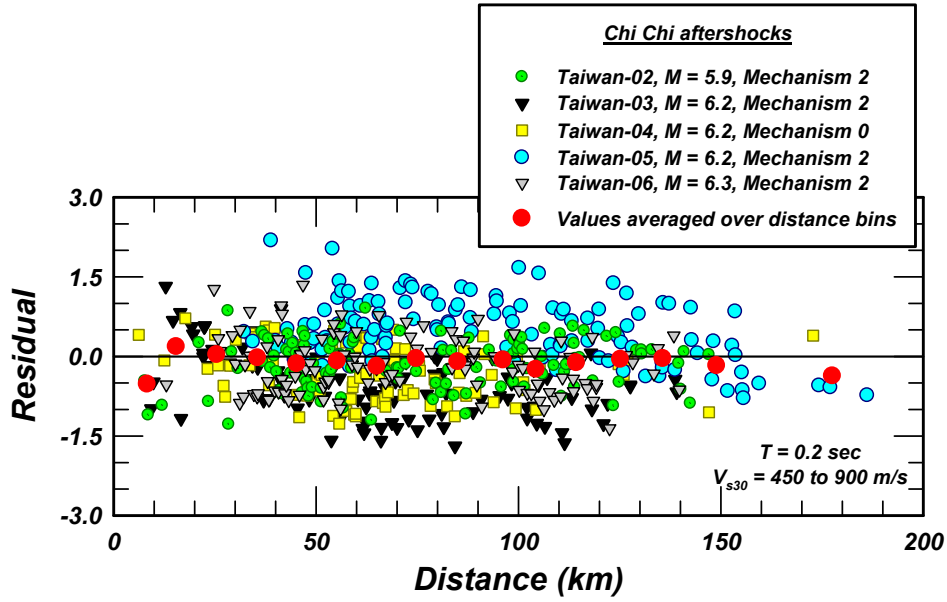


Figure C-3 Residuals versus closest distance for spectral accelerations ($T = 0.2$ sec) for motions recorded during the five Chi-Chi earthquake aftershocks obtained using the derived equation with magnitude and mechanism as shown in the legend

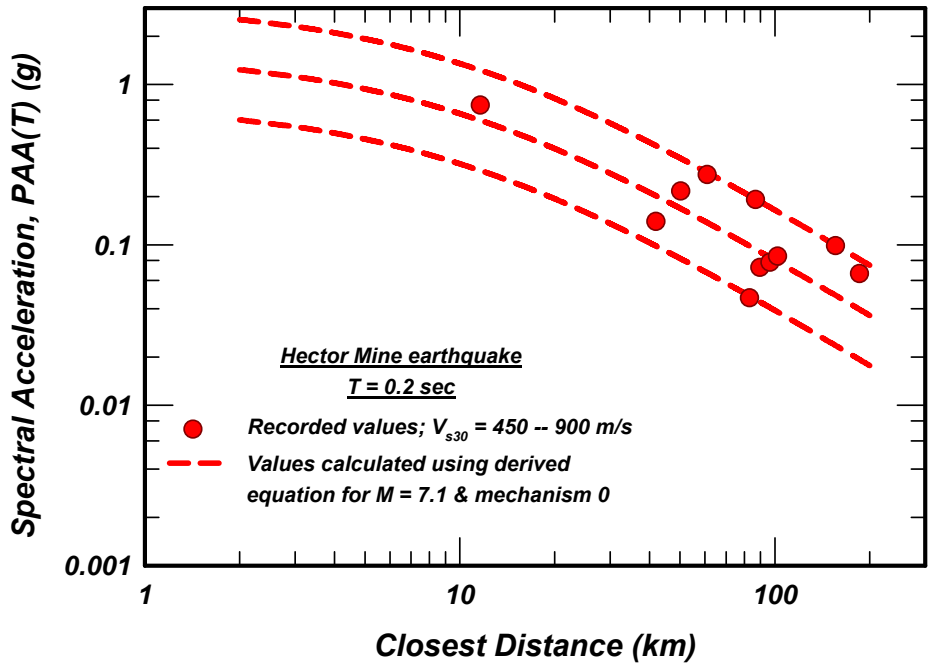


Figure C-4 Comparison of spectral accelerations ($T = 0.2$ sec) recorded during the 1999 Hector Mine earthquake with median, 16-percentile and 84-percentile values calculated using the derived equation with $M = 7.1$ & mechanism 0

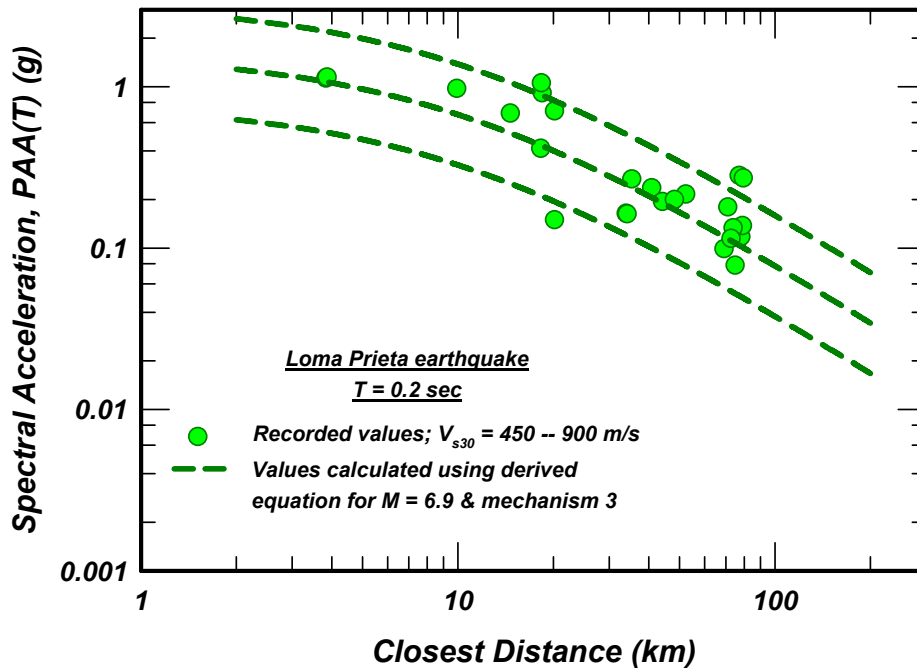


Figure C-5 Comparison of spectral accelerations ($T = 0.2 \text{ sec}$) recorded during the 1989 Loma Prieta earthquake with median, 16-percentile and 84-percentile values calculated using the derived equation with $M = 6.9$ & mechanism 3

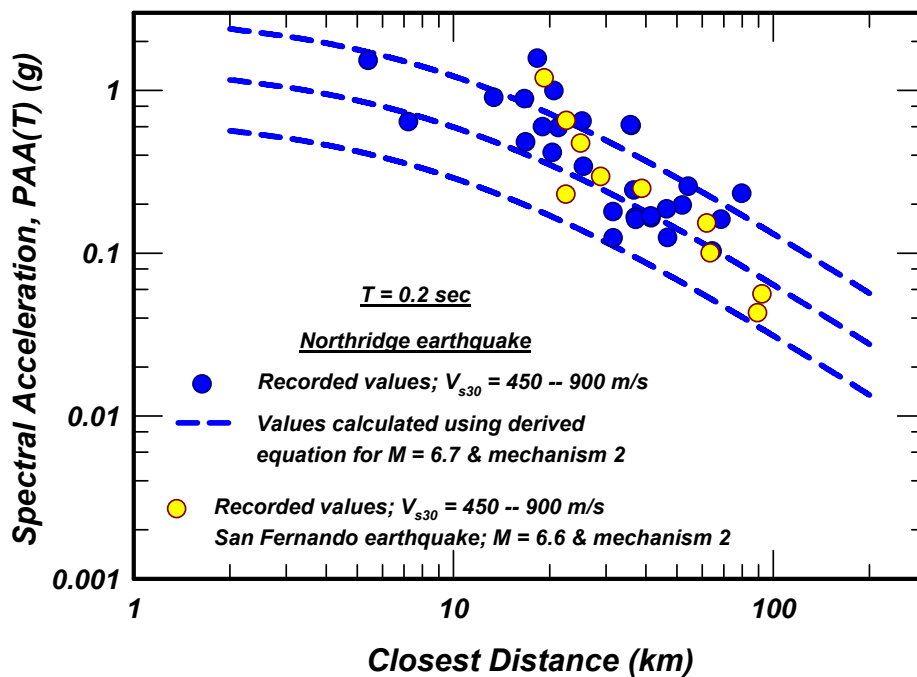


Figure C-6 Comparison of spectral accelerations ($T = 0.2 \text{ sec}$) recorded during the 1994 Northridge and the 1971 San Fernando earthquakes with median, 16-percentile and 84-percentile values calculated using the derived equation with $M = 6.7$ & mechanism 2

APPENDIX D
DERIVED PARAMETERS – SPECTRAL VALUES FOR $\tau = 1$ SEC

D.1 PARAMETERS FOR $\tau = 1.0$ SEC

The parameters, $\alpha_1(\tau)$, $\alpha_2(\tau)$, $\beta_1(\tau)$, and $\beta_2(\tau)$, factors $\gamma(\tau)$ and $\varphi(\tau)$, and standard error term for $\tau = 1.0$ sec derived using Eq. [1], are listed below:

Parameter / Factor for $\tau = 1.0$ sec	Magnitude Range	
	$M \leq 6\frac{3}{4}$	$M > 6\frac{3}{4}$
$\alpha_1(\tau)$	-2.1147	1.2135
$\alpha_2(\tau)$	0.5707	0.0777
$\beta_1(\tau)$	2.6904	2.0933
$\beta_2(\tau)$	-0.2371	-0.1487
$\gamma(\tau)$	0.00132	
$\varphi(\tau)$	0.12	
SE Term	0.77	

These values are listed and defined in Table 2.

D.2 EXAMINATION OF RESIDUALS -- $\tau = 1.0$ SEC

The residuals calculated using the parameters listed above are presented in Figure D-1 in terms of residuals versus magnitude, residuals versus distance, and residuals versus v_{s30} . The residuals obtained for the Chi-Chi main shock ($M = 7.62$) are shown separately and the trend of the residuals is shown for all events with and without the Chi-Chi main shock. The results shown in Figure D-1 indicate that the fitted parameters provide a very good representation of the data in the magnitude range of 5.2 to 7, for distances less than about 150 km, and for v_{s30} values less than about 700 m/s. The data for magnitudes smaller than about 5.2 and larger than 7.2 are rather sparse (except for the Chi-Chi main shock); the data for distances beyond 150 km and for v_{s30} greater than 725 m/s are also sparse.

The spectral values (at $\tau = 1.0$ sec) for the motions recorded during the Chi-Chi main event are somewhat overestimated. The latter observation is more clearly depicted in Figure D-2.

The residuals obtained for the five Chi-Chi aftershocks are presented in Figure D-3 in terms of residuals versus distance. Note that in the aggregate, the derived relationship for the spectral values at $\tau = 1.0$ sec provides an excellent representation of the values recorded during these five aftershocks in distance range of 30 to about 150 km. Note, however, that the number of data points is quite small at distances less than about 20 km or at distances greater than 150 km.

It is also worth noting that recordings from an individual aftershock can be either well over- or well under-estimated.

The values recorded during the Hector Mine earthquake are shown in Figure D-4 together with the curve calculated using the derived relationship for spectral values at $\tau = 1.0$ sec with $M = 7.1$ and mechanism 0. Similar plots for the values recorded during the Loma Prieta earthquake are shown in Figure D-5, and those recorded during the Northridge and the San Fernando earthquakes are presented in Figure D-6.

The plots in these figures indicate that the degree of fit varies for each earthquake but that the overall comparisons (as depicted in Figure D-1) indicate the reasonableness of the derived relationship.

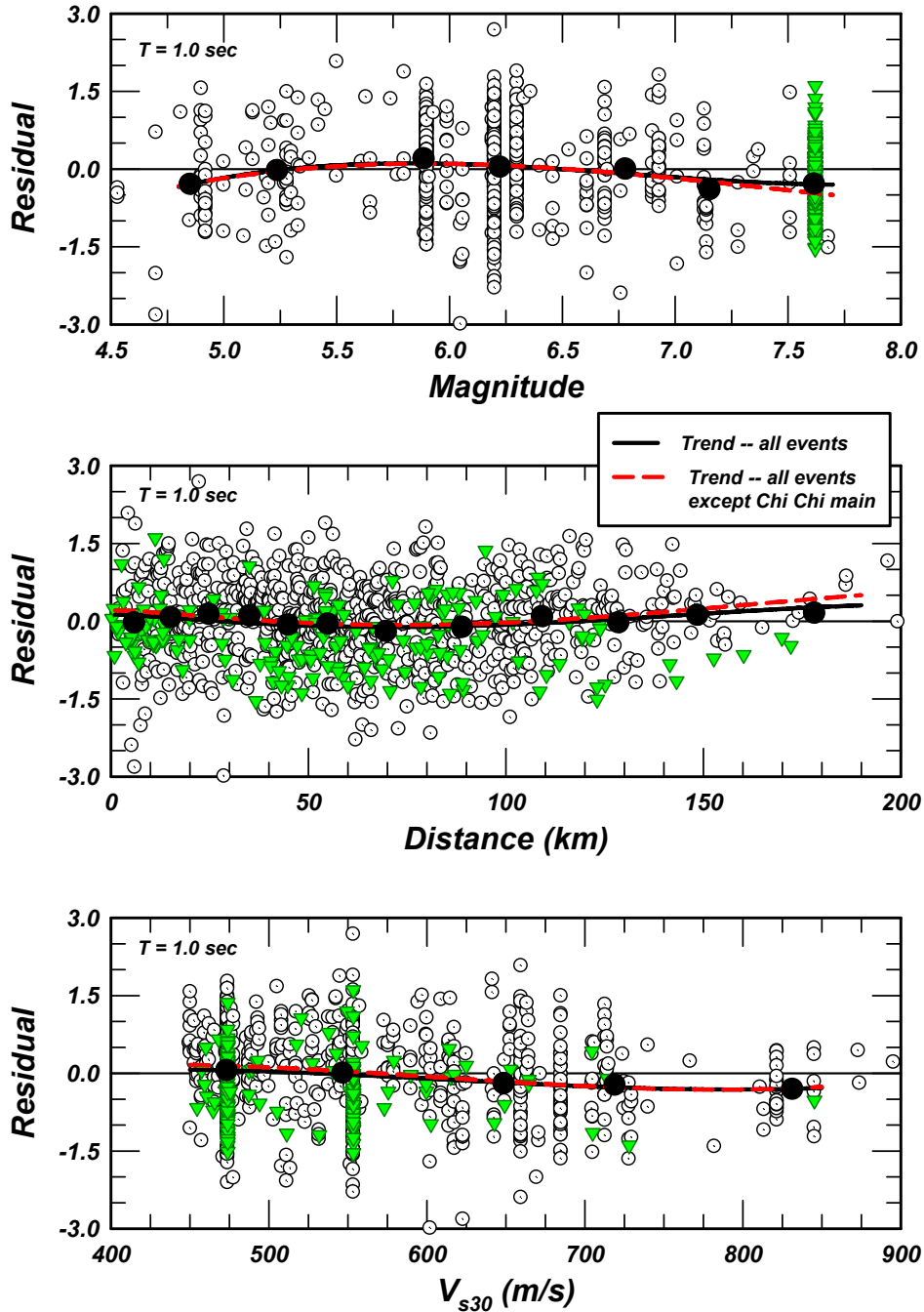


Figure D-1 Residuals versus magnitude, closest distance and V_{s30} using the derived equation for estimating PAA(T) for $T = 1.0 \text{ sec}$

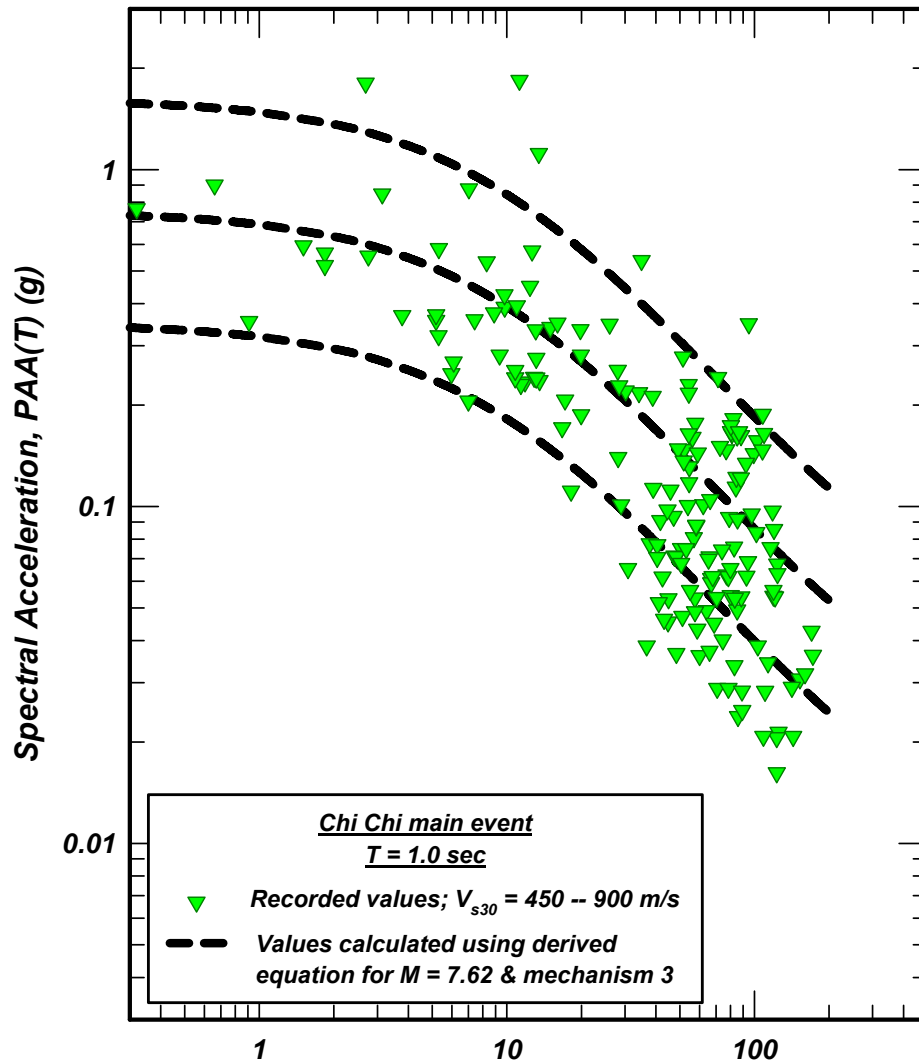


Figure D-2 Comparison of spectral accelerations ($T = 1.0$ sec) recorded during the 1999 Chi-Chi earthquake with median, 16-percentile and 84-percentile values calculated using the derived equation for $M = 7.62$ & mechanism 3

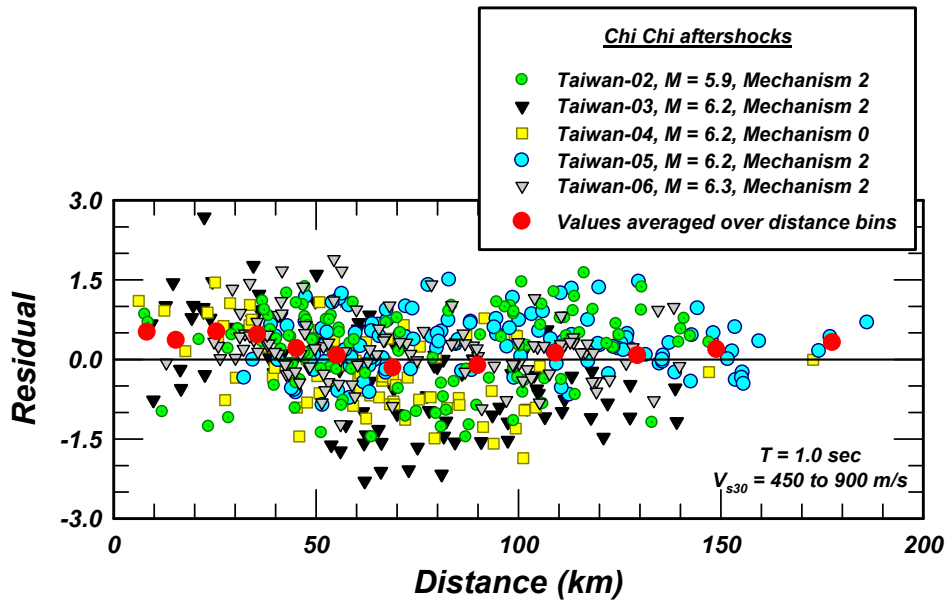


Figure D-3 Residuals versus closest distance for spectral accelerations ($T = 1.0$ sec) for motions recorded during the five Chi-Chi earthquake aftershocks obtained using the derived equation with magnitude and mechanism as shown in the legend

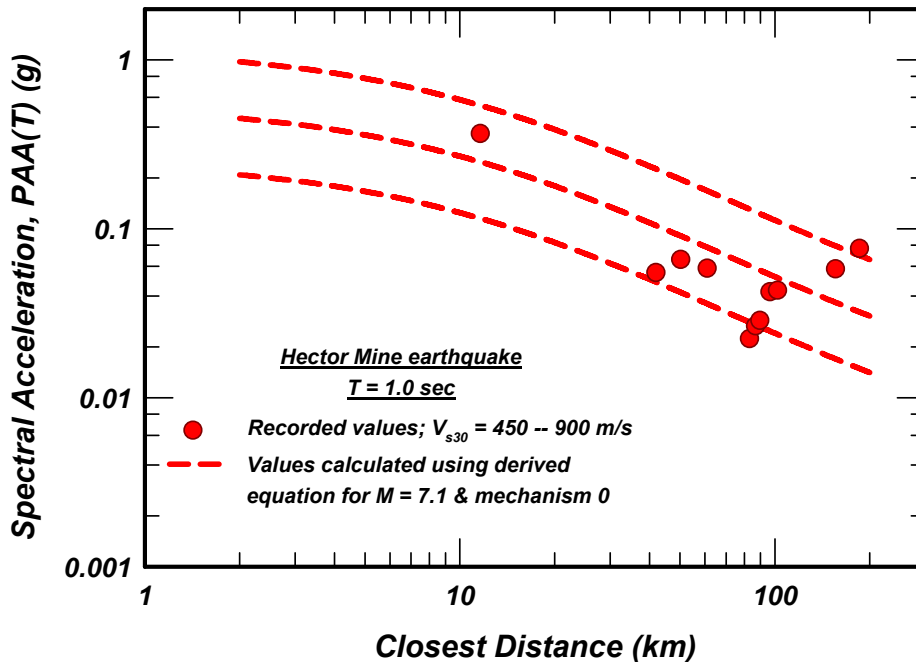


Figure D-4 Comparison of spectral accelerations ($T = 1.0$ sec) recorded during the 1999 Hector Mine earthquake with median, 16-percentile and 84-percentile values calculated using the derived equation with $M = 7.1$ & mechanism 0

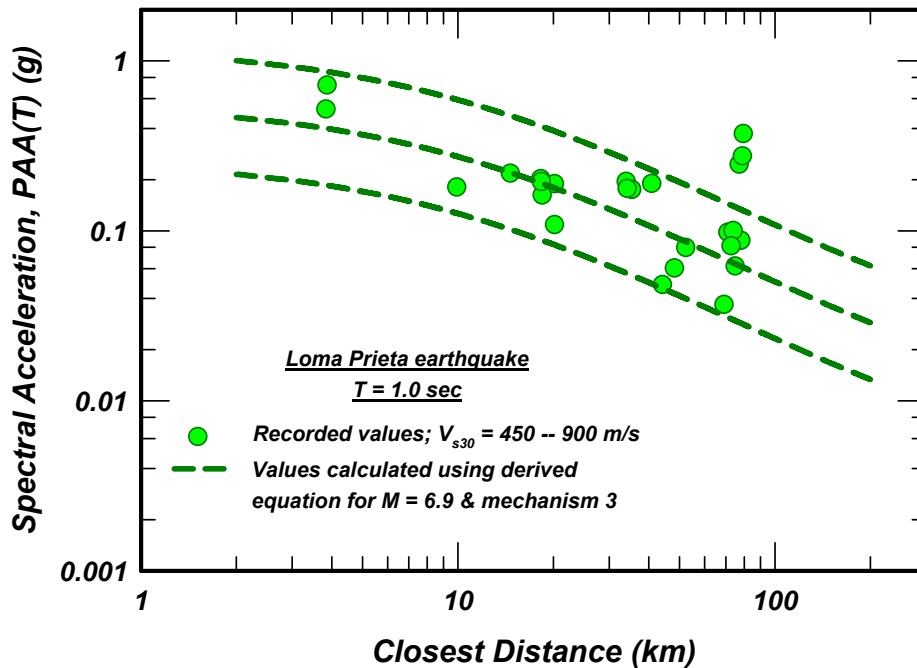


Figure D-5 Comparison of spectral accelerations ($T = 1.0$ sec) recorded during the 1989 Loma Prieta earthquake with median, 16-percentile and 84-percentile values calculated using the derived equation with $M = 6.9$ & mechanism 3

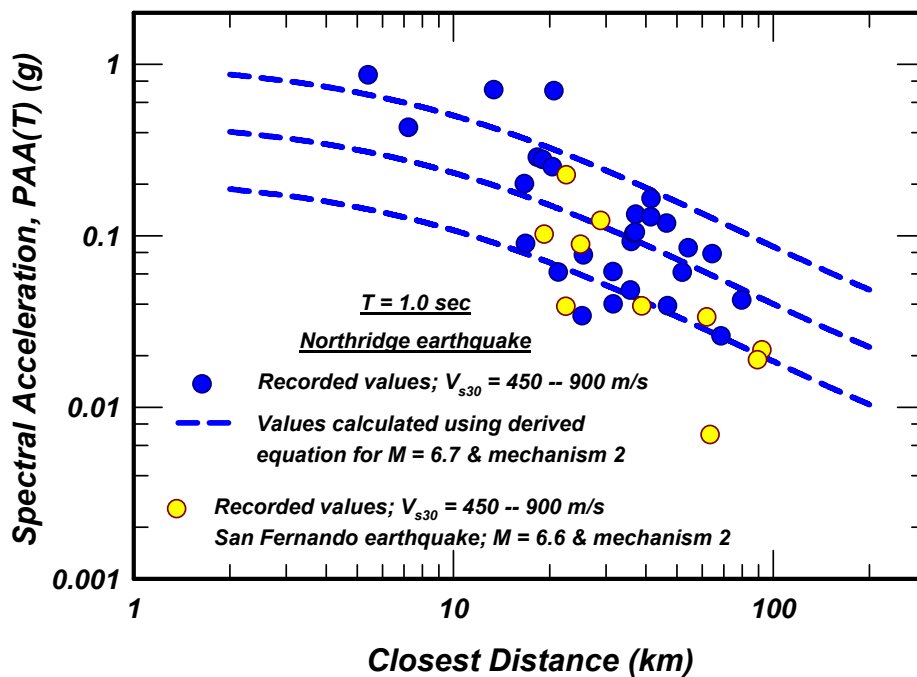


Figure D-6 Comparison of spectral accelerations ($T = 1.0$ sec) recorded during the 1994 Northridge and the 1971 San Fernando earthquakes with median, 16-percentile and 84-percentile values calculated using the derived equation with $M = 6.7$ & mechanism 2

APPENDIX E
DERIVED PARAMETERS – SPECTRAL VALUES FOR $\tau = 3$ SEC

E.1 PARAMETERS FOR $\tau = 3.0$ SEC

The parameters for $\tau = 3.0$ sec were derived using Eq. [1]. The derived parameters $\alpha_1(\tau)$, $\alpha_2(\tau)$, $\beta_1(\tau)$, and $\beta_2(\tau)$, factors $\gamma(\tau)$ and $\varphi(\tau)$, and standard error term are listed below:

Parameter / Factor for $\tau = 3.0$ sec	Magnitude Range	
	$M \leq 6\frac{3}{4}$	$M > 6\frac{3}{4}$
$\alpha_1(\tau)$	-6.2226	-2.2929
$\alpha_2(\tau)$	0.8805	0.2992
$\beta_1(\tau)$	2.6442	1.8270
$\beta_2(\tau)$	-0.2497	-0.1286
$\gamma(\tau)$	0.00023	
$\varphi(\tau)$	0.08	
SE Term	0.83	

These values are listed and defined in Table 2.

E.2 EXAMINATION OF RESIDUALS -- $\tau = 3.0$ SEC

The residuals calculated using the parameters listed above are presented in Figure E-1 in terms of residuals versus magnitude, residuals versus distance, and residuals versus v_{s30} . The residuals obtained for the Chi-Chi main shock ($M = 7.62$) are shown separately and the trend of the residuals is shown for all events with and without the Chi-Chi main shock. The results shown in Figure E-1 indicate that the fitted parameters provide a very good representation of the data in the magnitude range of 5.5 to 7.6 (i.e., including those recorded during the Chi-Chi main event) for distances less than about 140 km, and for v_{s30} values less than about 650 m/s. The data recorded during the Chi-Chi main event and the calculated values for $M = 7.62$ and mechanism 3 are presented in Figure E-2.

The residuals obtained for the five Chi-Chi aftershocks are presented in Figure E-3 in terms of residuals versus distance. Note that in the aggregate, the derived relationship for the spectral values at $\tau = 3.0$ sec provides an excellent representation of the values recorded during these five aftershocks in distance range of 40 to about 150 km. Note, however, that the number of data points is quite small at distances less than about 20 km or at distances greater than 150 km.

It is also worth noting that recordings from an individual aftershock can be either well over- or well under-estimated.

The values recorded during the Hector Mine earthquake are shown in Figure E-4 together with the curve calculated using the derived relationship for spectral values at $\tau = 1.0$ sec with $M = 7.1$ and mechanism 0. Similar plots for the values recorded during the Loma Prieta earthquake are shown in Figure E-5, and those recorded during the Northridge and the San Fernando earthquakes are presented in Figure E-6.

The plots in these figures indicate that the degree of fit varies for each earthquake but that the overall comparisons (as depicted in Figure E-1) indicate the reasonableness of the derived relationship.

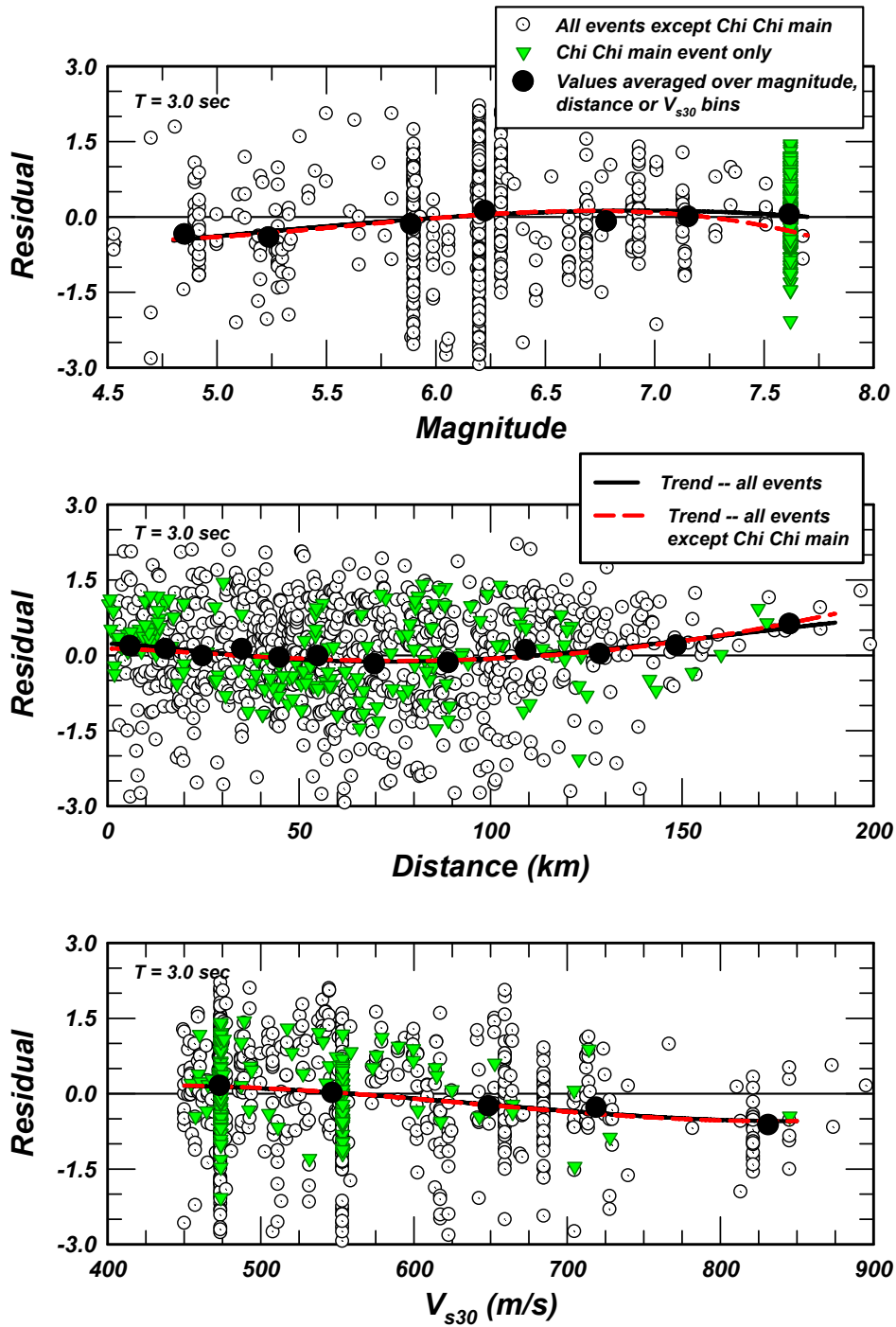


Figure E-1 Residuals versus magnitude, closest distance and V_{s30} using the derived equation for estimating $PAA(T)$ for $T = 3.0 \text{ sec}$

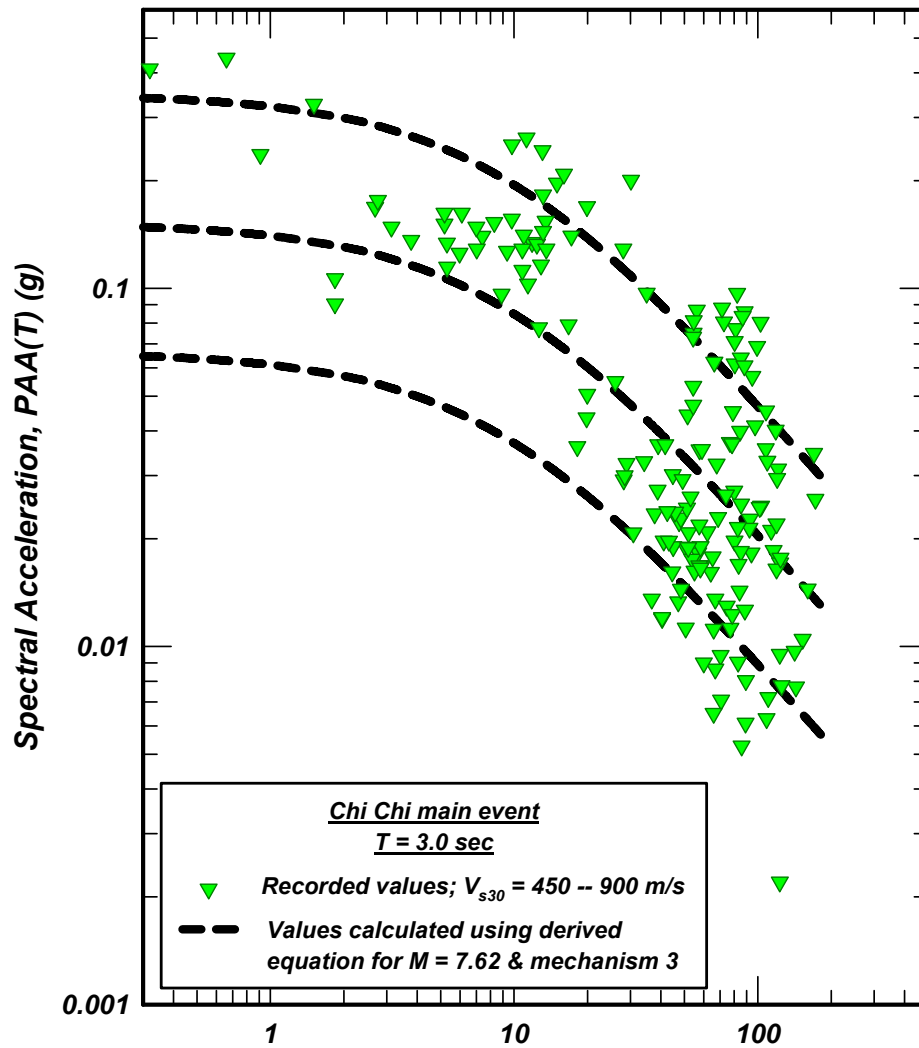


Figure E-2 Comparison of spectral accelerations ($T = 3.0$ sec) recorded during the 1999 Chi-Chi earthquake with median, 16-percentile and 84-percentile values calculated using the derived equation for $M = 7.62$ & mechanism 3

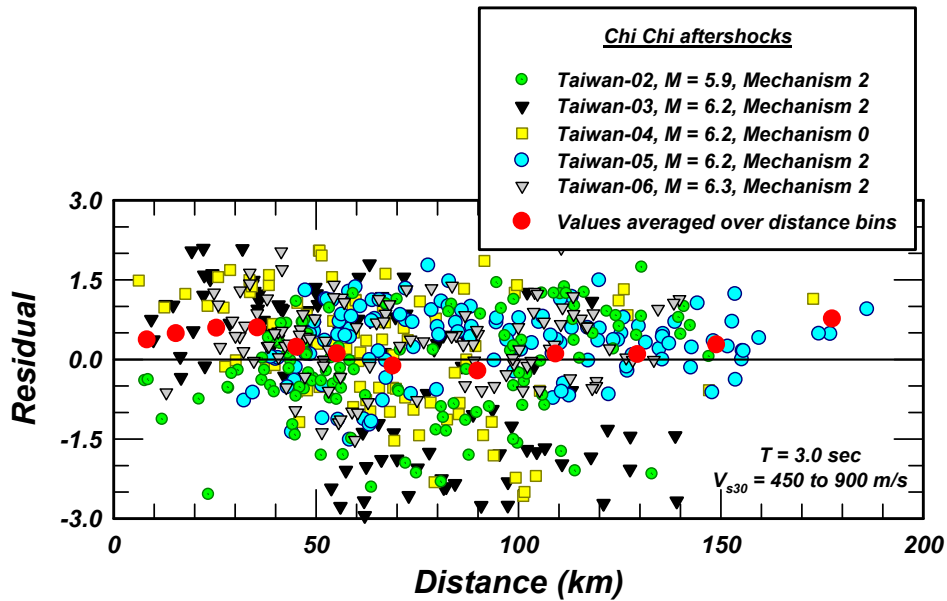


Figure E-3 Residuals versus closest distance for spectral accelerations ($T = 3.0$ sec) for motions recorded during the five Chi-Chi earthquake aftershocks obtained using the derived equation with magnitude and mechanism as shown in the legend

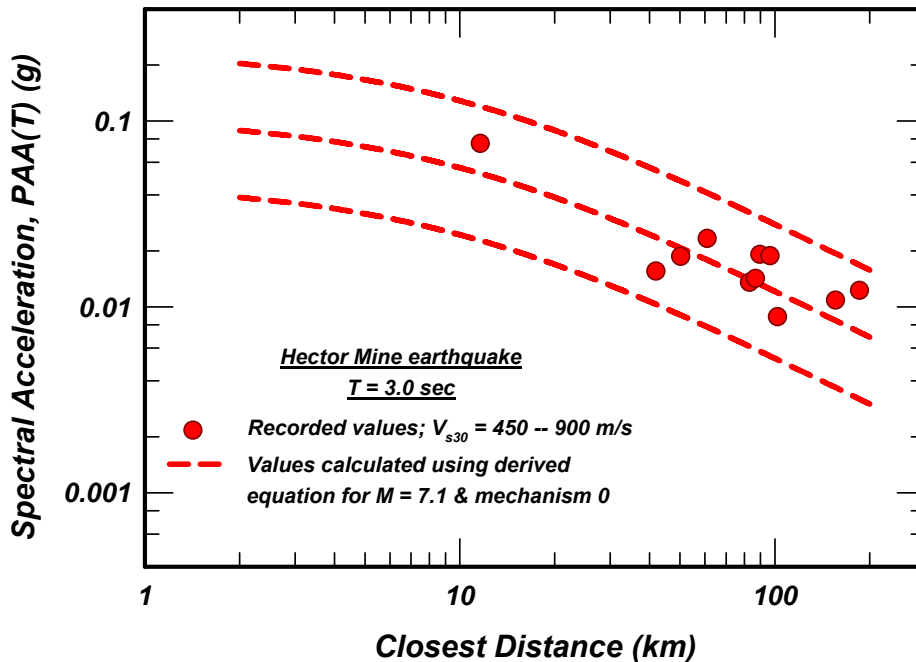


Figure E-4 Comparison of spectral accelerations ($T = 3.0$ sec) recorded during the 1999 Hector Mine earthquake with median, 16-percentile and 84-percentile values calculated using the derived equation with $M = 7.1$ & mechanism 0

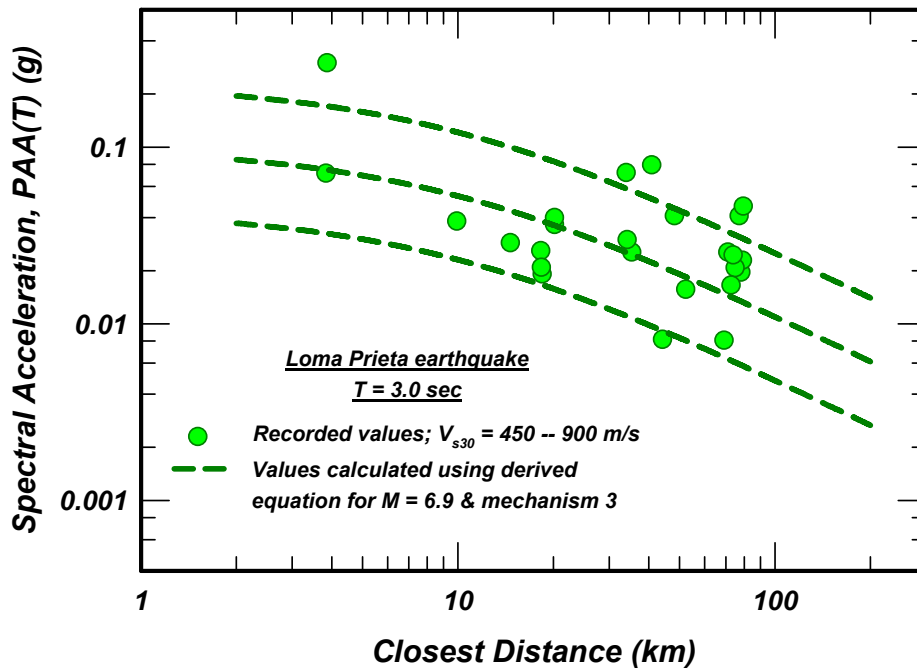


Figure E-5 Comparison of spectral accelerations ($T = 3.0$ sec) recorded during the 1989 Loma Prieta earthquake with median, 16-percentile and 84-percentile values calculated using the derived equation with $M = 6.9$ & mechanism 3

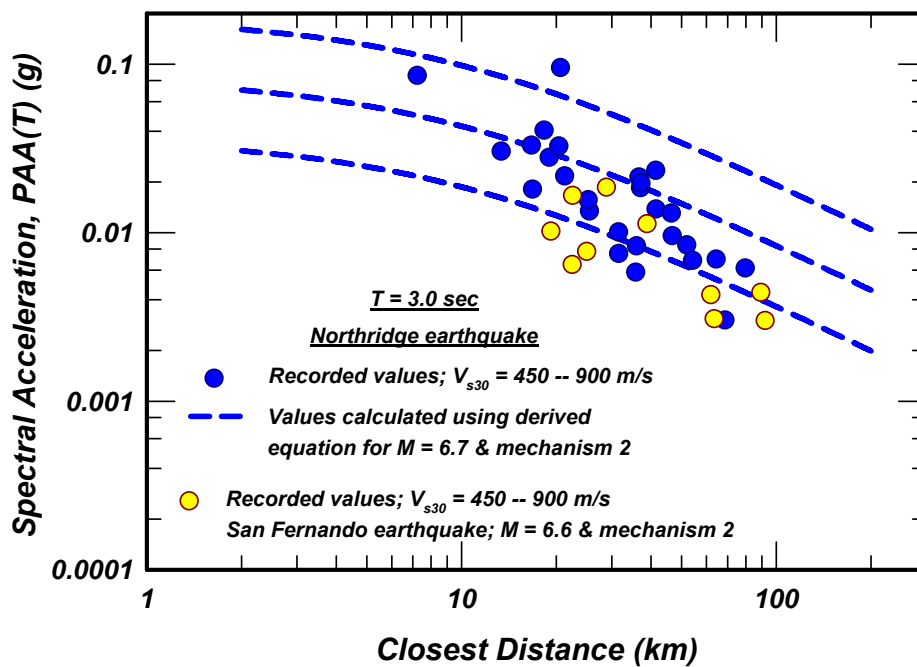


Figure E-6 Comparison of spectral accelerations ($T = 3.0$ sec) recorded during the 1994 Northridge and the 1971 San Fernando earthquakes with median, 16-percentile and 84-percentile values calculated using the derived equation with $M = 6.7$ & mechanism 2

APPENDIX F
ATTENUATION RELATIONSHIP DERIVED BY I. M. IDRIS IN 2002

F.1 INTRODUCTION

Just prior to the initiation of the NGA project, the writer had completed derivation of an attenuation relationship for "rock" or "rock-like" sites using the then available earthquake ground motion data from the PEER Strong Motion Database for shallow crustal earthquakes. Recordings obtained at the following locations were excluded: (i) dam abutments; (ii) any building with basements; (iii) buildings exceeding 2 stories; (iv) stations suspected of being affected by topographic features; (v) instruments known or suspected to have been placed on a pedestal; and (vi) motions recorded at distances beyond 100 km from the rupture plane. These exclusions were effected so that only "free-field" records are used to derive the attenuation relationships. The motions recorded at rock sites (Geomatrix site classification A) and at shallow soil sites (Geomatrix site classification B) were combined into a single "rock" or "rock-like" category for the purpose of deriving attenuation relationships for estimating horizontal spectral ordinates at such sites.

A total of 241 horizontal records (i.e., 482 horizontal components) were obtained from the PEER Strong Motion Database. The magnitude of the event, the closest distance from the rupture plane to the recording station, and the site classification given in the Database were adopted in this study. These 241 horizontal records were obtained during the 40 earthquakes listed in Table 1, which consist of 20 strike slip, 8 oblique and 12 reverse events. The date and time at which each earthquake occurred, the moment magnitude, and the mechanism of each earthquake are also listed in Table F-1.

F.2 ATTENUATION RELATIONSHIPS

The following form was adopted for estimating the median values of spectral accelerations:

$$\ln(y) = (\alpha_1 + \alpha_2 M) - (\beta_1 + \beta_2 M) \ln(R + 10) + F\phi \quad [F-1]$$

in which: y is the median value of peak horizontal acceleration or horizontal spectral ordinate in g's; M is moment magnitude; R is closest distance in km from the site to the rupture plane; F is fault type and is set equal to zero ($F = 0$) for a strike strip source and is set equal to unity ($F = 1$) for reverse and reverse /oblique sources; and ϕ is the style of faulting (or source mechanism) factor. The parameters $\alpha_1, \alpha_2, \beta_1,$ & β_2 are listed in Table F-2 for peak horizontal acceleration (pga) and for periods ranging from 0.03 sec to 5 sec, and for the three magnitude ranges used in the regression analyses.

The standard error for each period is given by the following relationships:

$$SE = \left\{ \begin{array}{ll} \varepsilon_{max} & \text{for } M \leq 5 \\ \varepsilon - 0.12M & \text{for } 5 \leq M \leq 7\frac{1}{4} \\ \varepsilon_{min} & \text{for } M \geq 7\frac{1}{4} \end{array} \right\} \quad [F-2]$$

Values of the parameters ε_{max} , ε , ε_{min} , and ϕ are listed in Table F-3 for pga and for all the periods considered.

TABLE F-1
List of Earthquakes Used to Derive Attenuation Relationships

Earthquake	Date			Time (GMT)	Magnitude (M)	Earthquake Mechanism
	Year	Month	Day			
Daley City	1957	03	22	1944	5.3	OB
Parkfield	1966	06	28	0426	6.1	SS
Lytle Creek	1970	09	12	1430	5.4	OB
San Fernando	1971	02	09	1400	6.6	RV
Hollister	1974	11	28	2301	5.2	SS
Gazli, USSR	1976	05	17		6.8	RV
Tabas, Iran	1978	09	16		7.4	RV
Coyote Lake	1979	08	6	1705	5.7	SS
Imperial Valley	1979	10	15	2316	6.5	SS
Livermore	1980	01	24	1900	5.8	SS
Livermore	1980	01	27	0233	5.4	SS
Anza (Horse Canyon)	1980	02	25	1047	4.9	SS
Mammoth Lakes	1980	05	25	1944	6.0	SS
Mammoth Lakes	1980	05	25	2035	5.7	SS
Mammoth Lakes	1980	05	27	1451	6	OB
Mammoth Lakes	1980	05	27	1901	4.9	SS
Mammoth Lakes	1980	05	31	1516	4.9	SS
Mammoth Lakes	1980	06	11	0441	5.0	SS
Westmorland	1981	42	06	1209	5.8	SS
Coalinga	1983	05	02	2342	6.4	OB
Coalinga	1983	05	09	0249	5	RV
Coalinga	1983	06	11	0309	5.3	RV
Coalinga	1983	07	09	0740	5.2	RV
Coalinga	1983	07	22	0239	5.8	RV
Coalinga	1983	07	22	0343	4.9	RV
Coalinga	1983	07	25	2231	5.2	RV
Coalinga	1983	09	09	0916	5.3	RV
Morgan Hill	1984	04	24	2115	6.2	SS
N. Palm Springs	1986	07	08	0920	6	OB
Chalfant Valley	1986	07	20	1429	5.9	SS
Chalfant Valley	1986	07	21	1442	6.2	SS
Chalfant Valley	1986	07	21	1451	5.6	SS
Whittier Narrows	1987	10	01	1442	6	RV
Whittier Narrows	1987	10	04	1059	5.3	OB
Superstition Hills(B)	1987	11	24	1316	6.7	SS
Spitak, Armenia	1988	12	07		6.8	OB
Loma Prieta	1989	10	18	0005	6.9	OB
Landers	1992	06	28	1158	7.3	SS
Northridge	1994	01	17	1231	6.7	RV
Kobe	1995	01	16	2046	6.9	SS

TABLE F-2
Parameters Derived for Estimating Median Horizontal Spectral Accelerations
Spectral Damping Ratio = 0.05

Period (sec)	Parameters for $M < 6$				Parameters for $M = 6$ to $M = 6\frac{1}{2}$				Parameters for $M > 6\frac{1}{2}$			
	α_1	α_2	β_1	β_2	α_1	α_2	β_1	β_2	α_1	α_2	β_1	β_2
pga	2.5030	0.1337	2.8008	-0.1970	4.3387	-0.1754	3.2564	-0.2739	6.5668	-0.5164	3.2606	-0.2740
0.03	2.5030	0.1337	2.8008	-0.1970	4.3387	-0.1754	3.2564	-0.2739	6.5668	-0.5164	3.2606	-0.2740
0.04	2.9873	0.0290	2.7850	-0.2081	3.9748	-0.1244	3.0378	-0.2468	6.1747	-0.4717	3.0156	-0.2461
0.05	3.2201	0.0099	2.7802	-0.2092	3.9125	-0.0972	2.9689	-0.2381	6.2734	-0.4675	2.9671	-0.2400
0.06	3.2988	0.0187	2.7784	-0.2083	3.8984	-0.0777	2.9481	-0.2355	6.4228	-0.4696	2.9677	-0.2396
0.07	3.2935	0.0378	2.7777	-0.2072	3.8852	-0.0613	2.9448	-0.2352	6.5418	-0.4704	2.9791	-0.2406
0.075	3.2702	0.0489	2.7774	-0.2068	3.8748	-0.0536	2.9458	-0.2354	6.5828	-0.4698	2.9850	-0.2413
0.08	3.2381	0.0606	2.7773	-0.2065	3.8613	-0.0462	2.9477	-0.2358	6.6162	-0.4685	2.9904	-0.2419
0.09	3.1522	0.0845	2.7770	-0.2061	3.8249	-0.0319	2.9527	-0.2367	6.6541	-0.4642	2.9989	-0.2429
0.1	3.0467	0.1083	2.7767	-0.2060	3.7774	-0.0181	2.9578	-0.2376	6.6594	-0.4580	3.0044	-0.2437
0.11	2.9308	0.1316	2.7763	-0.2061	3.7206	-0.0046	2.9623	-0.2385	6.6436	-0.4504	3.0071	-0.2442
0.12	2.8093	0.1541	2.7759	-0.2063	3.6562	0.0086	2.9659	-0.2393	6.6084	-0.4419	3.0077	-0.2446
0.13	2.6859	0.1758	2.7754	-0.2066	3.5860	0.0215	2.9685	-0.2401	6.5639	-0.4328	3.0067	-0.2448
0.14	2.5579	0.1966	2.7748	-0.2070	3.5111	0.0341	2.9703	-0.2407	6.5085	-0.4233	3.0044	-0.2448
0.15	2.4301	0.2166	2.7741	-0.2074	3.4327	0.0464	2.9712	-0.2412	6.4448	-0.4137	3.0012	-0.2448
0.16	2.3026	0.2357	2.7733	-0.2079	3.3515	0.0586	2.9713	-0.2416	6.3778	-0.4040	2.9974	-0.2447
0.17	2.1785	0.2541	2.7724	-0.2083	3.2683	0.0704	2.9708	-0.2420	6.3077	-0.3945	2.9931	-0.2446
0.18	2.0543	0.2718	2.7714	-0.2088	3.1837	0.0821	2.9697	-0.2423	6.2366	-0.3850	2.9885	-0.2444
0.19	1.9324	0.2888	2.7704	-0.2092	3.0980	0.0934	2.9681	-0.2425	6.1623	-0.3758	2.9836	-0.2442
0.2	1.8129	0.3051	2.7693	-0.2096	3.0117	0.1046	2.9660	-0.2426	6.0872	-0.3668	2.9786	-0.2440
0.22	1.5794	0.3360	2.7668	-0.2105	2.8382	0.1263	2.9608	-0.2428	5.9380	-0.3494	2.9684	-0.2436
0.24	1.3575	0.3646	2.7641	-0.2112	2.6648	0.1471	2.9544	-0.2428	5.7915	-0.3331	2.9580	-0.2431
0.25	1.2490	0.3782	2.7626	-0.2116	2.5786	0.1572	2.9509	-0.2428	5.7213	-0.3253	2.9529	-0.2428

TABLE F-2 (Cont'd)

Period (sec)	Parameters for $M < 6$				Parameters for $M = 6$ to $M = 6\frac{1}{2}$				Parameters for $M > 6\frac{1}{2}$			
	α_1	α_2	β_1	β_2	α_1	α_2	β_1	β_2	α_1	α_2	β_1	β_2
0.26	1.1435	0.3913	2.7611	-0.2119	2.4929	0.1671	2.9472	-0.2427	5.6485	-0.3178	2.9477	-0.2426
0.28	0.9381	0.4161	2.7580	-0.2126	2.3231	0.1863	2.9393	-0.2425	5.5097	-0.3035	2.9376	-0.2421
0.3	0.7437	0.4394	2.7548	-0.2132	2.1559	0.2049	2.9310	-0.2423	5.3744	-0.2900	2.9276	-0.2417
0.32	0.5553	0.4612	2.7514	-0.2137	1.9916	0.2228	2.9224	-0.2419	5.2428	-0.2774	2.9178	-0.2412
0.34	0.3755	0.4816	2.7480	-0.2143	1.8306	0.2400	2.9135	-0.2416	5.1167	-0.2656	2.9082	-0.2408
0.35	0.2883	0.4914	2.7462	-0.2145	1.7512	0.2484	2.9091	-0.2414	5.0563	-0.2600	2.9034	-0.2405
0.36	0.2049	0.5008	2.7445	-0.2147	1.6728	0.2567	2.9045	-0.2412	4.9957	-0.2545	2.8987	-0.2403
0.38	0.0362	0.5190	2.7410	-0.2152	1.5183	0.2728	2.8955	-0.2407	4.8752	-0.2441	2.8894	-0.2399
0.4	-0.1223	0.5361	2.7374	-0.2156	1.3671	0.2883	2.8864	-0.2403	4.7604	-0.2342	2.8803	-0.2395
0.45	-0.4985	0.5749	2.7285	-0.2167	1.0036	0.3251	2.8639	-0.2391	4.4900	-0.2119	2.8581	-0.2384
0.5	-0.8415	0.6091	2.7197	-0.2176	0.6598	0.3591	2.8419	-0.2379	4.2369	-0.1922	2.8367	-0.2374
0.55	-1.1581	0.6393	2.7112	-0.2185	0.3347	0.3906	2.8206	-0.2367	4.0027	-0.1747	2.8160	-0.2363
0.6	-1.7051	0.7087	2.7030	-0.2194	0.0271	0.4200	2.8002	-0.2356	3.7826	-0.1589	2.7960	-0.2353
0.7	-1.9821	0.7127	2.6878	-0.2211	-0.5407	0.4729	2.7624	-0.2334	3.3750	-0.1314	2.7580	-0.2333
0.8	-2.4510	0.7514	2.6742	-0.2228	-1.0522	0.5193	2.7283	-0.2315	3.0078	-0.1078	2.7227	-0.2314
0.9	-2.8715	0.7847	2.6624	-0.2244	-1.5147	0.5603	2.6980	-0.2298	2.6734	-0.0870	2.6901	-0.2295
1	-3.2511	0.8139	2.6522	-0.2259	-1.9343	0.5966	2.6712	-0.2284	2.3648	-0.0683	2.6603	-0.2278
1.5	-4.7813	0.9288	2.6206	-0.2326	-3.5364	0.7255	2.5803	-0.2246	1.1109	0.0068	2.5501	-0.2211
2	-5.9481	1.0246	2.6097	-0.2368	-4.5538	0.7945	2.5443	-0.2252	0.1818	0.0649	2.4928	-0.2176
3	-7.7976	1.2121	2.6086	-0.2385	-5.5133	0.8254	2.5790	-0.2354	-1.1016	0.1532	2.4711	-0.2168
4	-9.3398	1.4047	2.6012	-0.2336	-5.5624	0.7672	2.7072	-0.2537	-1.9306	0.2153	2.4953	-0.2190
5	-10.7364	1.5973	2.5703	-0.2250	-5.0154	0.6513	2.8979	-0.2773	-2.5042	0.2579	2.5107	-0.2199

TABLE F-3
Source Mechanism Factors and Standard Error Parameters

Period (sec)	ϕ	ϵ_{min}	ϵ	ϵ_{max}	Period (sec)	ϕ	ϵ_{min}	ϵ	ϵ_{max}
0.01 (pga)	0.320	0.450	1.320	0.720	0.26	0.355	0.546	1.416	0.816
0.03	0.320	0.450	1.320	0.720	0.28	0.357	0.550	1.420	0.820
0.04	0.320	0.450	1.320	0.720	0.3	0.360	0.555	1.425	0.825
0.05	0.320	0.450	1.320	0.720	0.32	0.360	0.559	1.429	0.829
0.06	0.320	0.460	1.330	0.730	0.34	0.360	0.562	1.432	0.832
0.07	0.320	0.469	1.339	0.739	0.35	0.360	0.564	1.434	0.834
0.075	0.320	0.473	1.343	0.743	0.36	0.360	0.566	1.436	0.836
0.08	0.320	0.477	1.347	0.747	0.38	0.360	0.569	1.439	0.839
0.09	0.320	0.483	1.353	0.753	0.4	0.360	0.572	1.442	0.842
0.1	0.320	0.490	1.360	0.760	0.45	0.360	0.579	1.449	0.849
0.11	0.324	0.495	1.365	0.765	0.5	0.360	0.586	1.456	0.856
0.12	0.327	0.500	1.370	0.770	0.55	0.350	0.592	1.462	0.862
0.13	0.330	0.505	1.375	0.775	0.6	0.340	0.597	1.467	0.867
0.14	0.332	0.509	1.379	0.779	0.7	0.322	0.607	1.477	0.877
0.15	0.335	0.513	1.383	0.783	0.8	0.307	0.615	1.485	0.885
0.16	0.337	0.517	1.387	0.787	0.9	0.294	0.623	1.493	0.893
0.17	0.339	0.521	1.391	0.791	1	0.282	0.630	1.500	0.900
0.18	0.341	0.524	1.394	0.794	1.5	0.236	0.630	1.500	0.900
0.19	0.343	0.527	1.397	0.797	2	0.204	0.630	1.500	0.900
0.2	0.345	0.530	1.400	0.800	3	0.158	0.630	1.500	0.900
0.22	0.348	0.536	1.406	0.806	4	0.125	0.630	1.500	0.900
0.24	0.352	0.541	1.411	0.811	5	0.100	0.630	1.500	0.900
0.25	0.353	0.544	1.414	0.814					